Informatik

Iyad Tumar

Resource Management of Disruption Tolerant Networks

JACOBS
UNIVERSITY

JACOBS
UNIVERSITY

Resource Management of Disruption Tolerant Networks

Iyad Khalil Tumar

A thesis submitted in partial fulfillment
of the requirements for the degree of
Doctor of Philosophy
in Computer Science

Approved, Thesis Committee:

Prof. Dr. Jürgen Schönwälder
Jacobs University Bremen, Germany

Prof. Dr. Harald Haas
Jacobs University Bremen, Germany
The University of Edinburgh, UK

Prof. Dr. Rolf Stadler
KTH Royal Institute of Technology, Sweden

Date of Defense: July 30th, 2010
School of Engineering and Science

Berichte aus der Informatik

Iyad Tumar

Resource Management of Disruption Tolerant Networks

Shaker Verlag
Aachen 2011

Bibliographic information published by the Deutsche Nationalbibliothek
The Deutsche Nationalbibliothek lists this publication in the Deutsche Nationalbibliografie; detailed bibliographic data are available in the Internet at http://dnb.d-nb.de.

Zugl.: Jacobs Univ. Bremen, Diss., 2010

Printed in Germany.

ISBN 978-3-8322-9346-8
ISSN 0945-0807

Shaker Verlag GmbH • P.O. BOX 101818 • D-52018 Aachen
Phone: 0049/2407/9596-0 • Telefax: 0049/2407/9596-9
Internet: www.shaker.de • e-mail: info@shaker.de

Abstract

Disruption tolerant networks (DTNs) is a research area aiming at developing network communication when connectivity is intermittent and prone to disruptions. The disruptions in DTNs occur due to many factors, such as node mobility, physical obstacles, depleted energy, and low node density. In such environments, data can be delivered by mobile nodes, which store, carry, and then forward data towards destinations. Unfortunately, many mobility scenarios depend on untethered devices with limited energy supplies. Therefore, power management schemes are highly needed in such networks in order to extend the network lifetime and to avoid degraded network connectivity.

A wireless interface is one of the largest consumers of energy in energy-limited devices and it can work in four different modes: listening, transmitting, receiving, and sleeping. Wireless interfaces consume a significant amount of energy even in the idle "listening mode". Therefore, a significant amount of energy can be saved by allowing nodes to put their wireless interfaces into sleeping mode. In DTNs, nodes need to discover neighbors to establish communication. Searching for neighbors in sparse DTNs can consume a large amount of power compared to the power consumed by infrequent data transfers. Thus, designing such power management schemes is challenging, because nodes need to know when to sleep, to save power, and when to wake up to search for neighbors. Ideally, power management schemes should not reduce network connectivity opportunities that would negatively affect the overall performance of the network.

In this thesis, we first present a power management scheme called Multi-Radio (MR) scheme, in which nodes are equipped with two complementary radios: a high-power radio and a low-power radio. In this scheme, energy can be conserved by using a low-power radio to discover communication opportunities with other nodes and waking up a high-power radio to undertake the data transmission. In addition, we investigate the impact of different node mobility patterns on the MR scheme: we study the effects of *Random Waypoint*, *Manhattan*, *Message Ferry*, *Human* and *Zebra* mobility models on the MR scheme. Finally, we introduce a Multi-Acoustic Modem power management scheme for sparse shallow underwater networks, in which nodes are equipped with two acoustic modems, low-power acoustic modem for neighbor discovery and high-power acoustic modem for data exchange.

I certify that I have written this PhD thesis by my own without any impermissible assistance.

Iyad Tumar
Matriculation Number: 10000398
School of Engineering and Science
Jacobs University Bremen, Germany
July 2010

To My Parents

To Mahmoud Darwish's Soul

Acknowledgements

Until writing this page, I have spent almost three years and a half for the PhD study. During the course of my study, I have received support from individuals and organizations. This thesis would not have been possible without their support.

I would like to thank my professor, Dr. Jürgen Schönwälder for giving me an opportunity to study and work in the Computer Networks and Distributed Systems group at Jacobs University. I would especially like to thank him for providing me the flexibility to choose projects while guiding me into the right directions. Also, for giving me constructive criticisms, which motivated and trained me to improve the quality of my research. Furthermore, his insights and experiences were so valuable for me to enhance my research and presentation skills. I would like to take this opportunity to thank my thesis committee members, Prof. Dr. Harald Haas and Prof. Dr. Rolf Stadler for their constructive comments on the structure and manuscript of this thesis.

Many Thanks go to European Network of Excellence for the Management of Internet Technologies and Complex Services (EMANICS) organization for funding my study, and to Jacobs University for providing me a great research environment. I am grateful to all of my present and former colleagues in the CNDS group: Ha Manh Tran, Anuj Sehgal, Matus Harvan, Vladislav Marinov, Georgi Chulkov, Nikolay Melnikov and Siarhei Kuryla for their support, whether it be through proofreading papers, listening to talks, or just offering their help, advice, and for bringing friendly atmosphere in the group and sharing pleasant excursions, which made my study more interesting. Again I would like to thank Anuj Sehgal with whom I have an opportunity to work. I would like to thank my friends Mohammed El-Shazly, Mohammed Nour, Raed Mesleh, Ahmed Moussa Eid, Hefzi Jarrar, Hamdy El-Sheshtawy, Khaled Hassan, Salahaldin Juba, Khodr Saaifan, Ahmed Deyab, Rami Tarawnah, Rami Abu Alhiga, Hany Elgala, Ghada Al kadamany, Liudmila Tarabashkina, Esther Ghanem, Samer Bali, Angelica Gutierrez, Thomas Raftis, who make my daily life less boring.

Last but not least, I am greatly obliged to my dearest parents, Khalil and Fatma, sisters and brothers for their constant support and encouragement.

Contents

1 Introduction

Traditional network architectures including the OSI reference model and the Internet architecture were designed with assumptions for specific applications and deployment scenarios. Some of the most important assumptions are the underlying network characteristics and network topologies, such as relatively short transmission delays, low error probability, and the existence of end-to-end paths. Today, some of these assumptions no longer hold due to the increasing number of communication scenarios that have more challenging environments with frequent connectivity disruptions and long transmission delays.

In the last few years, many research efforts have been devoted to provide networking services in challenging environments, where no infrastructure exists, such as, deep space, disaster and hostile areas, battle fields, underwater networks, and social networks [1, 2, 3, 4, 5, 6, 7, 8, 9]. However, building such networks is challenging because of disruptions in their connectivity due to mobility, geographical obstacles, sparsity and low density of nodes. Unlike traditional mobile ad hoc networks (MANETs), in which nodes are deployed dense enough to provide end-to-end communications, disruption tolerant networks are often sparse and do not support end-to-end communication. Sparsity deployments occur due to the expensive cost of nodes (e.g., deep sea networks) or sometimes it might be not easy to deploy a dense network (e.g., in a battle field in military areas, deep space networks). Therefore, the need for networks that support disruptions is important in such applications.

1.1 Disruption Tolerant Networks

Disruption tolerant networks (DTNs) is a research area aiming at developing network communication when connectivity is intermittent and prone to disruptions. The disruptions in DTNs occur due to many factors, such as node mobility, physical obstacles, depleted energy, and low node density. In such an environment, data can be delivered by mobile nodes which store, carry, and then forward data towards destinations [10, 11, 12, 13]. Figure 1.1 shows a scenario of message forwarding in a DTN. Initially, node S has a message for node D. However, node D is not within the radio range of node S. Since node R1 is within node S's radio range, node S forwards the message to node R1 as shown in Figure 1.1(a). Node R1 receives and stores the message, carries it until it encounters node R2 as in Figure 1.1(b), and then forwards it. When node R2 meets node D, it forwards the message to node D, as in Figure 1.1(c).

One of the major challenges in building a DTN architecture is the routing protocol. Recently, significant efforts have been spent on developing routing protocols and architectures for DTNs [15, 11, 16, 17, 18]. These protocols are designed to provide reliable and robust data

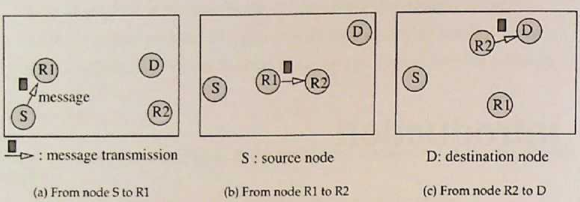

Figure 1.1: An example scenario of message forwarding in a DTN as time passes [14].

delivery services within DTN environments. DTNs can be applied to wireless networks with no end-to-end connectivity, satellite networks with long delays, wireless sensor networks with intermittent connectivity, and underwater acoustic networks with frequent interruptions.

Another major issue in DTNs is energy conservation. In general, DTNs are applicable in remote and hazardous areas where the energy sources are often constrained. DTNs are also often assumed to operate over a long period of time. Therefore, several research efforts have been devoted to developing power management schemes for DTNs to allow these networks to remain operational over a long period of time.

The wireless interface is one of the largest consumers of energy in energy limited devices [19] and it can work in four different modes: listening, transmitting, receiving, and sleeping. Wireless interfaces consume a significant amount of energy even in the idle listening mode. Measurements have shown that transmitting a single bit of information requires the same amount of energy as that needed for processing a thousand operations in a sensor node [20]. Studies also show that energy consumption of some radios in idle mode is almost as high as in receiving mode [21, 22]. Therefore, a significant amount of energy can be saved by allowing nodes to put their wireless interfaces into sleep mode.

In DTNs, nodes need to discover neighbors to establish communication. Searching for neighbors in sparse DTNs can consume a large amount of power compared to the power consumed by infrequent data transfers. Therefore, novel power management schemes are needed to address this problem and to save energy. Designing such power management schemes is challenging, because nodes need to know when to sleep, to save power, and when to wake up to search for neighbors. Ideally, power management schemes should not reduce network connectivity opportunities, which would negatively affect the overall performance of the network.

1.1.1 Disruption Tolerant Networks Characteristics

DTNs are supposed to operate over a long period of time, and they differ from traditional networks because of their characteristics. In this section we briefly review some important properties of DTNs [15, 23, 24]:

Latency: Due to frequent and random mobility of the nodes in DTNs, any two nodes may never meet each other for a long time. Therefore, the transmission rate may be considerably small and largely asymmetric with long latency of data delivery.

Disconnection: In DTNs, there is no end-to-end path due to network partition since these networks are prone to disruption.

Queuing Delay: In DTNs, the queuing delay is aggravated because disconnection is more common compared to traditional networks.

Network Lifetime: End nodes can be deployed in hostile and hazardous environments such as disaster areas. This implies that the end-to-end delay from a sensor node to the destination sink might be longer than the life time of the sensor node itself, due to power exhaustion or other failures.

Limited Resources: In general, DTN nodes are mobile and often battery operated with a wireless connection and they have limited resources (computing power, memory, and buffer space).

1.1.2 Sparse Network Architectures

Sparse networks are characterized by a sparse connectivity environment, where the density of nodes in the deployed area is insufficient to provide direct end-to-end communication. Many of these networks use mobility of nodes to deliver data to their destinations. When mobile nodes encounter each other opportunistically or intentionally, they pass messages to route them towards their final destinations.

This section presents some architectures for sparse networks:

1) Goodman et al. [25] propose the Infostation architecture, an array of isolated wireless ports for providing convenient and frequent access to high bit-rate connections. Infostations are distributed geographically to provide high data rate connections. They could be located at building entrances or on highways, streets, and in airports. The access between the Infostation and a gateway could be wired or dial-up, depending on traffic and latency demand.

2) Shah et al. [16] propose an architecture for collecting data in sparse sensor networks which is called DataMules. In this architecture, the data will be transported by a mobile node from static sensors to the access point in order to save energy in sensor nodes by using short range radios.

3) Fall [15] introduces a Delay Tolerant Network (DTN) architecture to interconnect challenged networks such as interplanetary networks and sensor networks. This architecture is based on an asynchronous message forwarding scheme using a store-and-forward approach.

4) Ahmed et al. [26] propose an architecture to address the partitions in sparse MANETs by using range of extension networks that consists of airplanes and satellites. These airplanes or satellite nodes maintain communication links with specific gateways in the deployed network areas to enable two separated networks to communicate with each other.

5) A vehicular network is a communication network connecting vehicles to each other and with mobile and fixed location resources, without the assistance of other communication infrastructure than carried on board. Several wireless technologies exist for vehicle-to-vehicle (v2v) and vehicle-to-roadside (v2r) communications, including Wireless Wide

Area Networks (WWAN), Wireless Local Area Networks (WLAN) using roadside base stations, and ad hoc networks using v2v communication. These technologies offer trade-offs in cost and performance, since a larger coverage area often leads to higher cost and lower capacity [27].

1.1.3 Underwater Acoustic Networks

Underwater sensor networks are attracting researchers' interests. These networks are envisioned to enable applications for oceanographic data collection, navigation, pollution monitoring, offshore exploration for disaster prevention, and tactical surveillance applications. These applications are based on underwater acoustic networking technology [2, 28, 29, 30]. In fact, the underwater channel is not conducive to use radio frequency (RF) for communications between sensor nodes since radio waves can only propagate through sea water at very low frequencies (30-300Khz).

Underwater acoustic networking introduces some challenges to achieve real-time communications because of the unique characteristics of the acoustic channel such as: limited bandwidth capacity, high and varying propagation delay. Underwater sensor networks are prone to disruptions and often have sparse topology to achieve the largest area of coverage [2], which means DTNs will arise in underwater networks.

The energy costs in underwater acoustic networks are different from terrestrial radio-based networks. In acoustic networks, transmission power is significantly higher than receiving power [9]. Thus, to save energy and to extend the network lifetime, and to obtain a good performance, it is essential to design networking schemes based on utilization of the opportunities presented by hostile deep-sea environments, taking into account long and varying propagation delays, high and varying ambient noise.

1.2 Motivation of Research

Due to the increasing number of communication scenarios that operate in challenging environments with frequent connectivity disruptions and long transmission delays, disruption tolerant networks (DTNs) arise as a feasible approach to address the technical issues in heterogeneous networks that may lack continuous network connectivity. DTNs are also dealing with opportunistic contacts for asynchronous communications in remote and hazardous areas where the energy sources are often constrained which makes energy conservation a major and critical issue. Therefore, this dissertation explores energy conservation techniques for disruption tolerant networks. This work combines asynchronous schemes in which nodes wake up based on their own schedules to communicate, with an on-demand schemes that often use additional low power radio to search for contacts and to awake the high power radio to undertake the data transmission. By using this combination (asynchronous and on-demand) more energy can be saved since achieving synchronization among nodes consumes much energy and keeping the high power radio in sleep mode and using it only for data exchanges saves energy by eliminating the idle time energy consumption. Furthermore, the dissertation explores the impact of the mobility modes on the energy conservation schemes in disruption tolerant networks.

DTNs have primarily been researched under the assumption of radio-based terrestrial networks and planned networks in space, yet many of the techniques are directly applicable in underwater networks since underwater sensor networks are prone to disruptions and often have a sparse topology to achieve the largest area of coverage [2]. This motivated us to explore the energy conservation techniques in underwater networks that based on acoustic communication modems.

1.3 Research Contribution

In this thesis, we explore energy conservation techniques for disruption tolerant networks. We design a power management scheme called Multi-Radio (MR) power management scheme that uses two complementary radios: a high bit rate, high-power radio and a low bit rate, low-power radio. By utilizing two radios instead of one, we are able to implement an asynchronous, on-demand energy conservation scheme that eliminates the idle time of a single high-power radio, and only allows the high-power radio to consume power in the sleep mode or while it is transmitting and receiving data. While the high-power radio is only called upon to perform data delivery when necessary, the low-power radio remains active for asynchronous neighbor discovery. For energy, we only account for the communication energy consumption of wireless interfaces and do not consider other sources such as computation or mobility.

The dissertation explores the impact of different mobility models on the MR power management scheme. We study the effects of the random waypoint mobility model, the most common model used to evaluate routing protocols in ad hoc networks. The Manhattan mobility model is based on the observed characteristics of road traffic in cities, especially in Manhattan. The Message ferry mobility model, in which nodes are classified into regular nodes (often static nodes) and ferries, which move around the deployed area in a deterministic path to collect messages from the regular nodes and to deliver messages to their destinations or to other ferries. The Zebra mobility model is based upon the observed mobility habits of zebras. Finally, the human mobility model is derived from human mobility traces collected at Disney World, Orlando, Florida.

The thesis presents a power management technique for shallow underwater networks. We investigate the use of two acoustic modems. We present a Multi-Acoustic Modem (MAM) power management scheme that is similar to the MR scheme. The MAM scheme uses two acoustic modems instead of two radios for communication underwater, a low power acoustic modem (low data rate) for neighbor discovery and a high power acoustic modem (high data rate) for data delivery.

1.4 Thesis Outline

Chapter 2 presents the routing protocols and mobility models for disruption tolerant networks. Power management schemes for disruption tolerant networks are discussed in Chapter 3. Chapter 4 describes underwater acoustic networks, considers acoustic channel models, communication scenarios, energy efficiency and routing protocols in underwater acoustic networks. A new multi-radio power management scheme for DTNs is discussed in Chapter 5. Chapter 6 focuses on energy consumption and power management for underwater acoustic networks.

Chapter 7 concludes the thesis with a discussion about the limitations and future direction of this study.

2 Routing Protocols and Mobility Models for Disruption Tolerant Networks

In this chapter, the routing problem and the mobility models for disruption tolerant networks are considered. There is no guarantee for an end-to-end connected path between a source node and a destination node at any time in DTNs. Therefore, traditional routing protocols are unable to deliver messages among nodes.

2.1 Routing Protocols for Intermittently Connected Networks

This section summarizes some commonly used routing protocols in intermittently connected networks such as: source routing, epidemic routing [31], message ferry routing [17], MaxProp routing protocol [12], and probabilistic routing [32]. In fact, we focus on the aforementioned routing protocols since they are used in the power management protocols that are discussed in this thesis.

2.1.1 Source Routing

In source routing protocols, the source node determines the routing path based on the topology of the network. In general, these routing protocols use knowledge-based mechanisms that utilize available knowledge about network dynamics and apply Dijkstras algorithm to find the shortest path in terms of expected delay [14].

2.1.2 Epidemic Routing

In epidemic routing, random pair-wise nodes exchange messages among mobile hosts to achieve message delivery. The epidemic protocol assumes that (i) the sender is never in range of any base station, (ii) the sender does not know the location of the receiver, (iii) the receiver may be a roaming wireless host, (iv) nodes can communicate when they become within each other communication range through node mobility.

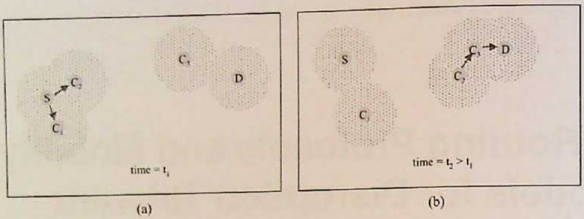

Figure 2.1: A source S wishes to transmit a message to a destination D but no connected path is available as shown in part (a). The carriers $C1 - C3$ are leveraged to transitively deliver the message to its destination at some later point in time as shown in part (b) [31].

The epidemic protocol distributes messages to random hosts through the connected portions of the network, which are called carriers. These carriers will distribute the messages to other portions of the network when they come into contact through node mobility. At this point the message spreads to an additional island of nodes. Through such transitive transmission of data, messages have high probability of eventually reaching their destinations. In epidemic protocol, each host stores a bit vector, called the summary vector that indicates which entries in their local hash tables are set. When two hosts come into communication range of one another, the host with the smaller identifier initiates an anti-entropy session [33] with the host with the larger identifier. To avoid redundant connections, each host maintains a cache of hosts that it has spoken with recently. Anti-entropy is not re-initiated with remote hosts that have been contacted within a configurable time period [31]. Figure 2.1 shows transitive transmission to send a message from node S to node D.

2.1.3 Message Ferry Routing Protocol

The message ferry (MF) model is another approach utilizing some mobile nodes (message ferries) to establish communication and carry messages to other nodes in the network. These ferries try to help deliver data by taking the responsibility for carrying data between nodes while they are moving around the deployment area [17, 34]. There are two scenarios of MF depending on who is initiates the proactive movement.

- Node Initiated Message Ferry (NIMF): In this scheme the node initiates the movement proactively. The ferries move around the deployment area to communicate with other nodes based on known routing, while the nodes move close to ferries according to the known routes in order to communicate with the ferry. The node has four operation modes (WORKING, GO-TO-FERRY, SEND/RECEIVE, and GO-TO-WORK). Figure 2.2 and Figure 2.3 show the transition diagram for nodes and the operations in NIMF.

- Ferry Initiated Message Ferry (FIMF): When a node wants to communicate with some other node, it sends a service request to a certain ferry using long range radio. After the ferry receives this request, it will adjust its trajectory to meet the node and communicate

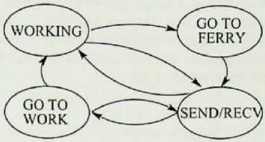

Figure 2.2: Mode transition diagram for nodes in NIMF [17].

1. Move according to a ferry route;
2. Broadcast `Hello` messages periodically;
3. On reception of an `Echo` message from a node:
   Exchange messages with the node;

Figure 2.3: Ferry operation in NIMF [17].

with it to exchange the messages using short range radio. The node has two operation modes (DISASSOCIATED and ASSOCIATED). At the beginning the node will be in the DISASSOCIATED mode. When the node sends a request message to the ferry it will enter the ASSOCIATED mode and waits for the interaction with the ferry. After the interaction, the node will return to the DISASSOCIATED mode.

2.1.4 Probabilistic Routing

PROPHET is a probabilistic routing protocol which uses a history of encounters and transitivity in order to determine future contact probabilities [32]. PROPHET is used for intermittently connected networks where there is no guarantee that a fully connected path between source and destination exists at any time.

The PROPHET algorithm relies on calculation of delivery predictability in order to forward messages to the most reliable node of which current knowledge exists. The calculated probability is used to decide if a certain node is reliable to forward messages to. This probability is calculated using a history of encounters, a data aging mechanism, and the transitivity property of network connections.

Whenever a node is encountered, the probability metric of node A encountering B is updated. As such, a node that is encountered more often has a higher delivery predictability than others. The probability of A encountering B can be calculated using (2.1). $P_{\text{encounter}}$ is an initialization constant with a value between 0 and 1.

$$P(A,B) = P(A,B)_{\text{old}} + (1 - P(A,B)_{\text{old}}) \cdot P_{\text{encounter}} \tag{2.1}$$

If a pair of nodes does not encounter each other during a time interval, they are less likely to be good forwarders of messages to each other and thus the delivery predictability values must be

reduced. Such an aging of knowledge is very important in order to constantly keep the most likely to be successful routes to be the ones that are selected. The aged delivery predictability values for node A encountering B can be updated according to (2.2). The parameter γ is the aging constant with values between 0 and 1, and t is the number of time units that have elapsed since the last time the metric was aged.

$$P(A,B) = P(A,B)_{\text{old}} * \gamma^t \tag{2.2}$$

There is also a transitive property in delivery predictability, which is based on the observation that if node A frequently encounters node B and node B frequently encounters node C, then node B probably is a good node to forward messages destined for node C from A. This transitive probability may be calculated using (2.3). The parameter β in (2.3) is a scaling constant with values between 0 and 1 that controls the impact of the transitivity property on the delivery predictability.

$$P(A,C) = P(A,C)_{\text{old}} + [1 - P(A,C)_{\text{old}}] \cdot P(A,B) \cdot P(B,C) \cdot \beta \tag{2.3}$$

When two nodes meet, they exchange the delivery predictability information they currently have stored. This information is used to update the estimated delivery predictability to the destination. A message is transferred to the other node if the delivery predictability of the destination of the message is higher at the other node.

The values for $P_{\text{encounter}}$, γ and β are set to 0.75, 0.98 and 0.25 respectively according to the optimal values suggested by the authors of the PROPHET protocol [32, 35].

2.1.5 MaxProp: Routing for Vehicle-Based Disruption-Tolerant Networks

The MaxProp routing protocol creates two schedules; one schedule for transmitted packets and the other for packets to be dropped. These schedules are based on the path likelihoods according to historical data and other mechanisms such as: acknowledgments that are propagated to the whole network, and not only to the source node, a head-start for new packets since MaxProp assigns a higher priority to new packets, and lists of previous intermediaries to prevent data from propagating twice to the same node [12]. MaxProp uses knowledge from previous encounters to calculate the shortest path to the destination. Each node has a vector called delivery likelihood, which is obtained using incremental averaging. When two nodes encounter each other, they exchange these vectors.

2.2 Mobility Models and Scenarios

Mobile systems are characterized by the movement of their devices. The movement parameters are speed, direction, and rate of change, which affect the protocols that support mobility. In this section we present some of the mobility models.

2.2.1 Random Waypoint Mobility Model

The random waypoint (RWP) model is a random mobility model used for testing and evaluation in mobile communication systems and it is the most common model used to evaluate routing protocols such as DSR [36] and AODV [37]. The mobility model is designed to provide possible movement patterns of mobile network nodes, and how their location, velocity and acceleration may change over time. As shown in Figure 2.4, the mobile nodes move randomly and freely without restrictions. The destination, speed and direction of each node is chosen randomly and independent of other nodes in the network. As such, the trajectory changes that occur in this model are random and no particular mobility pattern can be deciphered. This model is a good benchmark for worst-case mobile network performance since most DTN deployments are in scenarios where the mobility of nodes can be predicted with at least some probability.

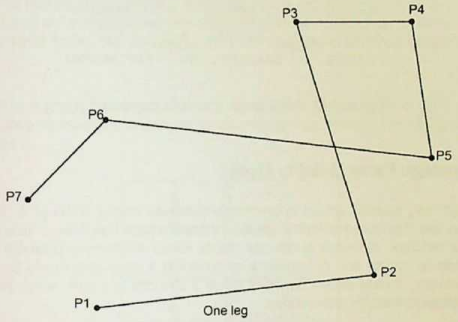

Figure 2.4: Random waypoint model [38].

Figure 2.4 shows an example. Nodes move from waypoint P_i to waypoint P_{i+1} with a speed of v_i. Each node waits a random pause time τ_i at each waypoint before it moves to the next waypoint.

2.2.2 Zebra Mobility Model

Zebra Mobility models are based on zebra's movement habit, explained in [1]. Each zebra has its own movement that can be classified into three states: grazing, graze-walking, and fast movement. At the beginning, zebras move in random waypoint to search for a grazing area, while searching for grazing area, zebras enter the fast movement state, in which they move faster and across longer distances following the random waypoint model. Once the zebras found the grazing area, they enter the grazing state in which they spent most of their time and they move slower with high turning angles, at other times they enter graze-walking state, in which they move a bit faster than in grazing state and across shorter distances between each movement with smaller turning angels. The movement patten within the grazing and the

grazing-walking states is modeled based on a real observation patterns [1]. Each zebra visits a watering hole by maintaining a timer that causes the zebra to move directly to a watering hole. After that a zebra either enters the fast movement state to search for another grazing area or it enters the grazing state.

Figure 2.5 shows the three states of the zebra movement, where the ($speed_g$, $speed_{gw}$, and $speed_{fm}$) represent the speed distributions in the three states (grazing, graze-walking,fast movement), and (P_{in}, P_{out}) represent the transition probabilities. The speed distributions and the transition probabilities are derived based on a feedback from biologist.

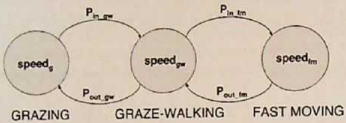

Figure 2.5: Three modes of zebra movement [1].

2.2.3 Message Ferry Mobility Model

The message ferry mobility model is commonly deployed across DTNs [17]. In this model, sensor nodes are distributed across a space in a pattern such that it maximizes the coverage of the sensor network. Message ferries are mobile nodes which move between these sensor nodes in order to collect and deliver data by providing a relay opportunity to static nodes. In such scenarios, mobile nodes normally follow a deterministic path which maximizes the connection opportunities for static nodes.

The route taken by the ferry is deployment dependent. In our case we chose to develop a message ferry model that maximizes the possibilities of connection, in case the static nodes are randomly distributed. As such, the message ferry topology was based on the Manhattan model's grid structure, as shown Figure 2.6. The static nodes were distributed randomly across the field, while the mobile ferry nodes were restricted to traveling on paths similar to the Manhattan model at a constant velocity of $5\ \mathrm{m/s}$.

2.2.4 Manhattan Mobility Model

The Manhattan mobility model uses a grid road topology and it is mainly used for the movement in urban areas. This mobility model is based on the observed characteristics of road traffic in cities, especially in Manhattan. In the Manhattan mobility model, mobile nodes move in horizontal or vertical streets. The map in Figure 2.7 shows an example of how the mobile nodes move in the Manhattan mobility model. Each street on the map has two lanes for both directions, north and south or east and west. The Manhattan model employs a probabilistic approach in the selection of nodes' movements. Each node moves on the horizontal or vertical lanes, once a node arrives at an intersection, it has three options: to continue strait on the same direction with a probability of 0.5 or to turn right or left with a probability of 0.25

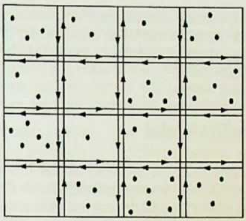

Figure 2.6: The message ferry mobility model; each line represents a single-lane in which the mobile nodes may move. The arrows represent the direction in which a mobile node is allowed to move. The static nodes, represented by the black dots, are distributed randomly across the field.

each [39]. This model forms a good basis for testing the performance of DTN deployments where the mobile nodes move in a highly structured fashion, thereby increasing the likelihood of connectivity.

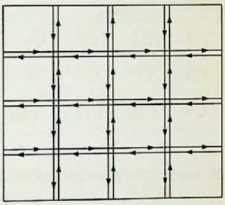

Figure 2.7: Map used in Manhattan mobility model; each line represents a single-lane in which the nodes may move. The arrows represent the direction in which a node is allowed to move [39].

2.2.5 Human Mobility (Orlando) Model

The Orlando mobility model is based on the actual data gathered from human mobility [40]. The Disney World traces were obtained from 40 volunteers who spent their thanksgiving or Christmas holidays in Disney World. Only the track logs from the inside of the theme parks are used for the study; the participants mainly walked in the parks and occasionally rode trolleys. Each participant was provided with GPS receivers that take reading of their current positions every 10 seconds and record them into a daily track log. Since GPS signals cannot be recorded indoors, such holes in the data are treated as the participant not having moved

between two locations for an extended period, and then moving at a rapid pace. The Orlando model provides an insight into human mobility in a structured environment and as such is a good basis to study the effects of human mobility on the performance of energy saving scheme in disruption tolerant networks.

2.2.6 Community Mobility Model

Lindgren et al. [32] designed a mobility model, which is called a community model, in order to evaluate the behavior of the PROPHET routing protocol. Since PROPHET is based on making predictions depending on the movement of the nodes, they preferred to use a more realistic mobility model compared to RWP model. This model has a 3000 m $\times$ 1500 m area divided into 12 subareas as shown in Figure 2.8. The model has 11 communities (C1-C11) and one gathering place (G). In each community there is a number of mobile nodes and one fixed node that works as a gateway. Each node has one home community that it visits more likely than other places. The mobility scenario works as follows: nodes select a destination and a speed, and move there. After reaching the destination, nodes pause for a while and then they select a new destination and speed. The destinations are selected as follows: if a node is at home, the node will go to the gathering place with a higher probability, but it might also go to other places. However, if the node is away from its home, it is likely to return to its home as shown in Table 6.1.

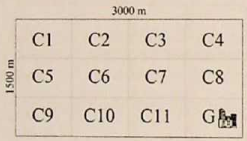

Figure 2.8: Destination selection probabilities [32].

From /To	Home	Gathering place	Elsewhere
Home	-	0.8	0.2
Elsewhere	0.9	-	0.1

Table 2.1: Destination selection probabilities [32].

2.3 Summary

In this chapter, five different routing protocols for intermittently connected networks are discussed. In source routing protocols, the source node determines the routing path based on the topology of the network. Epidemic routing protocols distribute messages to random hosts through the connected portions of the network through carriers. These carriers will distribute messages to other portions of the network when coming into contact through node mobility.

The message ferry protocol utilizes some mobile nodes to establish communication and to take the responsibility of carrying data between the nodes while they are moving around the deployment area. In probabilistic routing, nodes move in predictable manner (if the node visited a location several times before, it is likely to visit this location again). The MaxProp routing protocol creates two schedules; the first one for transmitted packets and the second one for packets to be dropped based on the path likelihoods according to historical data.

We also present different mobility models. The random waypoint model is the most widely used model to evaluate routing protocols for ad-hoc networks. It is a pure random model, in which the destination, speed and direction of each node is chosen randomly and independent of other nodes in the network. When a node reaches its destination, it waits a random pause time before moving to a new destination. The Zebra mobility model is designed based on zebras movement habit, and the model is classified into three states, grazing, graze-walking, and fast movement. The message ferry model depends on ferries which move around the deployed area in a deterministic path to collect messages and to deliver them to their destinations or to other ferries. The Manhattan mobility model uses a grid road topology and is mainly used for the movement in urban areas. In the Manhattan mobility model, mobile nodes move in horizontal or vertical streets. The human mobility model (Orlando) is based on actual data gathered from humans moving in a theme park. The community model was designed to evaluate the PROPHET routing protocol. Each node has one home community that it visits more likely than other places.

3 Power Management Schemes for Disruption Tolerant Networks

Power management schemes generally aim at saving maximum energy in the network to prolong the network life time. At the same time, they are trying to keep connectivity in the network to provide reasonable data delivery and delay. There have been many research efforts developing energy conservation schemes in wireless sensor networks [41]. These efforts include topology control schemes that exploit the network redundancy to save energy [42] and data reduction schemes [43]. Other efforts include energy management schemes that can be integrated with Media Access Control (MAC) protocol [44, 45, 46, 47, 48, 49, 50, 51] or implemented as independent sleep/wakeup protocols on top of MAC protocols [52, 53, 54, 55, 56, 57]. MAC protocols are motivated by the observation that transmissions of multiple nodes in a wireless network may interfere with each other. To avoid this interference, only two nodes can communicate with each other at any point in time. Therefore, significant energy can be saved if a node sleeps while others communicate without affecting network performance. MAC protocols propose mechanisms to increase sleeping time based on the traffic in the neighborhood. However, all the aforementioned protocols are useful in dense networks rather than DTNs (sparse networks).

This chapter describes several power management protocols that are implemented on top of the MAC layer for DTNs and it discusses their performance evaluation.

3.1 Oracles and Knowledge-Based Mechanisms

This power management mechanism based on knowledge of future contacts assumes that nodes have synchronized clocks. The scheme has two time intervals, contact time, when two nodes can communicate with each other, and waiting time, in which the node keeps waiting until the next contact. Jun et al. [58] used oracles to model the knowledge of the contacts (more details about these oracles can be found in [11]) as follows:

- **Mean Oracle**: provides information about the mean of contact time and waiting time durations between every pair of contacts.
- **Variance Oracle**: provides information about the variance of contact time and waiting time durations between every pair of contacts.
- **Contact Oracle**: provides precise information about the start time and the end time for every pair of contacts.

The mechanism uses these oracles based on the amount of knowledge it needs. The authors introduced three categories of knowledge. First, zero knowledge that does not use any oracle. Second, partial knowledge that uses either mean or both mean and variance oracles (statistic information). Finally, complete knowledge that uses the contact oracle (uses precise time of contacts and not statistic information).

The power management framework allows a node to be in one of three modes: dormant, search, and contact mode. In the dormant mode, the node does not expect any contact, therefore, it sleeps. The node wakes up frequently to discover contacts in the searching mode. In the contact mode, the node will stay awake to start communication with other nodes. The rest of this section presents the three mechanisms of power management based on the knowledge information categories.

3.1.1 Power Management with Complete Knowledge

In this scheme, nodes have complete knowledge about future contacts. A node can communicate with only one node or multiple nodes. When a node communicates with only one node, it wakes up at the beginning of the contact and sleeps at the end of the contact. If the node communicates with multiple nodes, it wakes up at the start time for the first contact and sleeps at the end time for the last contact as shown in Figure 3.1.

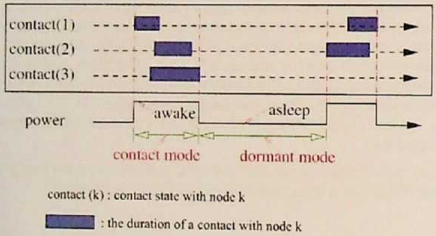

Figure 3.1: Transition among power management modes after aggregating multiple contact states in the complete knowledge class [58].

3.1.2 Power Management with Zero Knowledge

In zero knowledge scheme, a node has to discover contacts since it has no information when a contact starts and ends. A node broadcasts periodic messages called beacons to discover contacts. When a node receives a beacon from another node that is not in contact with, the node will consider this beacon from the new contact node and start to communicate with it. After that, the node will stay listening to the beacons from the same node. In case the node does not receive a number of consecutive beacons, it assumes that the contact is terminated [58].

A node has three time periods: First, the beacon window period in which the node chooses randomly a waiting time to send its own beacon. Second, the post-window space, which is a

small time after the beacon window to enable the node to listen to the beacons beyond the beacon window. The last one is the wake up period that represents the time between the beginning of two consecutive beacon windows.

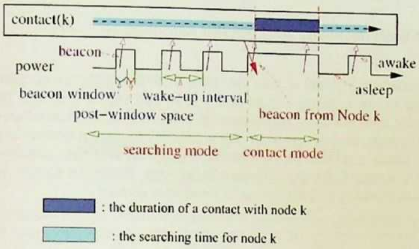

Figure 3.2: Transition among power management modes when a node has a contact with only one node [58].

Figure 3.2 shows the case when the node has contact with only one node. At the beginning the node will be in the searching mode. Within the beacon window, the node will choose a random time to broadcast the beacon. If the node does not receive any beacon, it will go to sleep at the end of the post-window space and keep sleeping until the next beacon window. However, if the node receives a beacon, it will switch to the contact mode and stay in that mode until it can not receive a consecutive number of beacons, after that it will go back to the search mode.

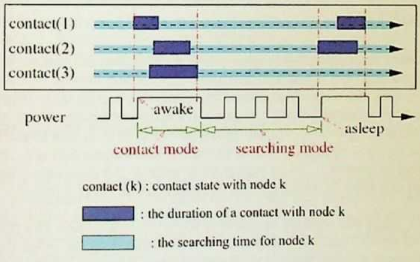

Figure 3.3: Transition among power management modes after aggregating multiple contact states in the zero knowledge class [58].

Figure 3.3 shows the case when a node has a contact with multiple nodes. The node alternates between sleeping and wake up within the search mode in case no contact is available. When a node receives a beacon from any other node, it will enter the contact mode. After the

connection is terminated, the node will check whether it has any other contact to stay in the contact mode, otherwise, it will go back to the search mode.

3.1.3 Power Management with Partial Knowledge

In the partial knowledge scheme, a node maintains statistics about the contact and the waiting time durations for the contacts. Therefore, a node can expect a contact based on these statistics. The basic idea is that a node wakes up to search for contacts when the probability to find a contact is high, and sleeps when the probability to have a contact is low. However, in this approach, there is a trade off between saving energy and data delivery performance. This mechanism is similar to the one with zero knowledge. Within the search mode, the node alternates between sleeping and waking up to discover a contact.

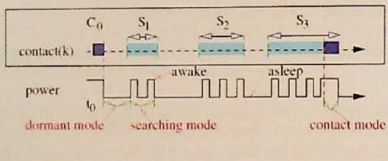

Figure 3.4: Transition among power management modes when a node has a contacts with only one node, node k [58].

In Figure 3.4, a node is in contact with node k and it terminates the contact at time t_0. At t_0, the node enters the dormant mode and estimates a searching interval S_1. At the beginning of S_1, the node enters the searching mode and periodically wakes up to discover a contact. If it does not discover a contact, it goes to sleep in the dormant mode at the end of S_1 and it estimates the next time interval to search. Since its trial during S_1 has failed, it may select a longer period of time $S_2 > S_1$ to search for a contact. If it fails again during S_2, it may select an even longer period of time $S_3 > S_2$ to search for a contact. If it discovers a contact, it enters the contact mode and repeats the procedure at the end of the contact [58].

The case when a node has multiple contacts is shown in Figure 3.5. The node estimates a searching interval for its neighbor nodes and enters dormant mode. After that it enters the searching mode when the first searching interval starts. The node will stay in the searching mode in case another searching intervals starts. Otherwise, it returns back to the dormant mode. Within the searching mode, if the node receives a beacon from any node, it enters the contact mode and stays in this mode as long as it receives beacons from other nodes. After the node finishes its contact with any node, it will check whether it has other contacts to stay in the contact mode. Then, it will check if it has an active searching interval to go back to the search mode, otherwise, it will go directly to the dormant mode.

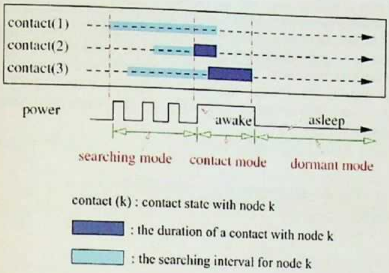

Figure 3.5: Transition among power management modes after aggregating multiple contact states in the partial knowledge class [58].

3.1.4 Performance Evaluation

Jun et al. [58] implemented the power management mechanisms using the knowledge oracles in ns-2 in order to evaluate their performance depending on four metrics: normalized energy consumption, data delivery, delivery delay, and energy consumption (average energy consumption to deliver a message). They used a network scenario consisting of 20 nodes distributed over 5 $\mathrm{km} \times 5\ \mathrm{km}$. The nodes move according to the random waypoint model with node speed between 5 $\mathrm{m/s}$ and 10 $\mathrm{m/s}$ and the pause time exponentially distributed with average 30 seconds. The transmission range for the wireless radio is 250 m and the bandwidth 2 $\mathrm{Mb/s}$. They also evaluated the mechanisms in another scenario that consists of 9 stationary nodes and one mobile node moves in a deterministic path to achieve communication with the stationary nodes. Simulation results show that with power management mechanisms, the network consumes $(10 - 50)\%$ of the energy without power management mechanisms.

3.2 Hierarchical Power Management

The hierarchical power management scheme is based on the previous work and tries to minimize the power consumed to search for other nodes within the searching mode. Jun et al. [59] use an additional low power radio to discover other nodes and awake the high power radio on-demand to undertake the data transmission. There are four variations of using the two wireless radios to discover contacts:

- **Continuous aware mechanism (CAM)**: uses only the high power radio that stays awake to search for other nodes. Therefore, no power saving is achieved in this scheme.
- **Power saving mechanism (PSM)**: uses only the high power radio that alternates between sleeping and waking up to discover nodes and save energy.

- **Short range radio dependent power saving mechanism (SPSM)**: uses both radios, the low power radio alternates between sleeping and waking up to discover contacts. When the low power radio discovers a contact, it will wake up the high power radio to undertake the data transmission. The high power radio stays awake as long as it receives beacons within the contact mode. When all contacts are terminated, the high power radio will return back to the dormant mode while the low power radio keeps searching for contacts as shown in Figure 3.6.

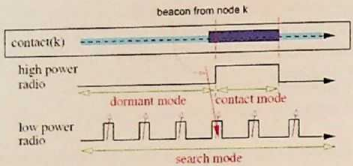

Figure 3.6: Transition between power management modes when a node has contacts with only one node k using SPSM [59].

- **Generalized power saving mechanism (GPSM)**: each radio has its own wake up interval. Therefore, both radios search for contacts. However, the wake up interval of the high power radio is larger than the wake up interval of the low power radio, which means that the low power radio searches more frequently for contacts as shown in Figure 3.7.

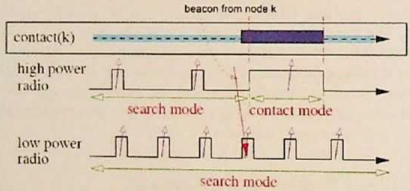

Figure 3.7: Transition between power management modes when a node has contacts with only one node k using GPSM [59].

3.2.1 Performance Evaluation

To evaluate the performance of the hierarchical power management mechanisms, the authors implemented these mechanisms in ns-2. They used two different mobility models (random waypoint (RWP), message ferry (MF)) and a setup consisting of 20 nodes distributed over an area of size 5 km $\times$ 5 km. In case of the MF mobile model, the network consists of 12 stationary nodes placed sparsely in a 5 km $\times$ 5 km grid area, and 8 mobile nodes called ferries moving

around the stationary nodes. The difference between the two models is that nodes encounter each other at much longer distances in the RWP model than in the MF model. The authors conclude that PSM works better than SPSM with the RWP model while SPSM works better than PSM with the MF model. The authors also show that GPSM achieves best performance among the four variations.

3.3 An Energy-Efficient Architecture for DTN Throwboxes

In this work, the authors present a hardware and software architecture for energy efficient throwboxes in DTNs. This architecture uses a multi-tiered, multi-radio, scalable, solar powered platform [60].

Throwboxes are stationary battery powered nodes with a radio interface, and a storage device. These nodes act as a router that enable mobile nodes to communicate with each other when they pass by the same location (throwbox) at different times. In previous work [61], the authors focused on algorithms that place throwboxes in locations that maximize network performance and they found that even a small number of throwboxes can significantly increase the delivery rate in DTNs. However, since throwboxes are constrained by power consumption, the authors presented this work to save energy without affecting the network performance and to address the power consumption problem. Banerjee et al. [60] found that the primary source of overhead is the energy cost of neighbor discovery. They show that using an 802.11 radio to search for contacts consumes 99.5% of the total energy.

Banerjee et al. [60] propose a power management architecture in DTNs that provides efficient neighbor discovery by detecting the mobility of nodes with a minimum cost and predicting the opportunity of each possible contact. Throwbox uses these predictions to limit the number of communication opportunities to save energy. This architecture pairs a tier-1 platform (a PDA-like Stargate and 802.11 radio) with a low-power tier-0 platform (a Mote and XTend radio). The XTend radio is a long-range, low-bitrate radio for neighbor discovery. The authors show that this coupling of the XTend radio and the low power mote reduces the total energy cost of the throwbox platform. The tier-0 platform searches for other nodes by listening to the beacons while tier-1 stays in a sleep state. If a node decides to take the transfer opportunity, tier-0 will wakeup tier-1 to undertake the data transmission. The tier-1 platform returns to a sleep state after the contact end.

3.3.1 Mobility Prediction Engine

The authors study the use of throwboxes in a vehicular network, where the mobile nodes have plentiful energy sources. They model the movement pattern of the mobile nodes as a Markovian process. They assume the location of a node at certain time t_0 is dependent only on its location at time t_{0-1}. This model is accurate for predictable and semi-predictable movement patterns such as vehicular networks movement.

The prediction algorithm is illustrated in Figure 3.8, it models the problem as a virtual square of width 2r, where r is the radius of the long-range radio. The throwbox is located at the center of the square. The large square is divided into square cells numbered from 0 to k. The algorithm makes use of a probability transition matrix T for mobile nodes in the network. Entry T_{ij} of

the matrix is the probability that a node will transition to cell j given that it is in cell i [60]. The prediction algorithm estimates:

- The probability that the mobile node n would be in any cell within the data transfer radio range after time ΔT, where ΔT is the transition time that required to wakeup tier-1 and start transferring application data (order of seconds).
- The predicted time when the node will be in range of the data transfer radio and the amount of data it is likely to transfer.

Figure 3.8 explains this process. At time t_0, the throwbox receives a beacon from cell A. The prediction engine estimates D_1 the distance until the node is within 802.11 range, and D_2 the distance for which the node stays within that range. If the predicted length of time until the mobile node reaches the range of the data radio (D_1/v) is greater than the transition time to wakeup tier-1, then the mobile node is ignored. Otherwise, the throwbox calculates the probability that the node will enter the range of the data radio (P_r).

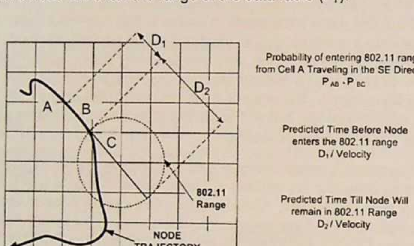

Figure 3.8: The figure depicts the working of the Mobility Prediction Engine [60].

3.3.2 Performance Evaluation

The authors of [60] evaluated the throwbox system through simulation and prototype experimentation. In their simulation, they placed three always-on throwboxes in UMassDieselNet [12] for three weeks changing batteries manually. They divided the area around each throwbox (1 $\mathrm{km} \times 1\ \mathrm{km}$) into 25 cells, each cell is $200\ \mathrm{m} \times 200\ \mathrm{m}$. These prototypes logged connection events on the 802.11b radio and the XTend radio and they fed the data into a Java-based simulator. They compared their results with three existing schemes: First, the Optimal (Dual platform) uses two radios with a perfect mobility prediction algorithm and an optimal scheduler. Second, the Power Saving Mode (PSM) [62] uses a single radio system in which the wireless interface periodically powers off to save energy. Finally, an adapted system from Wake-on-Wireless (WoW) [63] uses a second radio as a discovery radio. According to Banerjee et al. [60], their energy-efficient architecture reduces the power consumption of the throwbox

from 2500 mW to 80 mW, while delivering almost as many packets, and it saves energy better than PSM and WoW systems.

In their prototype experimentation, Banerjee et al. [60] deployed a two platform, two radios prototype with a power constraint of 80 mW, using the mobility prediction algorithm described before. The system was equipped with solar panels 220 cm^2 in area and a 1 Ah battery that was 20% full. The box was deployed in the UMassDieselNet for a day and it logged the battery capacity remaining in the battery as a function of time [60]. The authors show that during the day the throwbox stores excess energy and during night time it spends the excess accumulated energy. They determined through this experiment that the solar panels produce on an average power of 65 mW over 24 hours which is about 15 mW less than that the amount necessary to make the throwbox last perpetually. However, they mentioned that throwboxes can be made to run perpetually through the use of a slightly larger solar cell area (270 cm^2) since the amount of energy produced will vary from day to day depending on the intensity of the sun.

3.4 Context Aware Power Management Scheme

The context aware power management scheme (CAPM) is an asynchronous power management scheme that has an adaptive on period feature to achieve high data delivery and low delivery latency. Each node works on its own wake-up schedule independently. Figure 5.1 shows the sleeping pattern of CAPM that has a fixed duty cycle. Each duty cycle has two periods, wake up and sleep periods. Within this duty cycle each node wakes up for a fixed or adaptive period and sleeps for the rest of the time. The CAPM scheme includes two operations, neighbor discovery and data delivery.

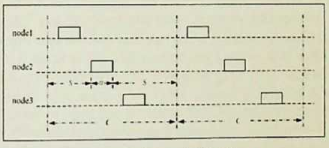

Figure 3.9: Random wakeup with fixed duty cycle [64].

3.4.1 Neighbor Discovery

In sparse networks, when a node has a message to be sent, it first needs to search for a neighbor (next hop) to send the message. This neighbor will forward the message to its destination. To find neighbors, CAPM assumes that each node (when the node wakes up) periodically broadcasts a beacon that includes information about its node identifier and the time duration that the node will stay active. The wake up node piggybacks a delivery notification extension to its beacon message in case it has data for delivery. This notification delivery provides information about the identifiers of the destination nodes. When an active node receives a delivery notification, it will send a delivery accept message to the source node.

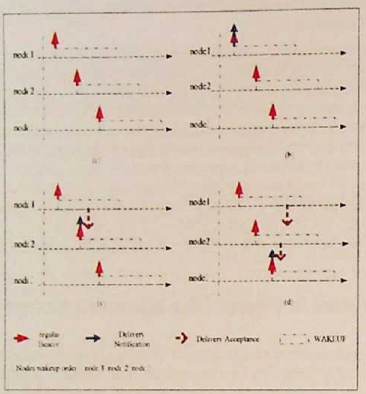

Figure 3.10: CAPM neighbor discovery [64].

Figure 3.10 explains the neighbor discovery procedure. In Figure 3.10(a) all nodes broadcast a normal beacon based on their wake up time since they have no messages for delivery. In Figure 3.10(b) node 1 broadcasts a beacon with attached delivery notification since it has data for delivery. When node 2 and node 3 wake up, they will send a regular beacon that will be received by node 1. After that, node 1 will deliver its data to node 2 and 3. In Figure 3.10(c) node 2 broadcasts a beacon with a piggybacked delivery notification extension because it has data for delivery. Since node 1 is active, it will send an accept delivery notification to node 2. When node 2 received this accept notification, it will start to send the data to node 1. In Figure 3.10(d) node 3 broadcast a beacon that includes a delivery notification to notify its neighbors that it has data for delivery. When node 1 and node 2 receive this beacon they will send an accept notification delivery to node 3. After that node 3 will send the stored messages to both nodes 1 and 2.

Figure 3.11 shows how each node maintains a neighbor list after receiving the beacon messages from its neighbors. Each node has a fixed on period (W). When node 1 receives a beacon from node 2, it will compute the remaining on time ($t_3 + W - t_4$) and send a delivery accept message to node 2. After that node 2 will insert the information provided by node 1 into its neighbor list. In a similar way, when node 2 receives node 3's regular beacon at time t_8, node 2 again updates its neighbor list as shown in Figure 3.11. Figure 3.11 also shows how node 1 updates its neighbor list upon receiving a beacon from node 2 and 3 [64].

3.4.2 Data Delivery

There are four scenarios for data delivery in CAPM as shown in Figure 3.12:

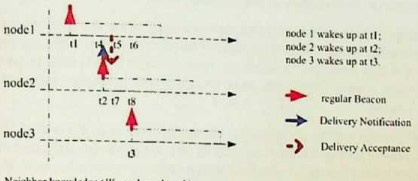

Neighbor knowledge (W : wakeup length):

node1

Node Id	Remaining Active Time	Time Stamp
2	W	t4
3	W	t6

node2

Node Id	Remaining Active Time	Time Stamp
1	W - (t5 - t1)	t7
3	W	t8

Figure 3.11: CAPM construction of neighbor list [64].

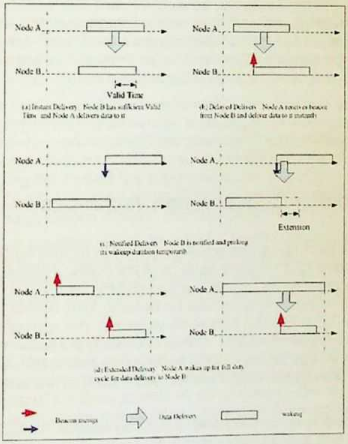

Figure 3.12: CAPM data delivery [64].

1. Sending and receiving nodes are active as shown in Figure 3.12(a). The sender node sends the packet immediately to the receiver node.

2. The sending node is active and has delivery data while the receiving node is inactive. When the sender node receives a regular beacon from the wake up receiving node, it will check if it has data for this wake up node. In case it finds data to be delivered to the wake up node, it will immediately send this data with a random back-off time as shown in Figure 3.12(b).

3. The sending node wakes up while the receiving node is at the end of its active time. In this case, the receiving node will extend its active time to be sufficient to receive all the data after receiving a beacon attached with a delivery notification from the sending node as shown in Figure 3.12(c).

4. The sending node and the receiving node do not have an overlapping period within the duty cycle. If the sending node has delivery data and can not send it after a certain number of duty cycles passed (K), CAPM allows the sending node to wake up for one whole duty cycle as shown in Figure 3.12(d) to find a next hop node.

3.4.3 Performance Evaluation

Xi and Chuah [64] implemented CAPM in ns-2 to evaluate its performance depending on four metrics: data delivery, normalized energy consumption, end-to-end delay, and average number of hops it takes for message delivery. They used a network scenario consisting of 40 nodes distributed randomly over 1 $\mathrm{km} \times 1\ \mathrm{km}$. These nodes move according to the random waypoint model with a maximum speed of 5 $\mathrm{m/s}$ and pause times of 10 seconds. The transmission range of the wireless radio is 250 m and the bandwidth is 2 $\mathrm{Mb/s}$.

At the beginning, they evaluated the performance of PROPHET without applying CAPM, after that they evaluated the same routing protocol with CAPM to illustrate the impact of CAPM. As a result, based on their simulations, they said that CAPM provides energy saving up to 85%.

3.5 Other Energy Conservation Techniques

Most DTN algorithms focus on garnering energy savings by utilizing schemes that take advantage of radio characteristics or mobility patterns of the nodes. However, the authors of [65] focus on deriving energy savings by implementing lossless adaptations of compression algorithms on the source nodes generating data for delivery. They develop a compression algorithm named Sensor LZW (S-LZW) and some variants of this approach that may be better applicable in certain specific conditions. In order to evaluate the performance of their methodology, they focus on energy savings as the performance metric and discover that local and downstream energy savings can reduce overall consumption up to a factor of 4.5 times across the network.

Since they expect there to be certain patterns that may develop in mobility of the nodes over time, the authors of [65] also develop methods for preconditioning the data so that it is best suitable for compression while considering data from every node as equally important. For such data, preconditioning using the proposed transforms can reduce energy consumption up to about 3 times compared with the baseline performance.

3.5.1 Compression Techniques

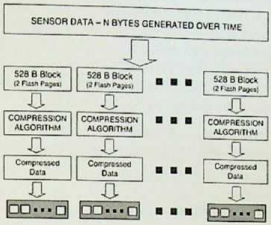

Figure 3.13: Overview of compression and transmission technique. The data is separated into smaller blocks which are compressed and then transmitted. Packets within a shaded region are dependent on prior packets to be decoded, however, each independent shaded region is independent of the others [65].

The basic compression algorithm proposed by the authors utilizes the LZW lossless dictionary compression method. This method provides an initial dictionary with 256 entries for all 8-bit characters and since both the sender and receiver have the initial dictionary, new entries are created based on existing entries without any additional transmission overhead. The S-LZW algorithm separates the data stream into smaller blocks with a bias towards small block sizes in order to minimize data loss. An overview of the compression and transmission scheme can be seen in Fig 3.13.

The S-LZW algorithm uses 512 dictionary entries and block sizes of 4 pages or less for compressing the data. It was discovered by experimentation that the compression ratio increases with dictionary size for large amounts of data but it is most efficient when data is compressed in blocks of 2 pages. Using this method, the authors were able to achieve a compression ratio improvement of 25.5%, 12.9%, 4.6% and 3.3% for SensorScope (SS), Great Duck Island (GDI), Zebranet (ZNet) and Calgary Corpus (Calgeo) datasets respectively.

Since most sensor data is repetitive over short intervals, the S-LZW algorithm can be further optimized with an additional mini-cache (S-LZW-MC) to the dictionary, which maintains a list of most recently used and created entries. Experimentation showed that a mini-cache size of 32 or 54 entries performs the best on an average, with only about 4.5% computational overhead for the S-LZW algorithm.

Local energy evaluations using the S-LZW-MC32 variant exhibited an average improvement of energy saving of about 1.7 times over using no compression to transmit the data. Since overall transmitted data was now smaller in size, there were significant downstream energy savings as well, an average of about 1.8 times against no compression. The results obtained here argue strongly for using compression even if there is no energy consumption benefit apparent on the compressing node.

The authors note that even though the S-LZW-MC variant takes advantage of local patterns in sensor data, these patterns could be increased if reversible transforms are used before applying compression techniques. As such, performance of the Burrows-Wheeler Transform (BWT)

and the Structured Transpose with Run Length Encoding (RLE-ST) is also tested. The S-LZW-MC-BWT variant shows an average energy consumption improvement of nearly 2 times for long range radios and 3 times for mid range radios on average, while there is a saving of approximately 10.7% at each hop in short range radio transmissions. The S-LZW-MC-RLE-ST variant exhibits local and downstream savings of nearly 3 times for the mid range radio. When reliability and replication are taken into account the S-LZW algorithm still appears to perform quite well. In case of considering reliability higher energy savings are achieved over a greater number of hops with lower delivery ratios. Replication provides a similar result since the higher the replication factor, the more the energy saving at each hop.

The authors demonstrate that using compression techniques can greatly reduce energy consumption in DTNs and networks with poor reliability tend to benefit even more.

3.5.2 Performance Evaluation

In order to have results that reflect real world performance, the compression algorithms proposed in the paper were tested upon datasets derived from SensorScope (SS), Great Duck Island (GDI), Zebranet (ZNet) and Calgary Corpus (Calgeo) field deployments. Using this wide spread of data allows them to test energy savings as a result of compression on indoor and outdoor stationary and mobile networks.

While performing their evaluations and calculations of local and downstream energy consumption 100% delivery reliability was assumed by the authors. However, as a special case they also investigate effects of packet loss, retransmission and replication in DTNs.

All experiments were performed on a TI MSP430 $\times$ 1611 microcontroller with 10 kB of RAM and 48 kB of flash memory. Running at a clock speed of 4 MHz and consuming 5.2 mW, this microcontroller is representative of actual sensor node deployments and thereby provides for fair comparisons. Since the evaluated networks are assumed to be DTNs, all data from the chosen datasets is stored in flash until enough is available to compress. Some of the datasets contain special headers, which are stripped for the purpose of this work since only sensor readings are stored and compressed on the nodes during the experiments. Additionally, a 0.5 MB flash module with 264 Byte pages that consumes 512 $\mu\mathrm{J}$ to write and 66 $\mu\mathrm{J}$ to read is utilized to store the test data before it is read one page at a time, compressed and then written back.

Furthermore, to obtain results which are truly representative of real world deployments, the authors use the Chipcon CC2420, CC1000 and MaxStream XTend radios for short, medium and long range testing. All data is divided into 64 byte packets that have a 10 byte header and source routing and epidemic routing is utilized for testing purposes.

3.6 Discussion and Comparison

In this section we compare the aforementioned power management schemes of DTNs that are described in this chapter. As shown in Table 3.1, Oracles, and CAPM schemes use a single radio (high power radio) while the other schemes use two radios (high and low power radios). Table 3.2 summarizes the routing protocols, mobility models, and evaluation environment for each scheme. As shown in Table 3.2, Oracles and Hierarchical schemes use the same routing

Table 3.1: Radios that are used in each power management scheme

Scheme	High Power Radio (HPR)	Data Rate (HPR)	Low Power Radio (LPR)	Data Rate (LPR)
Oracles	Lucent IEEE 802.11 WaveLAN PC Card	2 Mbps	-	-
Hierarchical	Lucent IEEE 802.11 WaveLAN PC Card	2 Mbps	Chipcon CC1000	76.8 Kbps
Throwbox	PDA-like Stargate and IEEE 802.11 Radio	2 Mbps	Mote and XTend (Low Power Mode)	115.2 Kbps
CAPM	Lucent IEEE 802.11 WaveLAN PC Card	2 Mbps	-	-

protocols and the same mobility scenarios for evaluation. The authors show that using two radios (high power and low power radios) instead of one single high power radio will save significant amount of power. However, in their first work (Oracles) the authors show that power management mechanisms consume around 50% of the energy expended when the network operates without power management scheme. Their second work (Hierarchical) shows that the energy comsuption could be reduced up to 73% from the energy expended when the network operates without power management scheme. The advantage of both schemes is that they can be used in more than one mobile scenario. However, the disadvantage of both schemes is that nodes need to be equipped with a GPS to achieve synchronization, and this increases the cost of the network.

The throwbox scheme uses the MaxProp routing protocol and a Markovian process mobility model. This scheme has an advantage since it can save power without sacrificing connection opportunities that affect the network performance. On the other hand, this scheme has many disadvantages such as a complex architecture in addition to the expensive cost since each node needs to be equipped with a GPS to achieve synchronization. It is efficient only for the DTN scenarios that allow using stationary nodes as well for predictable and semi-predictable movement patterns such as a Markovian process.

The CAPM scheme uses PROPHET with different mobile scenarios. The authors show that the CAPM scheme is adaptive to different network environments and can provide energy saving of up to $70-80\%$. The advantage of CAPM is that it is an asynchronous power management scheme that allows the nodes to work on their own wakeup schedule without time synchronization. The authors tested CAPM using the random waypoint and the Zebranet mobility models and they show that CAPM can give the same performance in both mobility scenarios. Then they compared the energy efficiency of the CAPM scheme and the PSM scheme described in the Hierarchical power management scheme and their results indicate that CAPM can achieve a 80% energy saving at low load and $70-80\%$ energy saving at high load and yet achieve a delivery ratio and an average delay that are comparable to the case without sleeping. However, the PSM scheme can only achieve a 40% energy saving.

Table 3.2: Comparison of the power management approaches

Scheme	Routing Protocol	Mobility Scenario	Evaluation Environment	Synch.
Oracles	Source Routing and Epidemic	Mobile Access Point (Message Ferry) and Random Waypoint (RWP)	Trace-driven Simulation	Yes
Hierarchical	Source Routing and Epidemic	Mobile Access Point (Message Ferry) and Random Waypoint (RWP)	Trace-driven Simulation	Yes
Throwbox	MaxProp	Markovian Process	Trace-driven Simulation and Prototype Experimentation	Yes
CAPM	PROPHET	Random Waypoint (RWP) and Zebranet Mobility Model [66]	Trace-driven Simulation	No

4 Underwater Acoustic Networks

Underwater sensor networks are attracting researchers interests. These networks are designed to enable applications ranging from oceanographic data collection, navigation, pollution monitoring, offshore exploration to disaster prevention, and tactical surveillance applications. These applications are based on underwater acoustic networking technology [2, 28, 29, 30]. In fact, the underwater channel is not conducive to use radio frequency (RF) for communication between sensor nodes since radio waves can only propagate through sea water at very low frequencies (30-300KHz).

Underwater acoustic networking presents some challenges to achieve real-time communications because of the unique characteristic of the acoustic channel such as: limited bandwidth capacity, propagation delay, low battery power. Underwater sensor networks are prone to disruptions and they often have sparse topology to achieve the largest area of coverage [2].

The energy costs in underwater acoustic networks are different from terrestrial radio-based networks. In acoustic networks, transmission power is significantly higher than receiving power [9]. Thus, to save energy and extend network lifetime and to obtain good performance it is essential to design networking schemes that are based upon utilizing the opportunities presented by the hostile deep-sea environment taking into account long and varying propagation delays, high and varying ambient noise.

4.1 Differences between Underwater Networks and Terrestrial Networks

The underwater acoustic channel is different from a terrestrial radio channel in many aspects:

- The transmission speed of acoustic signals in salty water is often bigger by 5 times than free space, which makes the propagation delay in an underwater channel significant.
- The attenuation of acoustic signals increases with frequency and range [67, 68, 69] which makes the bandwidth small. Based on the range, the bandwidth changes from hundred kHz (systems operating over several tens of meters) to a few kHz of bandwidth (systems operating over several tens of kilometers) [70, 71].
- Underwater networks are more expensive than terrestrial networks due to the complex underwater transceivers and the hardware protection.
- Underwater networks consume more power than terrestrial networks due to the underwater channel characteristics.

- Underwater nodes move with water current and the underwater channel varies with time depending on the location of the transmitter and receiver. Therefore, the fluctuation nature of the channel causes the received signals to be easily distorted.
- Underwater networks have much higher probability of bit error, which is caused by noise, multi-path and Doppler spread. Sometimes these networks have temporary loss of connectivity (shadow zone) due to the characteristics of the underwater channel.

4.2 Underwater Acoustic Propagation Model

The propagation model affects the performance of the underwater channel. The greatest changes in the acoustic models are caused by the attenuation model chosen. The rest of this section discusses the propagation delay and the attenuation models.

4.2.1 Propagation Delay

The underwater channel is affected by many factors such as: temperature, salinity, and depth. While most research efforts consider the speed of sound in water to be approximately 1500 $\mathrm{m/s}$, it is important to keep in mind the effects of mentioned factors on the speed of sound in water to have an accurate model since these factors may also be interdependent or varying across the ocean [72, 73].

MacKenzie et al. [72] provide an estimate of the speed of sound in water with an error in the range of approximately 0.070 $\mathrm{m/s}$ and they provide a general equation (4.1) that shows how temperature, salinity and depth affect the sound speed in water.

$$\begin{aligned} v &= 1448.96 + 4.591 \cdot T - 5.304 \times 10^{-2} \cdot T^2 + 2.374 \times 10^{-4} \cdot T^3 \\ &\quad + 1.340 \cdot (S - 35) + 1.630 \times 10^{-2} \cdot D + 1.675 \times 10^{-7} \cdot D^2 \\ &\quad - 1.025 \times 10^{-2} \cdot T \cdot (S - 35) - 7.139 \times 10^{-13} \cdot T \cdot D^3 \end{aligned} \tag{4.1}$$

- v = sound speed in $\mathrm{m/s}$
- T = temperature in degrees celsius
- S = salinity in parts per thousand (ppt)
- D = depth in meters

4.2.2 Propagation Loss

There are many factors that affect signal strength in underwater networks such as: absorption caused by magnesium sulphate and boric acid, particle motion, and geometrical spreading. Propagation loss is composed of geometrical spreading, attenuation, and the anomaly of propagation.

Geometrical spreading of a signal comes into effect when the acoustic intensity decreases exponentially with a certain range. Spherical spreading normally occurs when the transmission distance is large, while cylindrical spreading is common in short range underwater acoustic communications [74, 75]. In the deep sea sound channel a transition from the cylindrical to spherical transition also occurs such that if the range r is used between the sender and receiver, and r_N represents the transition range then

$$\begin{aligned} r < 2\text{km} &: r_N = 1000\text{m} \\ 2\text{km} \leq r < 10\text{km} &: r_N = 1200\text{m} \\ r \geq 10\text{km} &: r_N = 5000\text{m} \end{aligned} \tag{4.2}$$

The anomaly of propagation is nearly impossible to model. Therefore, the attenuation that occurs over a transmission range l for a signal frequency f spreading can be obtained from (4.3) where α is the absorption coefficient in dB/km, and k represents the geometrical spreading factor.

$$10 \log A(l, f) = k \cdot 10 \log l + l \cdot 10 \log \alpha \tag{4.3}$$

In general, the overall propagation loss can be obtained from (4.3) by substituting a suitable value of the geometrical spreading factor values shown in Table 4.1 based on the type of spreading that occurs and by using an appropriate attenuation model that provides the absorption coefficient α.

Table 4.1: Values for representing types of geometrical spreading via the geometrical spreading coefficient k [76].

	Spherical	Cylindrical	Practical
k	2	1	1.5

4.2.3 Absorption Coefficient

In underwater networks, attenuation by absorption occurs due to the conversion of acoustic energy into heat. This attenuation by absorption depends on frequency, at higher frequencies more energy is absorbed. At low frequencies, the absorption in seawater is so small that immense quantities of such water are required to create measurable losses of sound energy into heat which make the existing models inaccurate to calculate the results for low frequencies. Many mathematical models have over time improved the applicability and accuracy to obtain the signal absorption coefficient according to environmental and signal characteristics [77].

4.2.3.1 Thorp Model

The absorption coefficient can be obtained in dB/km from the Thorp model that only takes into consideration the effect of the frequency utilized and ignores the effect of relaxation frequencies, salinity, and acidity levels of the ocean [78, 79]. These limitations make (4.4) difficult to be utilized in general applications.

$$10\log\alpha = \frac{0.1f^2}{1+f^2} + \frac{40f^2}{4100+f^2} + 2.75\times10^{-4}\cdot f^2 + 0.003 \tag{4.4}$$

4.2.3.2 Fisher & Simmons Model

The Fisher & Simmons model is one of the most commonly used and referenced models [74, 80, 75]. This model takes into account the effect of temperature, depth, and it also introduces the effects of relaxation frequencies caused by boric acid and magnesium sulphate as shown in (4.5), where A_1, A_2, A_3 are functions of temperature and P_1, P_2, P_3 are functions of the constant equilibrium pressure. The values of P are represented in atm (the relationship between P and depth in meters is $P = D/10$) and f_1, f_2 are represented in Hz.

$$10\log\alpha = A_1P_1\frac{f_1f^2}{f_1^2+f^2} + A_2P_2\frac{f_2f^2}{f_2^2+f^2} + A_3P_3f^2 \tag{4.5}$$

$$\begin{aligned}
A_1 &= 1.03\times10^{-8} + 2.36\times10^{-10}\cdot T - 5.22\times10^{-12}\cdot T^2\\
A_2 &= 5.62\times10^{-8} + 7.52\times10^{-10}\cdot T\\
A_3 &= [55.9 - 2.37\cdot T + 4.77\times10^{-2}\cdot T^2 - 3.48\times10^{-4}\cdot T^3]\cdot10^{-15}\\
f_1 &= 1.32\times10^3(T+273.1)e^{\frac{-1700}{T+273.1}}\\
f_2 &= 1.55\times10^7(T+273.1)e^{\frac{-3052}{T+273.1}}\\
P_1 &= 1\\
P_2 &= 1 - 10.3\times10^{-4}\cdot P + 3.7\times10^{-7}\cdot P^2\\
P_3 &= 1 - 3.84\times10^{-4}\cdot P + 7.57\times10^{-8}\cdot P^2
\end{aligned}$$

The Fisher & Simmons model operates under some restrictions such as: the depth has to be less than 8 km and the salinity has been restricted to a value of 35 ppt, while the pH value has been set to 8.

4.2.3.3 Ainslie & McColm Model

The Ainslie & McColm model is based on the Fisher & Simmons model with some extra relaxations and simplifications as shown in (4.7). The Ainslie & McColm model also takes into account the effects of the acidity of sea water. It is based on depth (not pressure), which increases the range of applicability of the equation and provides the possibility of yielding more accurate results [81].

$$\begin{aligned}
\alpha &= 0.106\frac{f_1f^2}{f_1^2+f^2}e^{\frac{pH-8}{0.56}}\\
&\quad +0.52\left(1+\frac{T}{43}\right)\left(\frac{S}{35}\right)\frac{f_2f^2}{f_2^2+f^2}e^{\frac{-D}{6}}\\
&\quad +4.9\times10^{-4}f^2e^{-\left(\frac{T}{27}+\frac{D}{17}\right)}
\end{aligned} \tag{4.6}$$

The frequency equations for f_1 and f_2 are also simplified and represented in kHz:

$$f_1 = 0.78\sqrt{\frac{S}{35}}e^{\frac{T}{26}}$$
$$f_2 = 42e^{\frac{T}{17}}$$

The Ainslie & McColm model and the Fisher & Simmons model have similar performance in predicting the attenuation coefficient, while the Thorp model stops functioning after about a frequency of 200 kHz and it is restricted to a particular depth and temperature value.

4.2.4 Ambient Noise Model

Ambient noise in the ocean is a Gaussian distribution with continuous power spectral density (p.s.d.). The ambient noise occurs due to the turbulence, shipping, wind driven waves, and thermal noise. The spectral density is measured by dB re μ Pa per Hz as shown in the following equations [69], where N_t represent the turbulence noise, N_s the shipping noise (with s as the shipping factor which lies between 0 and 1), N_w the wind driven wave noise (with w as the wind speed in m/s) and N_{th} the thermal noise.

$$10\log N_t(f) = 17 - 30\log f \tag{4.7}$$

$$10\log N_s(f) = 40 + 20(s - 0.5) + 26\log f - 60\log(f + 0.03) \tag{4.8}$$

$$10\log N_w(f) = 50 + 7.5w^{\frac{1}{2}} + 20\log f - 40\log(f + 0.4) \tag{4.9}$$

$$10\log N_{th}(f) = -15 + 20\log f \tag{4.10}$$

The noise caused by distant shipping is dominant in frequency rage 10 Hz - 100 Hz, while turbulence noise influences only very low frequencies ($f < 10$ Hz). The wind driven waves affect the frequency range between 100 Hz - 100 kHz, which is the operating region used by the majority of acoustic systems. Thermal noise affects frequencies $f > 100$ kHz. In general, the overall noise p.s.d. can be obtained from (4.11).

$$N(f) = N_t(f) + N_s(f) + N_w(f) + N_{th}(f) \tag{4.11}$$

4.3 The Underwater Acoustic Channel Model

The underwater acoustic channel is time varying and based on many factors such as: received signal power (which is dependent on the transmission power), signal-to-noise ratio (SNR), and the capacity bound.

4.3.1 Received Signal Power

The received signal power P_{rx} is shown in (4.12) where f is the signal frequency and P_{tx} is the transmitted power over distance l. This equation focuses only on directional transmission (the most direct propagation path from transmitter to receiver), but it can be extended for indirect routes as well.

$$10 \log P_{rx} = 10 \log P_{tx} - 10 \log A(l, f) \tag{4.12}$$

The received signal power is dependent upon the propagation loss factor, which means, the attenuation model choice also adds a dependence upon depth, temperature, salinity and acidity of the area of interest.

4.3.2 Signal-to-noise ratio

Using the noise p.s.d $N(f)$ and the signal attenuation $A(l, f)$, the SNR at the receiver can be calculated from (4.13), where $SNR(l, f)$ is the SNR over a distance l and f is the transmission center frequency.

$$10 \log SNR(l, f) = 10 \log P_{tx} - 10 \log A(l, f) - 10 \log N(f) - 10 \log B(l) \tag{4.13}$$

In SNR, the attenuation model choice adds a dependence upon depth, temperature, salinity and acidity of the specific oceanic region that is of interest.

4.3.3 Channel Capacity

In designing networks and protocols, the channel capacity is an important metric that has an affect on the throughput and the topology of the network. The channel capacity c is shown in (4.14) based on Shannon's theorem, where B is the channel bandwidth, s is the signal power, and N is an additive white Gaussian noise.

$$c = B \log_2 \left(1 + \frac{s}{N}\right) \tag{4.14}$$

The channel capacity equation can be extended to be applicable in cases where the noise is dependent on frequency as shown in (4.15).

$$c = \int_B \log_2 \left(1 + \frac{s(f)}{N(f)}\right) df \tag{4.15}$$

The total capacity can be obtained by dividing the total bandwidth into multiple narrow sub bands and summing their individual capacities. In this case each sub band has a width of a small Δf, which is centered around the transmission frequency. Based on (4.14) and (4.15), the channel capacity over distance can be obtained as shown in (4.16).

$$c(l) = \int_B \log_2 \left(1 + \frac{P_{tx}}{A(l, f)N(f)B(l)}\right) df \tag{4.16}$$

4.4 Routing Protocols in Underwater Acoustic Networks

Many routing protocols have been designed for terrestrial ad hoc and sensor networks [82, 83]. These protocols have some drawbacks when applied directly in underwater networks due to the channel characteristics. These routing protocols are classified into three categories: proactive, reactive, and geographical routing protocols.

Proactive routing protocols such as Destination Sequence Distance Vector (DSDV) [84] and Temporally Ordered Routing Algorithm (TORA) [85] maintains up-to-date routing information to minimize the message latency by broadcasting control packets that contain routing table information (e.g., distance vectors). These protocols are not suitable for underwater networks since they provoke a large signaling overhead to establish a route for the first time and during a network topology change due to mobility or link failures.

Reactive routing protocols such as Ad hoc On-demand Distance Victor (AODV) [86] and Dynamic Source Routing (DSR) [87] initiate a route discovery process on demand when a route to a destination is required. These protocols may not be suitable for underwater networks due to the high latency when they establish a route. However, in [88], DSR was applied to underwater shallow networks and it shows good performance in terms of reliability, routing overhead, and path optimality.

Geographical routing protocols such as Greedy Face Greedy (GFG) [89] and Partial Topology Knowledge Forwarding (PTKF) [90] establish a path between a source and a destination based on localization information, which means each node selects its next hop based on the location of its neighbors and the destination. These protocols could be better for underwater networks but they face challenges in achieving accurate localization since synchronization is difficult due to high propagation delay. Furthermore, terrestrial localization systems such as the Global Positioning Systems (GPS) do not work underwater.

Most of the aforementioned routing protocols are based on packet switching (the routing function is performed for each single packet separately). In underwater networks, other techniques could be considered such as virtual circuit routing that establish a priori path between each source and sink, and each packet follows the same path. Virtual circuit switching routing protocols usually lack flexibility and how to adapt some degree of flexibility into virtual circuit switching routing protocols is a question that needs further research. The rest of this section shows the state of art of routing protocols in underwater networks.

4.4.1 A Network Layer Protocol for Underwater Networks

A simple multi-hop routing for shallow water networks, in which a central manager establish routes among nodes based on collected information from neighbor nodes, is proposed in [91].

The authors of [92] presented a routing protocol for underwater acoustic networking that provides a mechanism for network control and management. This protocol is self-configuring and it relies on a centralized manager running on a surface station to take care of network management. The centralized manager establishes the routing path based on the collected information from routing agents.

4.4.2 Data Collection, Storage, and Retrieval with an Underwater Sensor Network

In [93], a hardware and software architecture for long term monitoring is described. In this architecture, nodes communicate point-to-point using optical communication that provides high bandwidth when large amounts of data needs to be transferred and the nodes broadcast using an acoustic protocol for event signaling, low-bandwidth communication, and for 3D localization.

4.4.3 Vector-Based Forwarding Protocol (VBF)

Xie et al. [94] proposed a routing protocol, called vector-based forwarding (VBF). The VBF is a position based routing approach. Each packet carries the positions of the sender, the forwarder, and the destination. The nodes determine the forward path based on the routing vector. When a node receives a packet it calculates its relative position to the forwarder based on the distance between itself and the forwarder and based on the angle of arrival of the signal. If the node decides that its close enough to the routing vector (less than a predefined distance threshold), it adds its new position to the packet and forward the packet to its destination, otherwise it discards the packet. VBF also adopts a localized and distributed self-adaptation algorithm to enhance the performance of the protocol.

4.4.4 A Resilient Routing Algorithm for Long-term Applications

Pompili et al. [95] proposed a two-phase resilient routing algorithm for long-term monitoring tasks in 3D underwater sensor networks. This algorithm is based on virtual circuit routing techniques, i.e., the multi-hop connections between a source and a destination are established a priori and each packet with a particular connection follows the same path. In the first phase, energy-efficient node-disjoint primary and backup multi-hop data paths are optimally configured based on topology information gathered by a centralized manager (surface station). In the second phase of the resilient routing algorithm, an on-line distributed solution guarantees survivability of the network, by locally repairing paths in case of disconnections or failures.

4.4.5 Routing Algorithms for Delay-insensitive and Delay-sensitive Applications

The authors of [96] introduced two geographical routing algorithms for delay-insensitive and delay-sensitive applications. The two algorithms allow each node to select its next hop with the objective of minimizing the energy consumption. They algorithms are tailored to the underwater channel characteristics such as, the propagation delay which may vary in horizontal and vertical links, the transmission loss, and the limited bandwidth.

The first algorithm deals with delay insensitive applications and it relies on the packet-train transmission scheme. In order to minimize the total energy consumption, the algorithm allows each node to select its best next hop, the transmitted power, and the FEC code rate for each packet. This algorithm as well tries to maximize the probability of getting correct decoded packets at the receiver by exploit links that guarantee low packet error rate. The second algorithm deals with delay sensitive applications and it tries to minimize the energy consumption

while at the same time limit the end-to-end delay and packet error rate by estimating at each hop the time to reach the sink. This algorithm includes two new constraints to statistically meet the delay-sensitive application requirements: the end-to-end packet error rate should be lower than a certain threshold, and the end-to-end packet delay should be lower than a certain application dependent parameter.

4.4.6 Focused Beam Routing Protocol

In [97] a routing protocol called Focus Beam Routing (FBR) for static and mobile underwater networks is proposed. This protocol is based on location information to minimize the energy consumption per bit. FBR adopts a cross-layer approach, which means the routing protocol, the medium access control, and the physical layer functionalities are coupled by power control. The FBR assumes that nodes know their own locations and the location of the final destination, and they establish the route on-demand when a packet traverses a network to the final destination. Each node select its next hop at each step within the path from a source to a destination. Jornet et al. [97] mentioned that FBR can be coupled with any MAC protocol and in their work, they have chosen DACAP [98], a collision avoidance protocol based on virtual carrier sensing.

4.4.7 A Distributed Energy-Aware Routing Protocol

Domingo et al. [99] introduced a Distributed Underwater Clustering Scheme (DUCS), an energy-aware routing protocol for long-term non-time-critical monitoring applications using underwater wireless sensor networks with random node mobility and without GPS support. DUCS is an adaptive self-organization protocol, the nodes organize themselves into clusters and each cluster has a head node that is selected from all the nodes within that cluster. Nodes send their data via single hop to the head node which in turn aggregates the data and then send it to the sink via multi-hop forwarding. The head node is responsible for communication with the nodes in a local cluster and with other clusters head as well.

4.4.8 Adaptive Routing in Underwater Disruption Tolerant Sensor Networks

The authors of [100] proposed a routing protocol for underwater disruption tolerant sensor networks that establish routing adaptively based on the types of messages and application requirements. The authors assume that all sensor nodes know their 3D location. The routing protocol has two types of packets: *HELLO* packets and *data* packets. The *HELLO* packets are used for neighbor discovery. Each node in sparse underwater networks broadcasts *HELLO* packets that include node location, node ID, and available buffer size. The *data* packets include the normal payload with two fields; an emergency level and packet generating time, which are used in packet priority calculation. The priority of a packet takes into account the characteristic of the packet and the conditions of the network. The priority is calculated based on packet emergency level, packet age, node spatial-temporal density, and node battery level. After a node calculates a priority for a packet, it needs to make routing decisions accordingly to forward the packet toward to the sink. The adaptive routing protocol partitions the priority scale into 4 intervals [0, 25], (25, 50], (50, 75] and (75, 100], which correspond to the 4 routing states. For

each routing state, there is a corresponding forwarding area. Therefore, the adaptive routing protocol forwards packets to one of the forwarding areas based on the priority interval. With assist of localization service, the authors use geographic routing in their protocol. Figure 4.1 shows the routing decision procedure. Node A is the node which needs to make routing decisions based on the routing states of its packets in transit, and it has 4 neighbor nodes (node B, node C , node D, and node E). Node S is the sink, and R is the transmission rage of sensor nodes. Each packet at routing state i, has a corresponding forwarding area i, which is a sphere tangent to the transmission sphere of node A at the intersection point of $\vec{AS}$ (the forwarding vector from the current node to the sink) and the transmission sphere of node A. The authors choose the same size for forwarding areas 1 and 2 with a diameter $(\mathrm{R}/2)$ due to the sparsity of underwater, and they set area 3 to $3\mathrm{R}/4$, and area 4 to R. In general, a higher priority corresponds to a larger forwarding area. For example, if node A has a packet with a priority of 45, which means routing state 2, then node A will forward one copy of the packet to a neighbor node in the forwarding area 2 (node B). After that node A wait until the next neighbor moving into the forwarding area 2 to forward another copy. In case there are multiple neighbors at different layers, a node prefers those neighbors at the upper layer since they are closer to the sink [100].

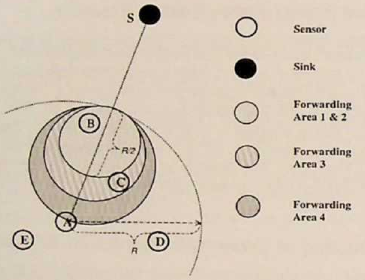

Figure 4.1: Illustration of routing decision procedure [100].

4.5 Energy Consumption Analysis in Underwater Acoustic Networks

Domingo et al. [101] analyzed the total energy consumption in underwater acoustic networks for two different scenarios: shallow water where the depth of the network is lower than 100 m and deep water that is used for deeper ocean.

4.5.1 Energy Consumption in Shallow Water

In shallow water, the authors of [101] consider a linear network that includes $N+1$ nodes and a distance d between each two nodes as shown in Figure 4.2. This network transmits packets of k bits from sensor nodes to the underwater sink and it represents the worst case scenario for network lifetime.

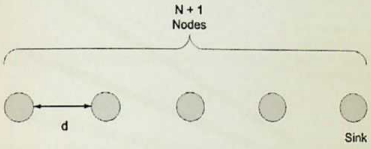

Figure 4.2: Simple linear network for the shallow water scenario [101].

In shallow water the spreading loss is cylindrical since the acoustic signals propagate with a cylinder bound by the surface and the sea floor. Therefore, the power level crossing the cylindrical surface is:

$$P = 2\pi \mathrm{dHI} \tag{4.17}$$

and energy consumed during transmission for one node in Joule $(\mathrm{W.s})$ would be:

$$E_{total} = hPT_{\mathrm{tx}}\mathrm{M} \tag{4.18}$$

where I is the intensity of the signal in $\mathrm{W/m^2}$, H is the height between the bottom and the surface of the sea, h represents the number of hops towards the surface sink and T_{tx} represents the transmission time for one packet and M represents the total number of the transmitted packets from the source node.

Figure 4.3 shows the total energy consumption using direct transmission and packet relaying. Domingo et al. [101] consider the height between the bottom and the surface of the sea to be H = 75 m, and the number of the transmitted packets to be 1000 packets within transmission time T_{tx} = 40 ms. Its clear from Figure 4.3 increasing the distance between the sensors will increase the energy consumption, and increasing the number of the nodes will increase the energy consumption as well since the additional nodes will be far away from the sink. However, there is no significant difference between the energy consumption in direct transmission and packet relaying since in shallow water the transmission power is linear proportional to the distance between sensor nodes.

4.5.2 Energy Consumption in Deep Water

In deep water, the authors of [101] consider a linear network that includes $N+1$ nodes and a distance d between each two nodes as shown in Figure 4.4. This network transmits packets

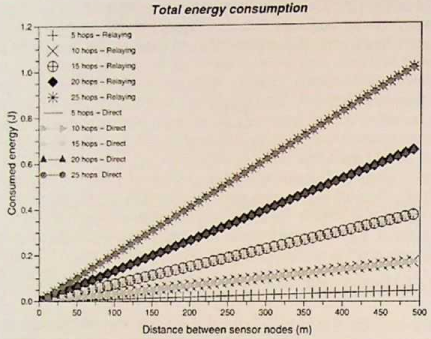

Figure 4.3: Total energy consumption in shallow water via direct links or through multi-hop paths (relaying) [101].

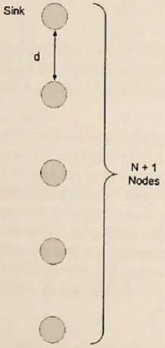

Figure 4.4: Simple linear network for the deep water scenario [101].

of L bits from sensor nodes to the underwater sink and it represents the worst case scenario for network lifetime.

In deep water the spreading loss is spherical since in deep water the acoustic signals propagation range is not bounded by the surface and the sea floor. Therefore, the power generated on the sphere surface is:

$$P = 4\pi \mathrm{d}^2 \mathrm{HI} \tag{4.19}$$

and energy consumed during transmission for one node would be:

$$E_{total} = hPT_{\mathrm{tx}}\mathrm{M} \tag{4.20}$$

where I is the intensity of the signal, H is the high between the bottom and the surface of the sea, h represents the number of hops towards the surface sink and T_{tx} represents the transmission time for one packet and M represents the total number of the transmitted packets from the source node.

Figure 4.5 shows the total energy consumption using direct transmission and packet relaying. The number of the transmitted packets is 1000 packets within transmission time T_{tx} = 40 ms. Its clear from Figure 4.5 using direct transmission from the sensor nodes to sink consumes more energy than relaying the packet through multi-hop. Increasing the number of the nodes will increase the total energy consumption since the additional nodes will be far a way from underwater sink and increasing the distance between the sensors will increase the energy consumption proportionally to the square of distance between sensor nodes.

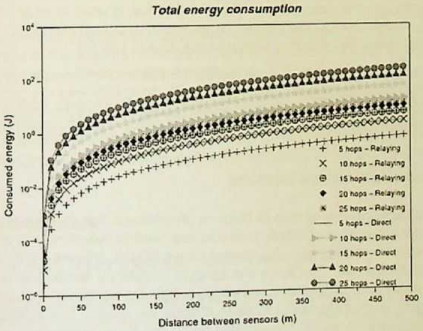

Figure 4.5: Total energy consumption in deep water via direct links or through multi-hop paths (relaying) [101].

4.6 Underwater Acoustic Network Topologies, Mobility and Sparsity

Underwater networks have sparse deployments and they differ from traditional terrestrial networks that assume fairly dense, continuously connected coverage of an area using inexpensive stationary nodes. Underwater sensor nodes are expensive and these nodes should cover a large area in oceans. Static underwater networks have to deal with natural ocean currents that bring in an added degree of complexity that is generally attributed only to mobile deployments, which led to the widespread use of mobile Autonomous Underwater Vehicles (AUVs) [9]. The sparsity and mobility of many underwater networks make disruption tolerant networks (DTNs) a feasible solution in underwater networks.

4.6.1 Static Networks

The network topology should be carefully designed since it is an important factor that affects the energy consumption, the capacity and the reliability of a network. In monitoring applications, the deployed network has to be highly reliable to avoid failure of monitoring due to failure of single or multiple devices [2].

4.6.1.1 2-D Underwater Sensor Networks

In 2-D underwater sensor networks, a group of sensor nodes are anchored to the bottom of the ocean with deep ocean anchors as shown in Figure 4.6. These anchors are interconnected to one or more underwater sinks using acoustic links. The underwater sinks are equipped with a vertical and a horizontal acoustic transceiver. The horizontal transceiver enables the sensor nodes to communicate with each other and the vertical link is used to relay collected data to a surface station. The surface station can be equipped with long range RF and/or satellite transmitters to communicate with an onshore or ship-based sink [2].

Underwater sensors can send the gathered data to the selected underwater sink, either directly or by relaying through intermediate nodes (multi-hop). Multi-hop links are normally preferred since they save energy by reducing the transmission power consumption that would be needed in case of long transmission distances and since they increase the reliability of the network [28].

4.6.1.2 3-D Underwater Sensor Networks

Two dimensional networks are unable to observe phenomena that do not occur at the ocean bottom. Three dimensional underwater networks are used to overcome this shortcoming. In three dimensional underwater networks, sensor nodes float at different depths in order to observe a given phenomenon. To deploy the sensors in different levels, the sensor could be attached to a surface buoy which has wires whose length can be regulated to adjust the depth, and then modifying the weight of the node to change the depth. This solution allows rapid deployment of the network but multiple floating buoys can be an obstruction in busy shipping lanes and floating buoys are vulnerable to weather and can also move due to ocean currents.

Figure 4.7 shows an architecture for 3D underwater sensor networks and a different way to deploy the sensors in different depths. In this architecture, a sensor is equipped with a floating

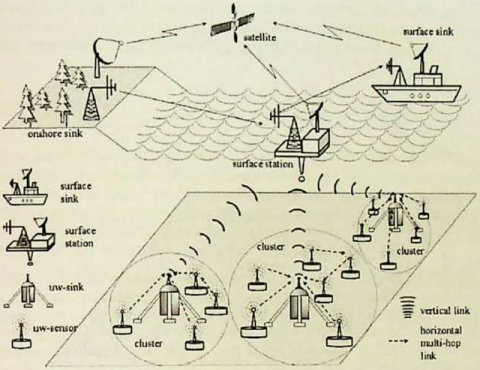

Figure 4.6: A typical 2-D underwater network [2].

buoy and then it is anchored to the ocean bottom. The floating buoy can be inflated by a pump to regulate the depth [28].

Many challenges arise with such an architecture, that need to be solved in order to enable 3D monitoring:

- Sensing coverage: Sensors should collaboratively regulate their depth in order to achieve 3D coverage of the ocean column and obtain sampling of the desired phenomenon at all depths, according to their sensing ranges.
- Communication coverage: In 3D underwater networks, network devices should coordinate their depths in such a way that the network topology is always connected, which allows the sensors be able to relay information to the surface station via multi-hop paths. This implies that at least one path from every sensor to the surface station always exists.

4.6.2 Mobile Network

The authors of of [102] classify underwater sensor networks into:

- Mobile underwater sensor networks for long-term non-time-critical aquatic monitoring: In these networks, local underwater sensors collect data and relay it to intermediate sensors. Then the intermediate sensors forward the packets to the surface nodes, after that, the surface nodes transmit data via radio to the on-shore command center. These networks have many applications such as: oceanography, marine biology, seismic predictions, pollution detection and oil/gas field monitoring.

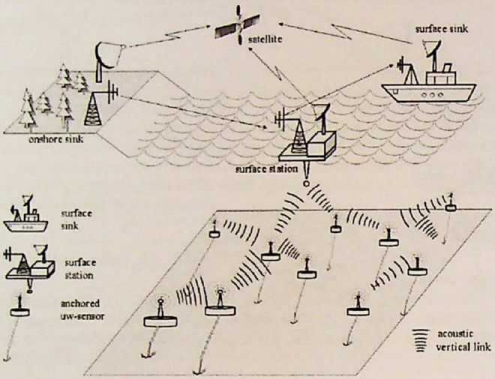

Figure 4.7: Architecture for 3D underwater sensor networks [2].

- Mobile underwater sensor networks for short-term time-critical aquatic exploration: In these networks, the underwater sensors use multi-hop acoustic routes to forward the collected data to a surface sink. Application for such networks could be underwater natural resource discovery, hurricane disaster recovery, and loss treasure discovery.

4.6.3 Disruption Tolerant Networks

DTNs have primarily been researched under the assumption of radio-based terrestrial networks and planned networks in space, yet many of the techniques are directly applicable in underwater networks. Most underwater networks comprise of mobile and sparse deployments [2, 28, 9]. Most approaches replicate packets epidemically during intermittent opportunities to transfer data and they use historic information regarding the past meetings of nodes to discover paths to destination nodes. When two nodes are in communication range of each other, they have transfer opportunities from the time they discover one another until they are out of acoustic range. The amount of data that can be transferred during each opportunity is the most constrained resource due to the limited bandwidth availability in the channel. In order to ensure data delivery, a series of dynamic or pre-arranged meetings between nodes can form a path to a destination. DTNs can also be used to connect geographically remote clusters of nodes.

The performance of a DTN can be greatly improved by using AUVs, mobile nodes that have controllable movements [103]. The authors of [104, 105] investigate DTN routing based on ferries that operate on pre-planned paths designed to optimize network performance and known

to all other nodes. In [106, 107], the authors proposed a method for robotic agents to dynamically adjust movements according to perceived network conditions and according to multiple network objectives to maximize delivery rate and minimize delivery latency.

4.7 Summary

In this chapter we introduced background and the state-of-art of underwater acoustic networks. We first discussed the differences between underwater networks and terrestrial networks. Underwater networks have higher propagation delay and signal attenuation than terrestrial networks, furthermore, the cost of building underwater networks is higher due to hardware protection. Underwater network consumes more energy than terrestrial networks due to the channel characteristics and they have a much higher bit error probability.

A propagation model for acoustic underwater networks is presented in Section 4.2. In this model, we discussed propagation loss, which is composed of geometrical spreading, attenuation, and anomaly propagation, and we presented three different absorption coefficient models (Thorp model, Fisher & Simmons model, and Ainslie & McColn model). Furthermore, ambient noise is discussed, which occurs due to turbulence, shipping, and wind driven waves. An underwater acoustic channel model is discussed in Section 4.3. We showed that the underwater channel is time varying and based on many factors such as, received signal power, signal to noise ratio (SNR), and the capacity bound.

Section 4.4 introduced routing protocols for underwater networks. The first type of these protocols relies on a central manager to establish the route among nodes, the second type uses the location of the nodes to establish the routes among nodes such as, vector-based forwarding (VBF) protocol, geographical routing algorithms for delay-insensitive and delay-sensitive applications, and focus beam routing protocol (FBR). The third type uses a hardware and software architecture for long term monitoring, in which nodes communicate point-to-point using an optical communication channel that provides high bandwidth and broadcast using an acoustic protocol for event signaling, and low bandwidth communication. The fourth type is based on clustering such as Distributed Underwater Clustering Scheme (DUCS) for long-term non-time-critical monitoring applications. The two-phase resilient routing algorithm for long-term monitoring protocol is based on virtual circuit routing techniques. Finally, adaptive routing in underwater disruption tolerant sensor networks. This protocol establishes routing adaptively based on the types of messages and application requirements

An energy consumption analysis for shallow water and deep water scenarios has been presented in Section 4.5. In addition, we introduced energy conservation techniques in underwater networks. At the end of this chapter, we discussed the underwater acoustic network topologies and mobility scenarios. These scenarios are prone to disruptions and they often have sparse topologies, which means disruption tolerant networks (DTNs) arise in underwater networks.

5 A Multi-Radio Power Management Scheme for Disruption Tolerant Networks

In this chapter, we design a power management scheme called Multi-Radio (MR) power management scheme that uses two complementary radios: a high bit rate, high-power radio and a low bit rate, low-power radio. By utilizing two radios instead of one, we are able to implement an asynchronous, on-demand energy conservation scheme that eliminates the idle time of a single high-power radio, and only allows the high-power radio to consume power in the sleep mode or while it is transmitting and receiving data. While the high-power radio is only called upon to perform data delivery when necessary, the low-power radio remains active for asynchronous neighbor discovery.

Since the neighbor discovery and data delivery radios are now separate, it is extremely important that the low-power radio is chosen with great care. The low-power radio is tasked with neighbor discovery and if the transmission range of this radio is greater than the high-power radio then there might be many delivery failures as nodes discovered by the low-power radio would not always be reachable by the high-power radio. Furthermore, there must be some frequency band independence between the two radios in order to avoid signal interference that may degrade network performance. For testing our multi-radio power management scheme, the XTend low-power radio was chosen, since its range and power consumption values are such that the high-power radio could still deliver data in every discovery scenario with energy savings. The WaveLan radio is used as the high-power radio, since it provides an opportunity to perform direct comparison with a single radio scheme [64]. Furthermore, we evaluate our MR power management scheme with different mobility models (random waypoint mobility model, the Manhattan mobility model, the Message ferry mobility model, the Zebra mobility model, and the human mobility model).

5.1 Neighbor Discovery

Neighbor discovery in the multi-radio scheme is extremely important in order to decide which nodes can be used as potential next-hop nodes for data forwarding. The nodes discovered are added as contacts in the routing table, along with a delivery predictability calculated using the PROPHET algorithm. In case of our multi-radio scheme, only the low-power radio is utilized to find neighbors.

Each node periodically wakes up for a period W in a fixed duty cycle of length C, as shown in Figure 5.1. Each time a node wakes up, it transmits a beacon containing it's node identifier. In case the node has data available for delivery, it piggybacks a delivery notification to the discovery beacon message. This delivery notification contains information about the destination nodes for the data to be transmitted. In case another suitable next-hop node has its low-power radio active, it replies with the delivery acceptance message to the node sending the delivery notification. After K duty cycles have passed, the nodes let their low-power radio remain active for the full cycle length C, before reverting back to the regular scenario. We refer to the tuple (W,C,K) as the sleep pattern [64].

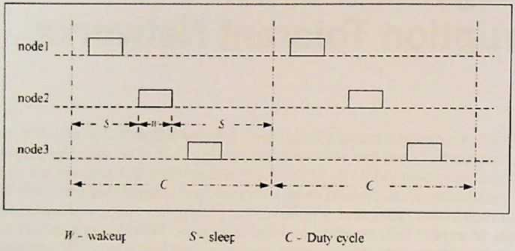

Figure 5.1: Random wakeup with fixed duty cycle [64].

Figure 5.2, which is similar to Figure 3.10, depicts some of the neighbor discovery scenarios that may be encountered. In Figure 5.2 (a), node 1 wakes up its low-power radio and transmits a discovery beacon message which is not received by any nodes since they are all inactive (sleeping) at this time. However, the discovery beacon for node 2 is received by node 1 and both nodes 1 and 2 receive node 3's discovery message, causing all nodes to be aware of node 3, only node 1 being aware of node 2 and no one aware of the existence of node 1 in their neighborhood. Figure 5.2 (b) extends this scenario by depicting a case when node 1 piggybacks a delivery notification to its beacon. Since no nodes are active when the beacon is sent, no node sends a data acceptance message. In Figure 5.2 (c) node 2 broadcasts a data delivery notification along with the beacon and receives an acceptance from node 1, since only that node is active when the beacon is sent. In Figure 5.2 (d) both nodes 1 and 2 respond to node 3's delivery notification since they are both active.

The neighbor discovery phase is not only used for signaling the data delivery, but also to calculate the delivery predictabilities to nodes in the network, to determine the best next-hop using the PROPHET routing protocol.

5.2 Data Delivery

Once a delivery predictability has been calculated, the next-hop node is identified and a delivery acceptance is received. Then, each node wakes up its high-power radio in order to undertake the data transmission. Figure 5.3 demonstrates a scenario when node A and node

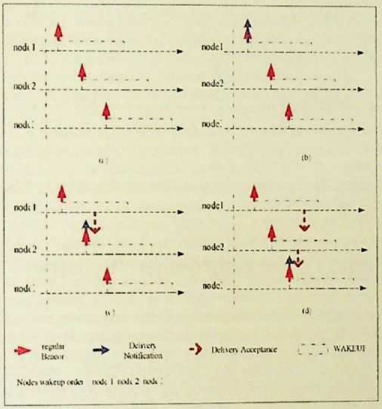

Figure 5.2: An illustration of the multiple possible neighbor discovery scenarios in the multi-radio scheme [64].

B are both still in their active beacon periods and a data delivery occurs in parallel. However, it is important to note that the multi-radio scheme does not require nodes to extend their awake period W in order to be able to receive a message, since a message will be received by the high power radio, thereby contributing towards energy savings. Each node only requires that the delivery acceptance message is received before the end of it's awake period.

Following this scheme ensures that the power usage impact of the high power modem is minimal, since it is only active during data transmission and reception phases and at all other times it is in the sleep mode. This does not just reduce the idle wait time but completely eliminates it.

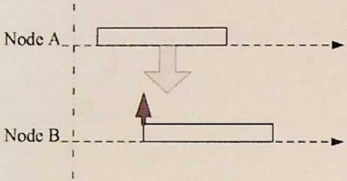

Figure 5.3: An illustration of the multi-radio data delivery scenario.

5.3 Multi-Radio Power Management Scheme

In this section, we describe what a node does in the MR power management scheme as shown in Figure 5.4. At the beginning each node reads the sleep pattern (duty cycle (C), wakeup period (W), and K), if $C_k == K$ (after K^{th} duty cycle), then a node sets $W = C$ and resets the C_k else $W_p = W$. The T_{start}=rand(t,t+C-W) and the SleepUntil(T_{start}) allow a node to start a wakeup time period randomly within each duty cycle and keep a node in a sleep mode until the begging of (T_{start}) at which a node wakes up its low power radio for W (Set(LPR,mode==ON)). After a node wakes up, it checks whether it has data to be delivered. If yes a node broadcasts a beacon (send(beacon(notificationDeliv))) that includes a notification delivery (destination ID). When a node receives a notification accept beacon from any other node, it activates the HPR (ActivateHPR_Tx()), which means a node wakes up its high power radio (Set(HPR,mode=ON)) in order to send the data, after sending the data, a node returns its high power radio to sleep mode (Set(HPR,mode=SLEEP)) as shown in the HPR Module in Figure 5.4. If the node does not receive any notification accept beacon, it will set its LPR to sleep mode at the end of W until the next duty cycle.

If the wake up node has no data to be delivered, it will broadcast a regular beacon (send(beacon(regBeacon)). When a node receives a beacon, it will check if this beacon is a delivery beacon (check(RxBeacon)==DelivRxBEACON), in that case a node starts to activate its HPR (ActivateHPR_Rx()), which means a node will send a notification acceptance (send(notificationAccept)) to the sender node and it will wake up its high-power-radio (Set(HPR,mode=ON)) to be ready to receive the data. After the node receives the data it will return its high-power-radio to

sleep mode as shown in the HPR Module in Figure 5.4. In case the received beacon is a regular beacon, a node will update its neighbor list, and go back to sleeping mode. In general, if the wake up node does not receive any beacon because it has no neighbor nodes or because of lost beacons, then this node will go to sleep mode at the end of W and it keeps in sleep mode until the next duty cycle.

The same procedure will be repeated every duty cycle. Since a node might not get in contact with another node for a long time, the MR power management scheme allows a node to turn on its low-power-radio for the whole duty cycle (W=C) after the K^{th} duty cycle in order to find contacts.

We present the relationship between W, C, and K that allows the packets to be transmitted between two nodes. For example, assume that we have two nodes (node A, and node B) in communication range; in our power management scheme node B can be discovered if it's awake period overlaps with the awake period of node A (offset time between node A and node B is less than $2W$). Otherwise, node B can be discovered by node A during the full awake cycle (after K^{th} cycle). From [108], the minimum W ($W_{\min}$) has to be larger than the time it takes the RF circuit to turn on and transmit a beacon between the two nodes A and B. The duty cycle C also has to be larger than the time it takes for neighbor nodes to send beacon messages. Xi et al. [64] assume that $C > C_{\min} = nW_{\min}$, where $C_{\min}$ is the minimum duty cycle, n is the active number of neighbors. If K becomes 0, a node wakes up the whole duty cycle ($W = C$) and no energy saving can be achieved, while if K goes to infinity, then W never equal C and in this case two nodes A and B might not communicate with each other. Using larger values for W increase the communication opportunities, enhance network performance, and consume more power while using smaller values for W save more energy. However, we should keep in our mind that the wakeup time W has to be larger than $W_{\min}$. If the contact time between any two nodes becomes very small (less than the time needed to exchange messages) then the nodes will return to sleep at the end of W and wait until the next duty cycle to search for contacts. Also, if the nodes move very fast this could worsen the network performance since the nodes cannot establish communication. In case of a static network, the nodes will be always within the communication range of each other and then the problem will turn into a synchronization problem, in which nodes need to wake up at the same schedule to communicate.

The authors of [64] provide an extensive discussion on how optimal values may be derived for (W, C, K) through the relationship between the Sleeping Pattern Impact Factor (SPIF) and the Traffic Threshold Line (THH) as shown in Figure 5.6. To understand what are the SPIF and THH factors, assume that we have a certain node called N, then neighbors of node N can be grouped into two groups, depending on how they are discovered by node N. In the first group, nodes can be discovered if their awake period overlaps with the awake time of node N, therefore, the average number of the nodes that can be discovered within the offset time ($2W$) is $(2W/C) \cdot n$. Otherwise, nodes can be discovered in the full awake cycle ($W = C$), in that case, the number of nodes that can be discovered is $[(C - 2W)/C)] \cdot n$. During the full awake cycle, traffic from both groups needs to be sent out, and therefore we have:

$$(C - C_{\min}) \cdot \Theta > \frac{2\mathrm{W}}{\mathrm{C}} \cdot \mathrm{nCf_{ij}} + \frac{\mathrm{C} - 2\mathrm{W}}{\mathrm{C}} \cdot \mathrm{nKCf_{ij}} \tag{5.1}$$

The traffic load for both groups 1 and 2 is listed in the first and the second terms at the right hand side of (5.1) respectively, where f_{ij} is the traffic generated by the source node in one wakeup cycle. The left hand side of (5.1) shows the amount of traffic that can be supported

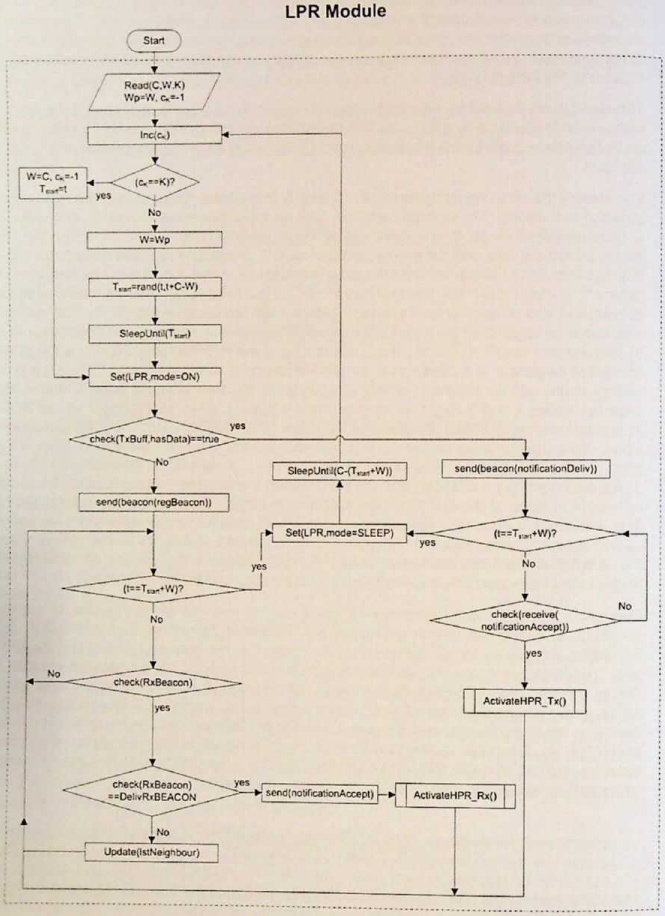

Figure 5.4: Flow Chart of a single node in the multi-radio (MR) power management scheme

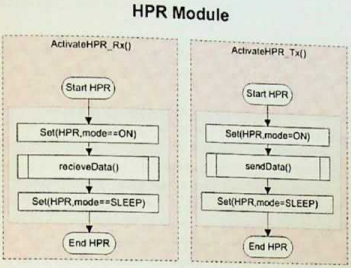

Figure 5.5: Flow Chart of ActivateHPR_Rx() and ActivateHPR_Tx() subroutines

by the radio. $C_{\min}$ is used to exchange beacons and can not be used for traffic transmission, where Θ is the high power radio bandwidth. From (5.1) we can get:

$$\frac{(C - C_{\min})}{2W + (C - 2W)K} > \frac{nf_{ij}}{\Theta} \tag{5.2}$$

The left hand side expression of (5.2) is called the SPIF factor, and the right hand side expression is called the THH factor. Figure 5.6 shows that the SPIF is a family of convex curves with respect to the C. From Figure 5.6, we can choose K and W values, and given a traffic load requirement, one can compute the THH. The largest K value need to be chosen such that the convex family of the SPIF curves lies above the THH line. More information about W, C, and Kcan be found in [64].

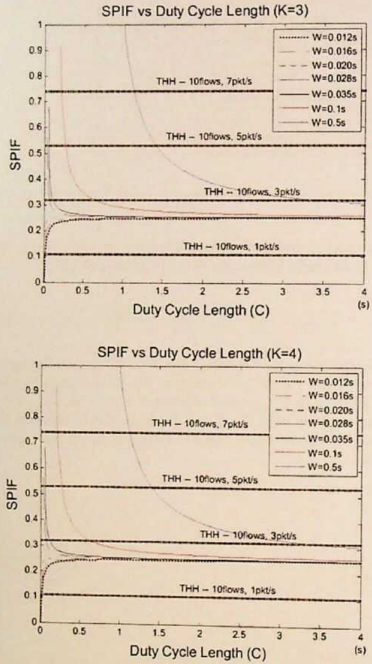

Figure 5.6: SPIF versus duty cycle length [64]

5.4 Energy Consumption

Three different radios are presented in this thesis, a high-power radio WaveLan 802.11 [59], and two low-power radios: the XTend [60] and the CC1000 [109]. More studies on the power consumption model can be found in [21]. In our work, we use the same power usage parameters as in [59, 60]. The values of the energy parameters are replicated in Table 5.1 and Table 5.2. We adjust the transmission range for the XTend radio to 250 m and we calculated the new transmit power consumption based on the Friis transmission equation in (5.3) [110], where P_r is the power received by the receiving antenna, P_t is the power input to the transmitting antenna, G_t and G_r are the antenna gain of the transmitting and receiving antennas, respectively, λ is the wavelength, and R is the transmission range. In (5.3) and (5.4), P_r (the minimum power required by the receiver to detect signals) needs to be fixed, the values of G_t, G_r, and λ are constant. By dividing (5.3) by (5.4), we get the new transmit power consumption is equal to 1/16 of the old transmit power consumption, where R_{old} = 1000 m and R_{new} = 250 m.

$$P_{r(old)} = P_{t(old)} G_t G_r (\frac{\lambda}{4\pi R_{old}})^2 \tag{5.3}$$

$$P_{r(new)} = P_{t(new)} G_t G_r (\frac{\lambda}{4\pi R_{new}})^2 \tag{5.4}$$

From Table 5.1, we can see that, a node consumes less power in sleeping activity than idle activity, while it consumes almost the same power in both idle and receiving activities. In addition, the XTend and the CC1000 radios consume an order of magnitude less power than the WaveLan 802.11 radio for each activity. Thus, they can discover contacts using substantially less power.

Table 5.1: Power usage of different radio types (in Watt)

Radio Type	Transmit	Receive	Idle	Sleep
WaveLan	1.3272	0.9670	0.8437	0.0664
XTend	1	0.36	0.36	0.01
CC1000	0.0781	0.0222	0.0222	0.00003

Table 5.2: Physical characteristics of different radio types

Radio Type	Bit Rate	Bandwidth	Range
WaveLan	2 Mbps	83.5 MHz	250m
XTend	115.2 Kbps	36 MHz	250m
CC1000	76.8 Kbps	76.8 kHz	50m

The introduction of adaptive radios with multiple transmission modes (like high and a low-power modes) have also seen development of power management schemes that leverage this feature by performing neighbor discovery using an asynchronous scheme in the low-power mode, and then switching to a high power mode once there is deliverable payload available [111]. Though this method reduces the overall energy consumption, it is worth noting that it also reduces the overall node discovery opportunities since the mode change occurs during the wake-up

cycle. This happens because the radio frequency being utilized for node discovery in low-power mode will always be different from the frequency for data delivery in high-power mode, and the radio is capable of using only one frequency at a time (the radio is only used either for neighbor discovery or for data delivery at a time). By using two radios in DTNs, we are able to separate the neighbor discovery and the data delivery.

Results from initial investigation showed that it is better to use high-power radios for data transmission since these radios normally provide a high data rate. However, since the idle-power consumption for high-power radios is higher than those of low-power low-data-rate radios, they are unsuitable for use during the neighborhood discovery phase. Conversely, the comparatively low energy consumption in idle listening state makes the low-power radios more suitable for neighbor discovery.

5.5 Simulation Setup

The multi-radio scheme was evaluated using ns2 [112], one of the most popular mobile wireless networking simulators available. However, the current versions of ns2 only support a single radio interface implementation on the mobile nodes and this made it necessary to extend ns2 such that it would support multiple interfaces, in order to implement our multi-radio scheme.

Several propagation models are implemented in ns2: Free Space, Two Ray Ground, and Shadowing models to predict the signal power received by the receiver. The signal strength is used to determine whether the frame is transmitted successfully. The Free Space model is used to simulate path loss of wireless communication when line of sight path exists between transmitter and receiver. The Two Ray Ground model, which has been used in our simulations, is used when line of sight exists taking into account the reflection of ground. The Shadowing model considers the shadow effect of obstructions between the transmitter and receiver. Ns2 uses a signal strength threshold (CSThresh_) to determine whether a frame is detected by the receiver. If the signal strength of the frame is less than CSThresh_, this frame is discarded in the PHY layer. In ns2, there is another threshold (RxThresh_) for the signal strength of a frame received by the receiver. If a frame is received at the receiver with a signal strength stronger than RxThresh_, the frame is considered to be received correctly. Otherwise, the frame is considered a corrupted frame and the Mac layer will discard it [112].

As related to the interference problem, the Mac layer in ns2 versions prior to release ns-2.33 uses a RTS/CTS/DATA/ACK pattern for all unicast packets and sends out DATA for all broadcast packets. A Signal to Interference and Noise Ratio (SINR) error model is introduced in new ns2 releases. In this model, an error is calculated using received signal strength, noise and interference. "Interference is calculated using a Gaussian model to account for all transmissions which happen simultaneously to the one which is considered for reception" [112]. The SINR is used to calculate the Packet Error Rate (PER), and PER is used to determine packet losses [112]. Our simulator version is older than ns-2.33 and hence uses the RTS/CTS/DATA/ACK pattern.

In order to evaluate the multi-radio scheme, the Random Waypoint (RWP), ZebraNet, Message Ferry, Manhattan, and Orlando (real human mobility model) mobility models are used. To compare our results with the CAPM scheme, we use the same simulation scenario in [64]. Each scenario is set up with 40 mobile nodes that are distributed over 1000 x 1000 m^2. The

simulations were also performed with the nodes distributed in an area of 1150 x 1150 m^2, 1400 x 1400 m^2, 2000 x 2000 m^2, and 3000 x 3000 m^2. We use constant bit rate traffic with 10 CBR flows and a packet size of 512 bytes as in the CAPM scheme. The traffic generation for each flow varied from 0.25 pkts/s to 3 pkts/s. The sources and destinations of CBR flows are randomly selected prior to each run, amongst the 40 nodes. A maximum of 10 connections are allowed during each run.

Each simulation runs for 2000 seconds, with 1000 seconds being utilized as a warm-up period, and the performance data being recorded only for the last 1000 seconds of the simulation. In order to minimize the possibility of only a corner case being encountered, every reported result is an average taken over 5 runs, and the observed variance are within $\pm 3\%$. The WaveLan and the XTend radios in Table 5.1 are used for all the simulations.

5.6 Performance Evaluation and Direct Comparison Between the Multi-Radio and the CAPM Scheme

As we said in the previous section, to compare our results with the CAPM scheme, we use the same simulation scenario in [64]. The scenario is set up with 40 mobile nodes that are distributed over 1000 x 1000 m^2. Each of these nodes is setup to move at a constant velocity of 5 m/s following the RWP mobility model.

5.6.1 Performance Evaluation Metrics

In order to evaluate the performance of the multi-radio scheme, we utilize three metrics:

1. Normalized Energy Consumption: The ratio of the energy consumption when multi-radio scheme is applied divided by the energy consumption in the absence of energy conservation.
2. Delivery Ratio: The ratio of the number of the successfully received data packets divided by the number of the data packets sent.
3. Average End-to-End Delay: The average delay it takes to deliver a data packet from the source to the destination.

5.6.2 Multi-Radio Scheme Evaluation With the Optimal Values of (W, C, K)

In this experiment we test and evaluate the multi-radio scheme with the optimal values of the sleep pattern (W, C, K) as mentioned in Section 5.3. The authors of [64] provide an extensive discussion on how optimal values may be derived for (W, C, K). Following their guidelines, we use the values as shown in Table 5.3. The second column in Table 5.3 shows the node density (total number of nodes divided by the network area), for example 1000 x 1000-40 indicates that the network has 40 nodes distributed over 1000 x 1000 m^2. We first evaluate our multi-radio (MR) scheme using the CC1000 radio as low-power radio and the WaveLan 802.11 as

high-power radio. Figure 5.8 shows that using the CC1000 radio for neighbor discovery in our multi-radio scheme reduces the energy consumption by 95%, while the single radio (SR), CAPM, scheme only achieves 75%.

Table 5.3: Parameter values

Packet rate	Node density	Sleeping pattern (W,C,K)
3 pkt/s	1000 x 1000-40	(0.024, 1.67, 3)
	1150 x 1150-40	(0.024, 1.67, 3)
	1400 x 1400-40	(0.017, 1.46, 3)
	2000 x 2000-40	(0.01, 1,25, 4)
	3000 x 3000-40	(0.01, 1,6, 3)
0.25 pkt/s	1000 x 1000-40	(0.04, 0.4, 12)
	1150 x 1150-40	(0.04, 0.4, 12)
	1400 x 1400-40	(0.04, 0.4, 12)
	2000 x 2000-40	(0.01, 0.4, 12)
	3000 x 3000-40	(0.01, 0.4, 12)

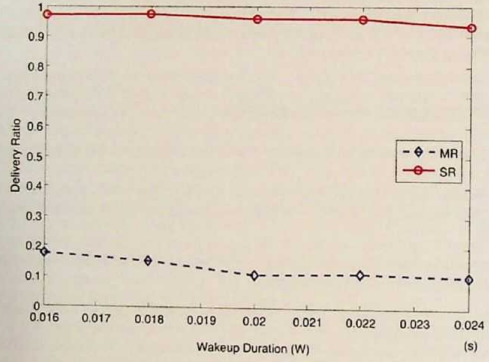

Figure 5.7: Delivery ratio using CC1000 radio for neighbor discovery in the single radio (SR) and the multi-radio (MR) schemes

Though the energy savings make the CC1000 radio an attractive option for the multi-radio scheme, it is important to also understand the effects that the scheme has on the overall delivery ratio. From Figure 5.7, it becomes clear that using the CC1000 radio for neighbor discovery has a very high impact on the delivery ratio. This ratio especially becomes very small once higher values for C and large distributed areas for nodes are used. However, this poor performance is only because the CC1000 radio has a very limited transmission range of 50 m. Using the multi-radio along with a low-power radio (XTend) that has a transmission range of 250 m,

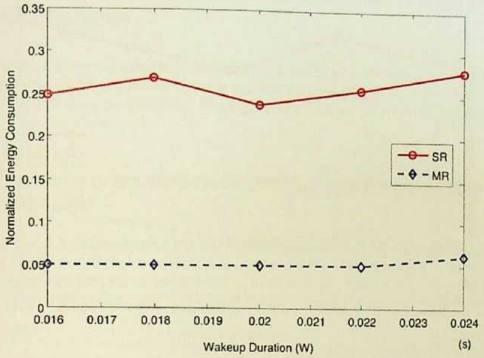

Figure 5.8: Normalized energy consumption using CC1000 radio for neighbor discovery in the single radio (SR) and the multi-radio (MR) schemes

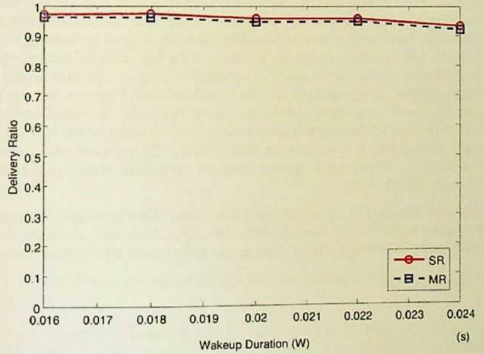

Figure 5.9: Delivery ratio using XTend radio for neighbor discovery in the single radio (SR) and the multi-radio (MR) schemes

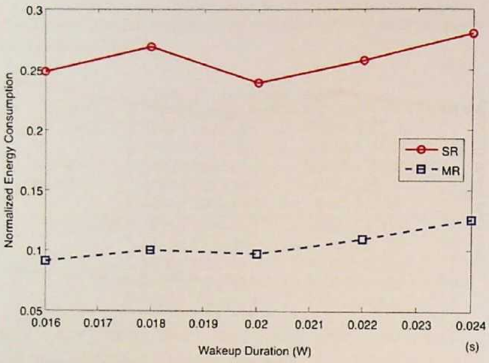

Figure 5.10: Normalized energy consumption using XTend radio for neighbor discovery in the single radio (SR) and the multi-radio (MR) schemes

the same as the long range high-power WaveLan radio, the multi-radio performs as well as the SR scheme in terms of the delivery ratio as shown in Figure 5.9, while it outperforms the SR by reducing the energy consumption by half the power consumption as shown in Figure 5.10. By decreasing the low-power radio power consumption, the total energy consumed in the network will be decreased, which enhances the performance of the MR scheme. For example, if there exist an ideal (zero) low power radio, then the consumed power in a network is only the power needed for data transfer, which leads to an optimal MR scheme. However, there is a limitation on how much the power consumption of the low-power radio can be decreased based on the sensitivity of the receiver, since there is a minimum power required by the receiver in order to receive signals without any problem at a certain distance. On the other hand, increasing the low-power radio power consumption will increase the consumed energy in the network and make the MR scheme inefficient.

From the previous results, it is clear that using the XTend radio for neighbor discovery in the multi-radio scheme is better than using the CC1000 radio. Therefore, all the following experiments in this thesis use only the XTend radio as low-power radio for neighbor discovery.

5.7 Impact of Different DTNs Mobility Scenarios on The Multi-radio Scheme

In this section we show the evaluation results for the multi-radio scheme with different mobility models. We first evaluate the MR scheme with random waypoint, then we use more realistic mobility models such as ZebraNet, Message Ferry, Manhattan, human mobility (Orlando) models.

5.7.1 Evaluation of the Multi-Radio Scheme with Random Waypoint Mobility Model

To evaluate the multi-radio scheme with the random waypoint mobility model, the network is set up with 40 mobile nodes that are distributed randomly over 1000 x 1000 m^2. The simulations were also performed with the nodes distributed in an area of 1150 x 1150 m^2, 1400 x 1400 m^2, 2000 x 2000 m^2 and 3000 x 3000 m^2. All nodes move at a constant velocity of 5 m/s.

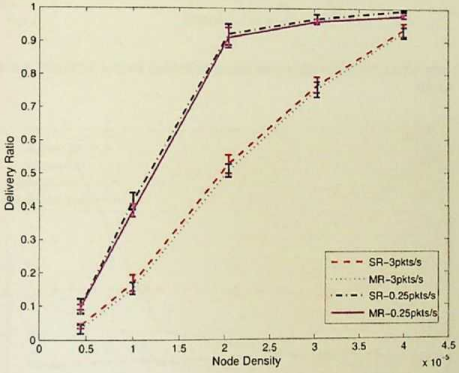

Figure 5.11: Impact of node density on the delivery ratio for the MR and the SR schemes using RWP model

Figure 5.11 and Figure 5.13 show the delivery ratio, and the normalized energy consumption over different node densities. From Figures 5.11, 5.13, it is clear that the delivery ratio of the multi-radio scheme is comparable to the single radio, CAPM, (SR) scheme, while the normalized energy consumption for the multi-radio (MR) is significantly less than the SR. The SR saves 85% energy at low load (0.25 pkts/s) and 73% energy at high load (3 pkts/s) over different node densities, while the multi-radio saves 90% energy at low load (0.25 pkts/s) and

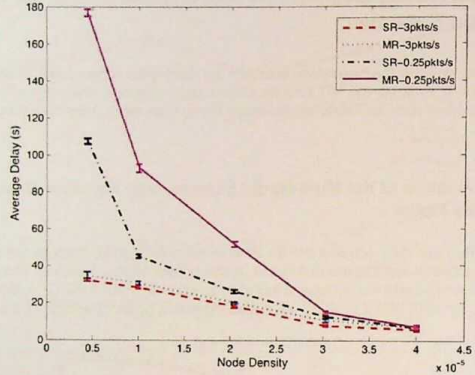

Figure 5.12: Impact of node density on average delay the for the MR and the SR schemes using RWP model

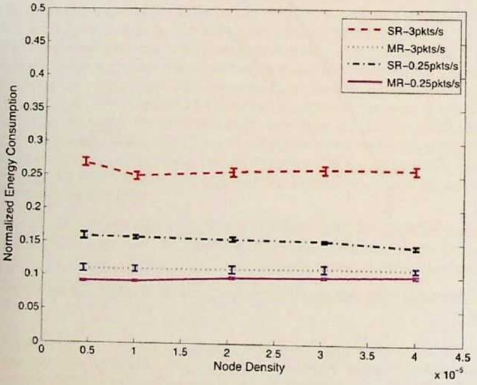

Figure 5.13: Impact of node density on normalized energy consumption for the MR and the SR schemes using RWP model

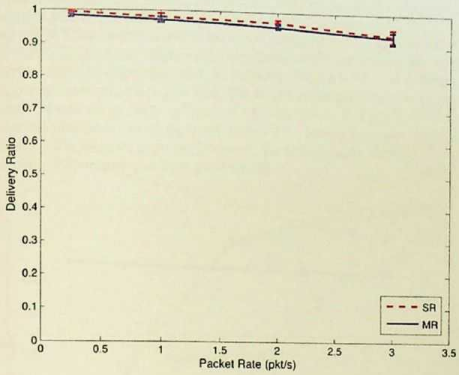

Figure 5.14: Impact of traffic load on delivery ratio for the MR and the SR schemes using RWP model

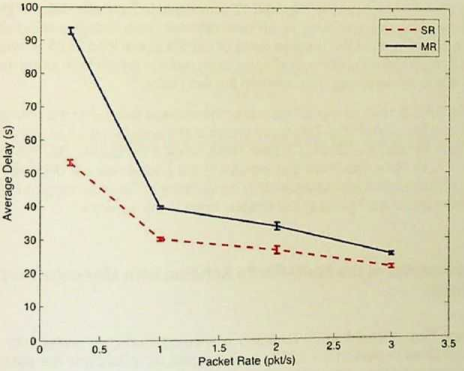

Figure 5.15: Impact of traffic load on average delay for the MR and the SR schemes using RWP model

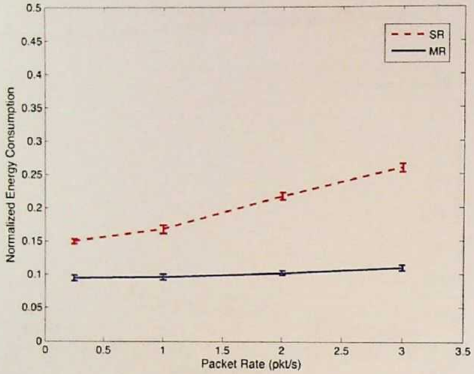

Figure 5.16: Impact of traffic load on normalized energy consumption for the MR and the SR schemes using RWP model

88% energy at high load (3 pkts/s). Figure 5.12 shows that the average delay of the multi-radio is comparable to the average delay of SR over different node densities and traffic load of 3 pkts/s, while its higher than the average delay of the SR at low load (0.25 pkts/s). This delay occurs due to the initialization time needed for each radio to switch from sleep mode to active mode, and due to the switching time between the two radios.

Figures 5.14, 5.15, 5.16 show the delivery ratio, the average delay, and the normalized energy consumption vs the packet rate. This figure shows that the multi-radio can still achieve almost the same delivery ratio for different packet rates, while it consumes half the power of SR. Figures 5.14, 5.15, 5.16 also show that increasing the packet rate will decrease the delivery ratio, while it increases the normalized energy consumption. The error margins in Figures 5.11-5.16 and in the rest of the figures in this chapter indicate the variance.

5.7.2 Evaluation of the Multi-Radio Scheme with Message Ferry Mobility Model

The Message Ferry model had 25 randomly distributed stationary nodes with 15 message ferries as explained in Section 2.1.3. The ferries moved on a fixed grid-like path, where each vertical and horizontal lane of the grid was separated by a constant distance of 250 m. As such, for the 1000 x 1000 m^2 scenario there were 4 vertical and horizontal lanes each. Similarly, the 2000 x 2000 m^2 and 3000 x 3000 m^2 had 8 and 12 vertical and horizontal lanes each respectively.

While using the Message Ferry model, the delivery ratio of the multi-radio approach is once again very similar to the performance of a single-radio, as per Figure 5.17. However, the energy consumption savings increased to be in the range of $90\% - 93\%$ for the multi-radio, as compared to $76\% - 86\%$ for the single-radio approach, while the packet rate was varied from high to low across different node densities, as shown in Figure 5.19. The average delay for the multi-radio approach tends to be higher than the single-radio approach, but this reduces with increasing node density as its clear in Figure 5.18. Figures 5.20, 5.21, 5.22 make it clear that varying the packet rate from low to high still allows the multi-radio approach to have delivery ratios similar to the single-radio scheme, however, the energy consumption reduces by a large amount, especially in the case of a high packet load.

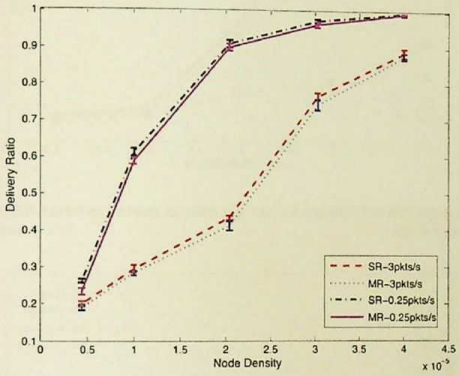

Figure 5.17: Impact of node density on the delivery ratio for the MR and the SR schemes using Message Ferry model

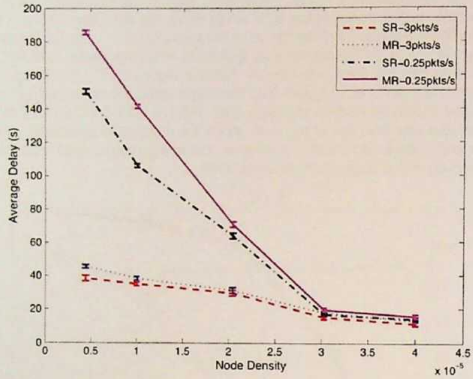

Figure 5.18: Impact of node density on average delay for the MR and the SR schemes using Message Ferry model

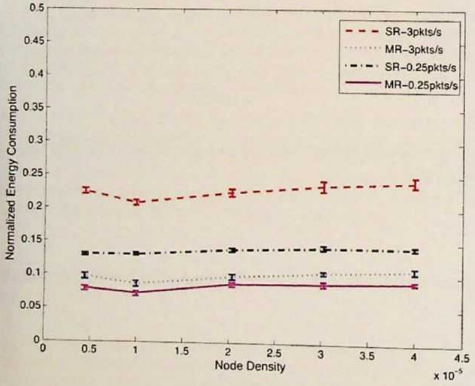

Figure 5.19: Impact of node density on normalized energy consumption for the MR and the SR schemes using Message Ferry model

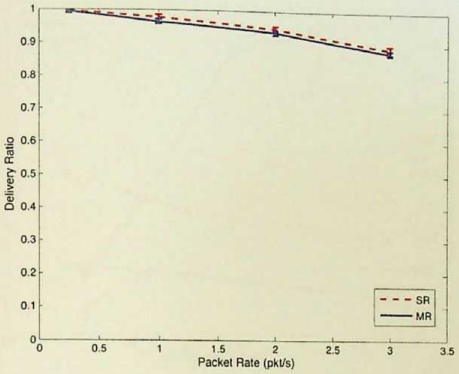

Figure 5.20: Impact of traffic load on delivery ratio for the MR and the SR schemes using Message Ferry model

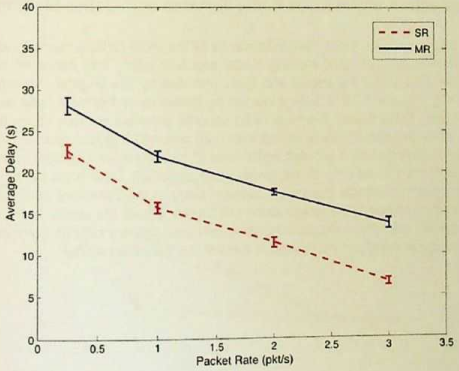

Figure 5.21: Impact of traffic load on average delay for the MR and the SR schemes using Message Ferry model

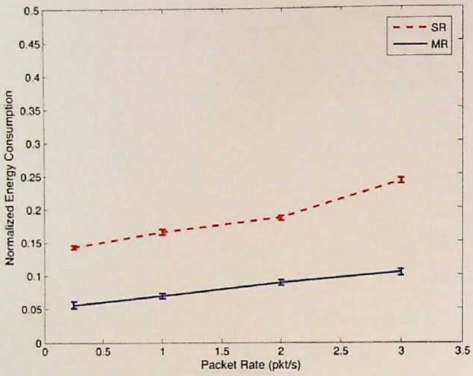

Figure 5.22: Impact of traffic load on normalized energy consumption for the MR and the SR schemes using Message Ferry model

5.7.3 Evaluation of the Multi-Radio Scheme with Zebra Mobility Model

In order to obtain an idea about the performance of the multi-radio scheme in more realistic mobility scenarios, the ZebraNet mobility model was also used. The ZebraNet mobility models were generated using the traces and tools provided by the original investigators of the ZebraNet [113]. Figures 5.23 to 5.28 show the performance of the multi-radio scheme in the ZebraNet model. Once again, the multi-radio scheme provides delivery ratios similar to the single radio when the packet rate is varied from 0.25 pkts/s to 3 pkts/s, while providing energy savings ranging between 89% (at high traffic load (3 pkts/s)) to 91% (at low traffic load (0.25 pkts/s)) against the 73% to 85% of the single-radio approach. The node density appears to have a much more prominent impact on average delay in the ZebraNet model compared to the RWP model, however, the average delay still closely follows the single-radio performance. Varying the packet rate still manages to achieve the same delivery ratio as a single-radio, while greatly reducing the energy consumption in case of the ZebraNet model.

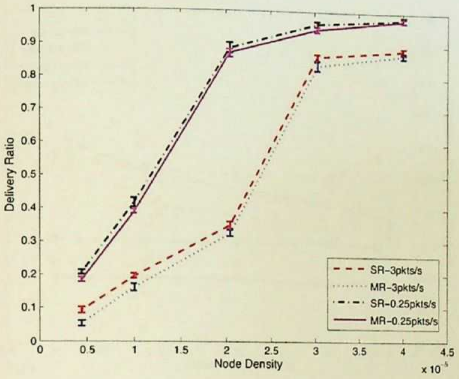

Figure 5.23: Impact of node density on the delivery ratio for the MR and the SR schemes using ZebraNet model

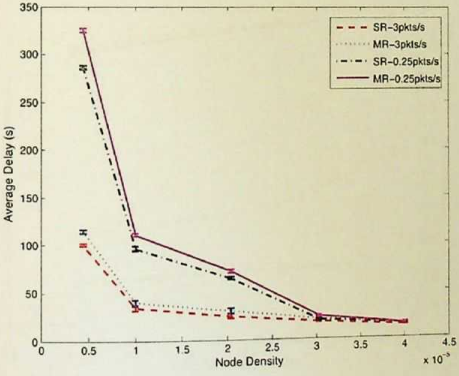

Figure 5.24: Impact of node density on average delay for the MR and the SR schemes using ZebraNet model

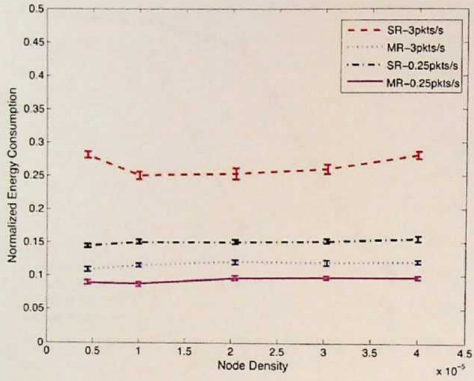

Figure 5.25: Impact of node density on normalized energy consumption for the MR and the SR schemes using ZebraNet model

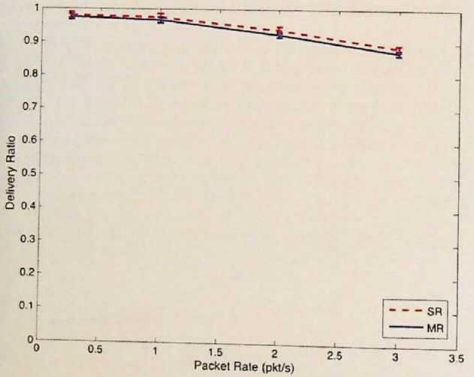

Figure 5.26: Impact of traffic load on delivery ratio for the MR and the SR schemes using ZebraNet model

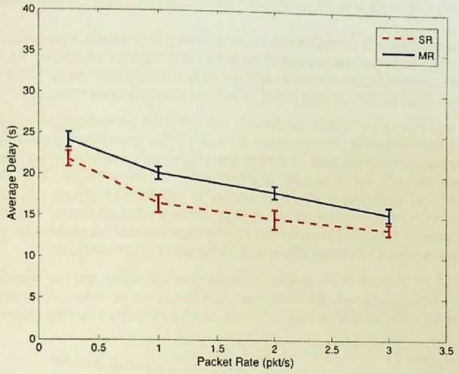

Figure 5.27: Impact of traffic load on average delay for the MR and the SR schemes using ZebraNet model

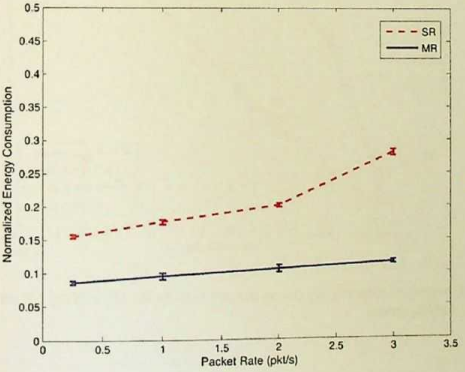

Figure 5.28: Impact of traffic load on normalized energy consumption for the MR and the SR schemes using ZebraNet model

5.7.4 Evaluation of the Multi-Radio Scheme with Manhattan Mobility Model

The Manhattan model had 40 nodes moving on a fixed grid-like path, where each vertical and horizontal lane of the grid was separated by a constant distance of 250 m. As such, for the 1000 x 1000 m^2 scenario there were 4 vertical and horizontal lanes each. Similarly, the 2000 x 2000 m^2 and 3000 x 3000 m^2 had 8 and 12 vertical and horizontal lanes each respectively.

Figure 5.29 and Figure 5.31 show the delivery ratio, and the normalized energy consumption over different node densities. From Figures 5.29, 5.31, it is clear that the delivery ratio of the multi-radio scheme is comparable to that of the single radio scheme, while the normalized energy consumption for the multi-radio is significantly less than the SR. The SR saves 84% energy at low load (0.25 pkts/s) and 72% energy at high load (3 pkts/s) over different node densities, while the multi-radio saves 89% energy at low load (0.25 pkts/s) and 86% energy at high load (3 pkts/s). Figure 5.30 shows that the average delay of the multi-radio is a bit higher than the average delay of SR over different node densities and traffic load.

Figures 5.32, 5.33, 5.34 show the delivery ratio, the average delay, and the normalized energy consumption vs the packet rate. These figures show that the multi-radio can still achieve almost the same delivery ratio for different packet rates, while it consumes half the power of SR.

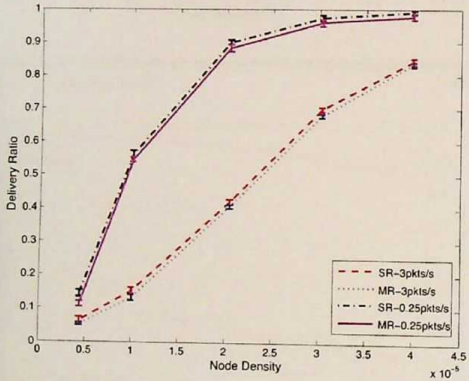

Figure 5.29: Impact of node density on the delivery ratio for the MR and the SR schemes using Manhattan mobility model

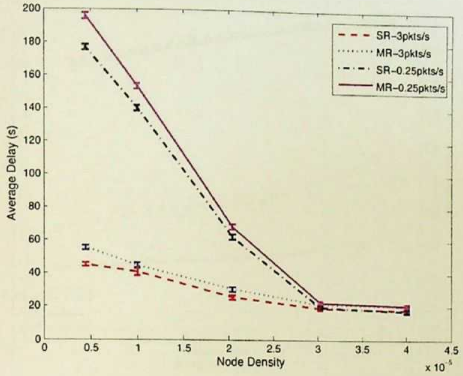

Figure 5.30: Impact of node density on average delay for the MR and the SR schemes using Manhattan mobility model

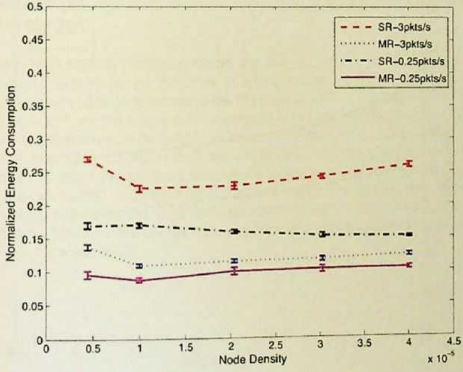

Figure 5.31: Impact of node density on normalized energy consumption for the MR and the SR schemes using Manhattan mobility model

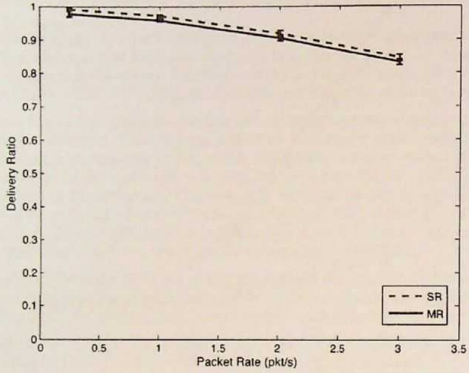

Figure 5.32: Impact of traffic load on delivery ratio for the MR and the SR schemes using Manhattan mobility model

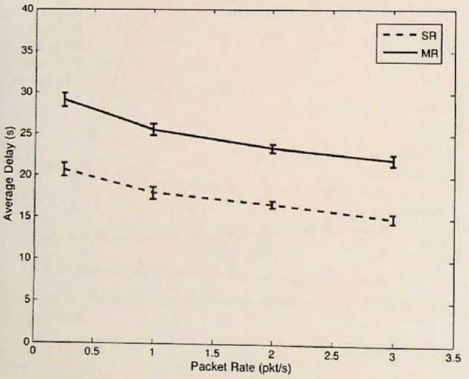

Figure 5.33: Impact of traffic load on average delay for the MR and the SR schemes using Manhattan mobility model

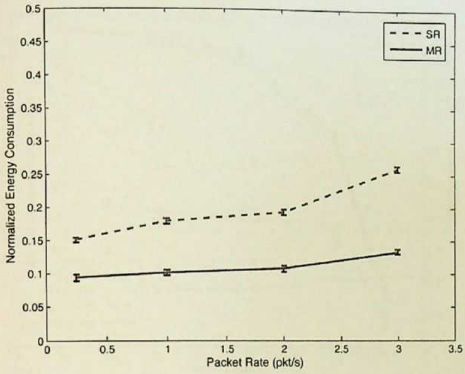

Figure 5.34: Impact of traffic load on normalized energy consumption for the MR and the SR schemes using Manhattan mobility model

5.7.5 Evaluation of the Multi-Radio Scheme with Human Mobility (Orlando) Model

While using the human mobility (Orlando) model, the delivery ratio of the multi-radio approach is once again very similar to the performance of a single-radio, as in Figure 5.35. However, the energy consumption savings increase to be in range of $84\% - 87\%$ for the multi-radio as compared to $67\% - 77\%$ for the single-radio approach, while the packet rate was varied from high to low across different node densities, as shown in Figure 5.37. The average delay for the multi-radio approach is a bit higher than the single-radio approach due to the initialization time needed for each radio to switch from sleep mode to active mode, and due to the switching time between the two radios. Figures 5.38, 5.39, 5.40 make it clear that varying the packet rate from low to high still allows the multi-radio approach to have delivery ratios similar to the single-radio scheme, however, the energy consumption reduces by a large amount, especially in the case of a high packet load.

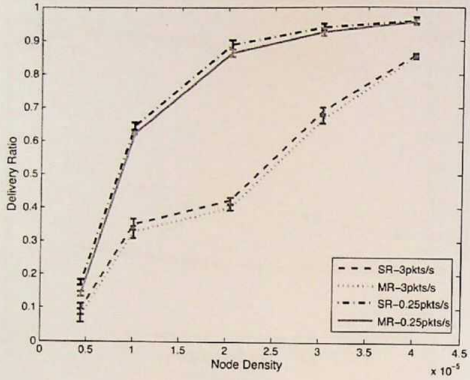

Figure 5.35: Impact of node density on the delivery ratio for the MR and the SR schemes using Orlando mobility model

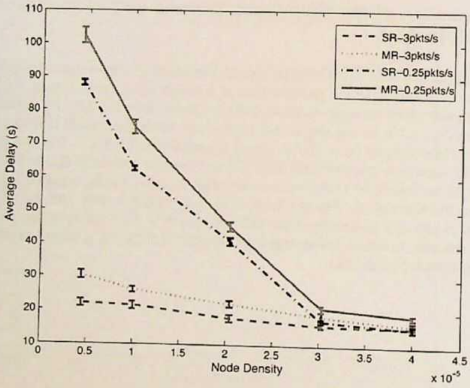

Figure 5.36: Impact of node density on average delay the for the MR and the SR schemes using Orlando mobility model

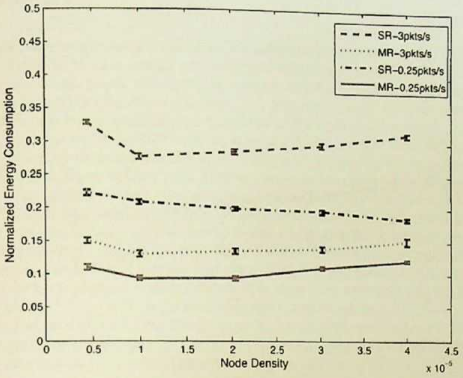

Figure 5.37: Impact of node density on normalized energy consumption for the MR and the SR schemes using Orlando mobility model

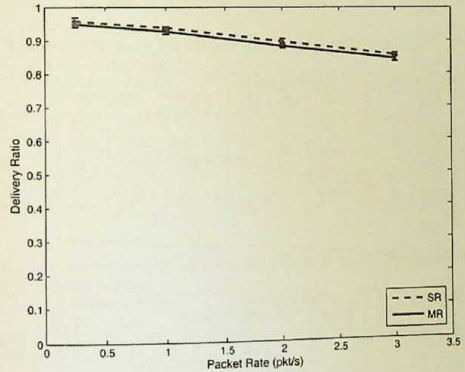

Figure 5.38: Impact of traffic load on delivery ratio for the MR and the SR schemes using Orlando mobility model

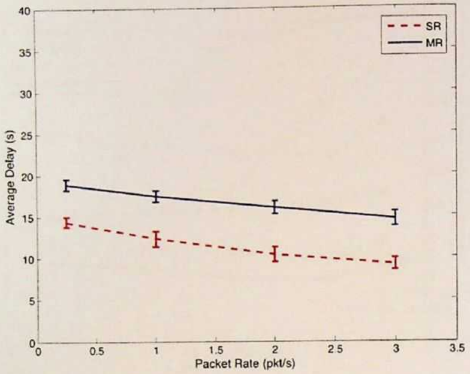

Figure 5.39: Impact of traffic load on average delay for the MR and the SR schemes using Orlando mobility model

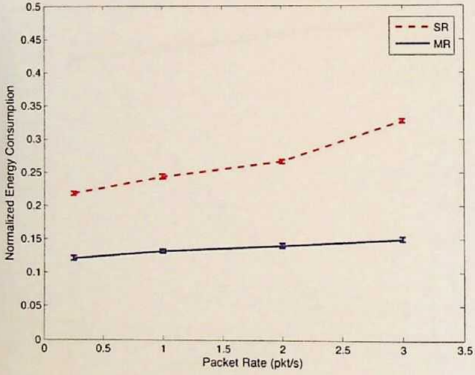

Figure 5.40: Impact of traffic load on normalized energy consumption for the MR and the SR schemes using Orlando mobility model

5.8 Summary

In this chapter, we investigated the use of an additional long range low bit rate radio in disruption tolerant networks to save energy with minimum effects on the network performance. We presented a multi radio power management scheme, in which nodes control two radio interfaces, low-power radio for neighbor discovery and high-power radio for data delivery. Using ns2 simulations, we first evaluate the performance of the multi radio scheme with high randomness in the node mobility (RWP) and we compare it with a single radio scheme (CAPM). Our simulation results show that the MR scheme can achieve significant energy savings, while achieving almost the same delivery ratio. Then we evaluate the MR scheme with more realistic and less random mobility models. Our simulation results from the four mobility models show that the MR scheme has a similar behavior under different mobility models and it still can save a significant amount of energy with respect to a single radio scheme while achieving a comparable delivery ratio for all mobility models. Table 5.4 shows a comparison between the single radio (SR) power management scheme and the multi-radio (MR) power management scheme at low data rate for 5 different mobility models. It is clear from this table that the MR scheme saves more energy ($87\% - 93\%$) while the single radio scheme saves ($77\% - 86\%$) . Increasing the data rate has less effect on the MR scheme than the single radio scheme, so when data rate is increased, the MR scheme still can save significant energy ($84\% - 90\%$) while the sigle radio saves less energy ($67\% - 76\%$) as shown in Table 5.5.

Based on the aforementioned results, our MR scheme is a robust power management scheme for disruption tolerant networks that outperforms a single radio scheme, since it achieves almost the same delivery ratio with a bit more latency while at the same time it saves a significant amount of energy compared to a single radio scheme. In addition, our MR scheme shows robust performance in the face of node mobility model.

Table 5.4: Comparison between the SR and the MR performance across different mobility models at low data rate (0.25 pkt/s)

	Delivery Ratio			Average Delay (s)			Energy Saving		
	SR	MR	Delta	SR	MR	Delta	SR	MR	Delta
RWP	99%	98%	1%	55	95	40	85%	90%	5%
MF	99%	99%	0%	22	29	7	86%	93%	7%
Zebra	98%	97.5%	0.05%	22	25	3	85%	91%	6%
Manhattan	99%	98%	1%	21	29	8	84%	89%	5%
Orlando	96%	95%	1%	14	19	5	77%	87%	10%

Table 5.5: Comparison between the SR and the MR performance across different mobility models at high data rate (3 pkt/s)

	Delivery Ratio			Average Delay (s)			Energy Saving		
	SR	MR	Delta	SR	MR	Delta	SR	MR	Delta
RWP	94%	93%	1%	32	35	3	73%	88%	15%
MF	90%	89.5%	0.05%	7	13	6	76%	90%	14%
Zebra	88%	87%	1%	14	15	1	73%	89%	16%
Manhattan	84%	83%	1%	15	22	7	72%	86%	14%
Orlando	86%	85%	1%	9	14	5	67%	84%	17%

6 Energy Conservation and Power Management for Underwater Acoustic Sensor Networks

Energy conservation is a challenging issue in underwater networks. The limited battery energy supply makes it important to find solutions that allow nodes to operate for months without having to recharge or replace batteries [9, 114]. Energy conservation techniques in underwater networks are not entirely different from terrestrial networks. Some efforts save energy in underwater networks by integrating power management protocols in the MAC layer. These protocols such as UWAN-MAC [115] use sleep schedules, as in S-MAC [116] for terrestrial sensor network. However, such protocols avoid RTS/CTS exchanges due to the high propagation delay and they are useful only in dense networks while the node density in underwater networks is expected to be lower due to the application requirements and due to the expensive cost of deploying such networks.

Achieving power efficient high bit rate communications underwater is of high importance since most existing acoustic modems provide either a very low bit rate or higher bit rate with a very high power consumption. To overcome this shortfall the authors of [117] have designed underwater sensor nodes equipped with an acoustic modem with a low data rate and also an optical modem with a high data rate in shallow water dense topology conditions. The method of switching between the acoustic modem and the optical modem to achieve the desired bit rate is effective in reducing the mode change time of the method proposed in [111] but the use of an optical method restricts the range of high bit rate communication to very short distances since optical data transfer methods do not work reliably over long ranges, if at all, underwater.

The authors of [118] highlight the need for developing algorithms to specifically maximize energy efficiency in sparse underwater acoustic networks in order to facilitate long term deployments of such networks, since once a network is deployed the issue of limited battery resources becomes particularly important as a result of the difficulty and high cost associated with recharging node batteries [119].

The authors of [118] show that there are significant differences between underwater acoustic modems and radio transmitters by comparing multiple idle-time power management techniques ranging from no sleep or wakeup state modes, an optimal sleep mode and a wakeup mode protocol. Their further work discussed in [111] uses a single acoustic modem with an ultra low power low bit rate mode that is used purely in listening mode in order to conserve power and switches to either a high bit rate or low bit rate receive and transmit mode. The authors of the paper recommend using the wakeup mode and switching between high power

and low power transmit/receive modes for the acoustic modem. Though this work addresses sleep-cycle based power efficiency in underwater networks, it does not focus on disruption tolerance and the likely sparse topology, thereby, creating the need for exploring such similar protocols as well.

Due to the adverse underwater environmental conditions, an underwater sensor network is usually viewed as Disruption Tolerant Network. In this chapter, we investigate the use of two acoustic modems in shallow underwater sensor networks to save energy. We present a Multi-Acoustic Modem (MAM) power management scheme that is similar to the MR scheme presented in Chapter 5.

6.1 The Multi-Acoustic Modem (MAM) Power Management Scheme

The MAM scheme uses two acoustic modems instead of two radios for communication underwater. The low power acoustic modem (low data rate) is used for neighbor discovery and the high power acoustic modem (high data rate) for data delivery. The MAM scheme flow chart is similar to the MR scheme shown in Figure 5.4 but with HPR now being a High Power Acoustic Modem (HPAM) and LPR a Low Power Acoustic Modem (LPAM). The sleep pattern (W,C,K) values is the MAM scheme are similar to the sleep pattern values of the MR scheme. To this end, we present an evaluation of the MAM scheme via simulation along with the PROPHET routing protocol, demonstrating that the use of a low power acoustic modem results in saving energy.

6.2 Acoustic Modems

Acoustic modem technology nowadays provides commercial modems such as the Teledyne-Benthos modem [120], the LinkQuest [121] modem as well as modems developed for research purposes such as the Woods Hole Oceanographic Institution's (WHOI) modem. In this evaluation we use the WHOI modem [122].

The WHOI acoustic modem has two modes of operations: low bit rate mode and high bit rate mode; the low rate transmission mode uses Frequency Shift Keying (FSK) modulation with 80 bits per seconds bit rate, while the high rate transmission mode uses Phase Shit Keying (PSK) with variable bit rate between 2500 and 5000 bits per second. The modem converts the electrical signal to acoustic signal and vice-versa using transducers.

The WHOI modem has five states, and each state has different power consumption. The first state is the transmit state, the modem consumes between 10 - 50 W based on the transmission distance. Second, the listen (Idle) state, in which, the modem consumes 80 mW while it is listening to packets. Third, the receive low rate state, in this state, the modem consumes 80 mW in order to receive low data rate packet. After that, the receive high rate state, in this state, the modem consumes 3 W while it is receiving high data rate packet. Finally, the sleep state, in which the modem is turned off. Table 6.1 shows the WHOI modem properties.

Table 6.1: Properties of the WHOI modems [111].

Name	Tx Power	Rx Power	Type	Data Rate
WHOI	50 Watt	3 Watt	High Power	5600 bps
WHOI	10 Watt	80 mWatt	Low Power	80 bps

6.3 Simulation Setup

In our work we used the underwater channel model that is introduced in [76]. We integrated this channel into ns2 [112, 123]. In general, ns2 divides the channel and the physical layer functions into four components: propagation model, channel model, physical model, and modulation model. The propagation model is responsible for the signal-to-noise ratio at the receiver taking into account the ambient noise and the attenuation. The total attenuation is calculated based on spreading loss [75] and the Thorp's approximation [78, 79] as explained in Chapter 4. The channel model in ns2 maintains the node list used to calculate neighbor sets and propagation delays. The calculation of the propagation delay taking into accounts: the speed of the sound, the depth of the water, the temperature of the water, and salinity. There are five zones in which the temperature change depends on the depth of the water [76, 124]. The salinity value is set to the global observed average value (35 parts-per-thousand). The physical layer is modified to approximate the properties of the WHOI acoustic modem.

To evaluate the Multi-Acoustic Modem (MAM) scheme, we use a grid area of 1000 x 1000 m^2 to evaluate the MAM scheme. Each scenario is set up with different number of stationary nodes varied between 3 - 25 nodes that are distributed randomly in the grid area. We use constant bit rate traffic with 10 CBR flows and a packet size of 512 bytes. The traffic generation for each flow varied from 0.25 pkts/s to 2 pkts/s. The sources and destinations of CBR flows are randomly selected prior to each run.

Each simulation runs for 2000 seconds, with 1000 seconds being utilized as a warm-up period, and the performance data being recorded only for the last 1000 seconds of the simulation. In order to minimize the possibility of only a corner case being encountered, every reported result is an average taken over 5 runs, and the observed variance are within $\pm 5\%$. In our simulation we utilized the properties of the WHOI Micromodem, as shown in Table 6.1, since it provides both, a high power and low power mode.

6.3.1 Performance Evaluation Metrics

In order to evaluate the performance of the multi-acoustic scheme, we utilize the following metrics:

1. Normalized Energy Consumption: The ratio of the energy consumption when multi-acoustic scheme is applied divided by the energy consumption in the absence of energy conservation.

2. Delivery Ratio: The ratio of the number of the successfully received data packets divided by the number of the data packets sent.

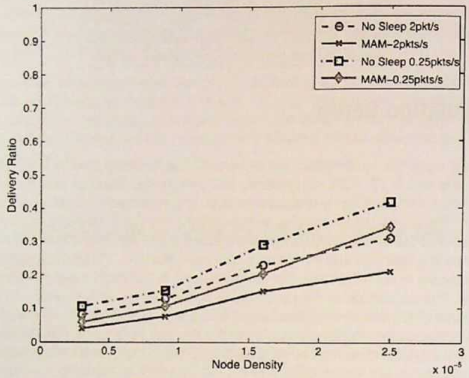

Figure 6.1: Impact of varying node density on the delivery ratio for the MAM scheme

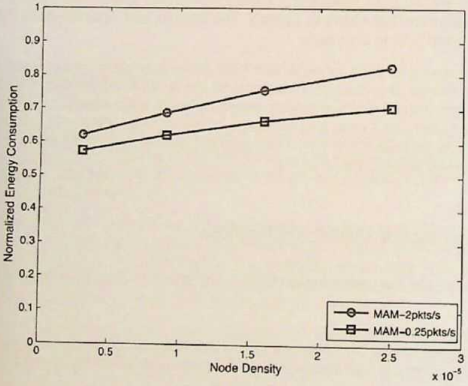

Figure 6.2: Impact of varying node density on normalized energy consumption for the MAM scheme

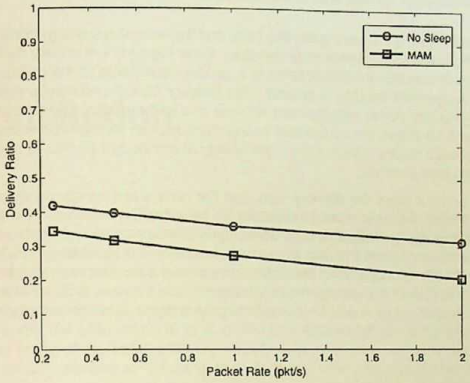

Figure 6.3: Impact of traffic load on delivery ratio for the MAM scheme

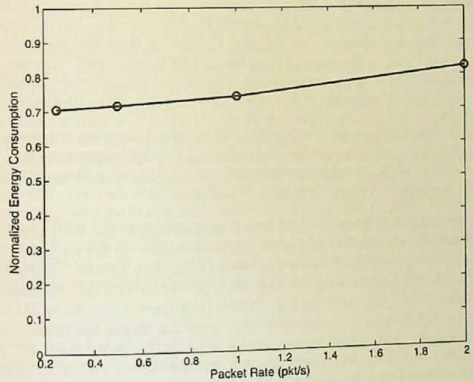

Figure 6.4: Impact of traffic load on normalized energy consumption for the MAM scheme

6.3.2 Evaluation of the Multi-Acoustic Modem Scheme

Figure 6.1 and Figure 6.2 show the delivery ratio, and the normalized energy consumption over different traffic loads and different node densities. From Figure 6.1, it is clear that the delivery ratio of the multi-acoustic modem scheme is a bit lower compared to the delivery ratio when no power management scheme is applied. The delivery ratio in underwater networks is low without applying any power management scheme due to the underwater channel characteristics. Figure 5.13 shows the normalized energy consumption for the multi-acoustic modem. The multi-acoustic modem saves $30\% - 42\%$ energy at low load (0.25 pkts/s) and $17\% - 38\%$ energy at high load (2 pkts/s).

Figures 6.3 and 6.4 show the delivery ratio, and the normalized energy consumption vs the packet rate. These figures show that increasing the packet rate will decrease the delivery ratio, while it increases the normalized energy consumption. In fact, using high traffic load (2pkts/s) overloads the network since this load exceeds the capacity of the acoustic modem. When the traffic load exceeds the capacity of the acoustic modem, the modem can not handle the extra packets and then these packets start to be accumulated in a queue. A network becomes fully saturated when the queue is full, which leads to packet drops, and this in turn decreases the delivery ratio as shown in Figures 6.3.

6.4 Summary

In this chapter, we investigated the use of two acoustic modems to save energy in underwater acoustic networks. We presented a multi acoustic modem power management scheme (MAM), in which nodes control two acoustic modems, a low power acoustic modem for neighbor discovery and a high power acoustic modem for data delivery. We evaluated the multi acoustic modem scheme using ns2 simulations. Our results show that the MAM achieve low delivery ratio while it can save energy both at low and high traffic load. However, the delivery ratio achieved by MAM in underwater networks is lower than the delivery ratio achieved by the MR scheme in terrestrial networks. In fact, the delivery ratio in underwater networks using the PROPHET routing protocol is low without applying any power management scheme due to the underwater channel characteristics. In general, most of the intermittent routing protocols in underwater networks achieve either low or medium delivery ratio [125]. For example epidemic routing [31], which is originally designed for terrestrial networks or protocols that are designed for underwater networks such as VBF [94] and FBR [97].

The multi acoustic modem scheme saves less energy compared to the MR scheme in terrestrial networks and this is due to the fact that the relative costs of various interface modes are different for acoustic devices than for radios. Most of the radios have similar costs for receiving and idling. On the other hand, acoustic modems have very high transmission costs compared to receive costs.

7 Conclusion

Disruption tolerant networks (DTNs) arise as a feasible approach to address technical issues in heterogeneous networks that may lack continuous network connectivity. One of the major concerns DTNs are dealing with is discontinuous connectivity and opportunistic contacts for asynchronous communications in remote and hazardous areas where the energy sources are often constrained. DTNs are also often assumed to operate over a long period of time, which makes energy conservation a major and critical issue. Though DTNs have primarily been researched under the assumption of radio-based terrestrial networks and planned networks in space, yet many of the techniques are directly applicable in underwater networks since underwater sensor networks are prone to disruptions and often have sparse topologies.

In this thesis, we address energy conservation for sparse DTNs that are characterized by frequent partitions, intermittent connectivity, and message delivery delays. Studies have shown that in DTNs, most of the energy is consumed while nodes search for contacts using radio interfaces. These contacts are used as relays to forward the data to its destinations. Therefore, we designed a power management scheme called the Multi-Radio (MR) power management scheme that uses two complementary radios: a high-power radio and a low-power radio. By utilizing two radios instead of one, we are able to implement an asynchronous, on-demand energy conservation scheme that eliminates the idle time of a single high-power radio, and only allows the high-power radio to consume power in the sleep mode or while it is transmitting and receiving data. While the high-power radio is only called upon to perform data delivery when necessary, the low-power radio remains active for asynchronous neighbor discovery.

We first evaluated the performance of the MR scheme with high randomness in the node mobility (RWP) and we compared it with a single radio scheme (CAPM). Our simulation results show that the MR scheme can achieve significant energy savings, while achieving almost the same delivery ratio. Then we evaluated the MR scheme with more realistic and less random mobility models to investigate the impact of different node mobility patterns on the MR scheme. We study the effects of *Manhattan*, *Message Ferry*, *Human* and *Zebra* mobility models. Our simulation results from the four mobility models show that the MR scheme has a similar behavior under different mobility models and it still can save a significant amount of energy with respect to a SR scheme while achieving a comparable delivery ratio for all mobility models. However, the MR scheme has more delay than the SR scheme along with all mobility models. It is worth to mention that though our results are obtained using specific technologies (WaveLan, XTend), the MR scheme still can save energy using different technologies as long as the low power radio consumes less power than the high power radio in the 4 states (transmit, receive, idle, sleep) and especially in idle state since in DTNs, most of the energy is consumed in searching mode while nodes listen to each other to communicate. However, the low power radio has to be chosen such that it provides a transmission range equal to the high power radio transmission range.

Finally, the dissertation presented a power management technique for shallow underwater networks. We presented a Multi-Acoustic Modem (MAM) power management scheme that is similar to the MR scheme. The MAM scheme uses two acoustic modems instead of two radios for communication underwater. A low power acoustic modem (low data rate) is used for neighbor discovery and a high power acoustic modem (high data rate) for data delivery. The simulation results show that the MAM scheme can save energy both at low and high traffic load. However, the delivery ratio achieved by the MAM scheme in underwater networks is lower than the delivery ratio achieved by the MR scheme in terrestrial networks. In fact, the delivery ratio in underwater networks using the PROPHET routing protocol is low without applying any power management scheme due to the underwater channel characteristics. Our simulation results also show that the multi acoustic modem scheme saves less energy compared to the MR scheme in terrestrial networks. This is due to two reasons: First, the relative costs of various interface modes are different for acoustic modems compared to radios. Most of the radios have similar costs for receiving and idling. On the other hand, acoustic modems have very high transmission cost compared to receive costs. The second reason are the underwater channel characteristics. From Shannons's law in (4.14), it is clear that achieving better throughputs requires more channel capacity and in turn increasing the channel capacity requires higher power signals, which means nodes need to consume much energy in transmission, and this affects the total energy saving in underwater networks.

7.1 Limitation of Thesis

Designing power management schemes in terrestrial and underwater disruption networks remains challenging due to the sparse topologies and rare communication opportunities in such networks. In this thesis we presented the MR power management scheme for terrestrial disruption tolerant networks and the MAM power management scheme for underwater disruption sensor networks. The final goal of both schemes is to save energy and extend the network lifetime with the minimum degradation of the network performance. Though the MR scheme saves significant energy and at the same time it achieves a good delivery ratio, it added some delay especially at low node densities, which might be an issue in some applications. We evaluated the MR scheme along with the PROPHET routing protocol, and having only one routing protocol being evaluated could be considered a limitation.

The MAM scheme was designed for 2D shallow underwater networks in order to save energy but it achieves low delivery ratio. However, most of the intermittent routing protocols in underwater networks achieve either low or medium delivery ratio [125]. For example epidemic routing [31], which is originally designed for terrestrial networks or protocols that are designed for underwater networks such as VBF [94] and FBR [97]. Therefore, the MAM scheme would need to be evaluated with more routing protocols such as adaptive routing protocol for underwater disruption sensor networks.

The thesis has limitation in the traffic models that had been used in our evaluation (simulations) for both the MR and the MAM schemes. We only use CBR traffic models, and we ignore retransmissions. Both schemes need to be evaluated with other traffic models. The thesis as well has lack of experimental validation.

7.2 Future Work

The design of power management schemes is greatly affected by routing protocols. In this thesis, we designed a MR power management scheme along with the PROPHET routing protocol. As a next possible step, it would be interesting to study the behavior of the MR scheme with other routing protocols such as MaxProp. Furthermore, it would be interesting to evaluate the MR power management scheme with other mobility models such as Truncated Levy Walk mobility.

All the power management schemes for disruption tolerant networks in the literature are evaluated in different scenarios and the authors compare the performance of their scheme by calculating the percentage of the saving energy in the network as related to the case when the network does not use any power management scheme. Therefore, an open issue and future work would be to evaluate all the aforementioned power management schemes in Chapter 3 for a set of well defined scenarios and to compare their performance relative to each other.

Another research direction is to explore adaptive radios for energy saving techniques in disruption tolerant networks. These radios use an RF management technology that allows nodes to determine their transmit power and channel settings based on what they detect. The nodes set their channel and power settings decisions based on the RF environment. It would be interesting to explore how adaptive radios behave in DTNs and how much energy they can save, and to study the adaptive radio effects on network performance as well.

Finally, we believe that DTN applications and resource management play a significant role in the future ubiquitous computing. Therefore, it would be interesting to explore what applications can DTNs be applied for, and to investigate how to manage the limited resources for such applications.

List of Figures

List of Tables

List of Abbreviations

AODV	Ad hoc On-demand Distance Victor
AUVs	Autonomous Underwater Vehicles
BWT	Burrows-Wheeler Transform
CAM	Continuous Aware Mechanism
CAPM	Context Aware Power Management
CBR	Constant Bit Rate
CTS	Clear To Send
DSDV	Destination Sequence Distance Vector
DSR	Dynamic Source Routing
DTNs	Disruption Tolerant Networks
DUCS	Distributed Underwater Clustering Scheme
FBR	Focus Beam Routing
FIMF	Ferry Initiated Message Ferry
FSK	Frequency Shift Keying
GFG	Greedy Face Greedy
GPS	Global Positioning System
GPSM	Generalized Power Saving Mechanism
MAC	Media Access Control
MAM	Multi Acoustic Modem
MANETs	Mobile Ad-hoc Networks
MF	Message Ferry
MR	Multi Radio
NIMF	Node Initiated Message Ferry

OSI	Open Systems Interconnection
PROPHET	Probabilistic Routing Protocol using History of Encounters and Transitivity
PSK	Phase Shit Keying
PSM	Power Saving Mechanism
PTKF	Partial Topology Knowledge Forwarding
RF	Radio Frequency
RLE-ST	Structured Transpose with Run Length Encoding
RTS	Request To Send
RWP	Random Waypoint
SNR	Signal-to-Noise Ratio
SPSM	Short Range Radio Dependent Power Saving Mechanism
SR	Single Radio
TORA	Temporally Ordered Routing Algorithm
VBF	Vector-Based Forwarding Protocol
WHOI	Woods Hole Oceanographic Institution
WLAN	Wireless Local Area Networks
WoW	Wake-on-Wireless
WWAN	Wireless Wide Area Networks

A Publications

A.1 Related Papers

1. I. Tumar and J. Schönwälder. *Resource Management of Disruption Tolerant Networks.* In proceedings of the 2nd Conference on Autonomous Infrastructure, Management and Security (AIMS 2008), Bremen, July 2008. Springer LNCS 5127.

2. I. Tumar, A. Sehgal, and J. Schönwälder. *Power Management for Sparse Acoustic Underwater Networks.* In proceedings of the 6th IEEE Conference on Sensor, Mesh and Ad Hoc Communications and Networks (SECON 2009), June 2009.

3. A. Sehgal, I. Tumar, and J. Schönwälder. *AquaTools: An Underwater Acoustic Networking Simulation Toolkit.* In proceedings of IEEE Oceans, Sydney, May 2010.

4. I. Tumar, A. Sehgal, and J. Schönwälder. *Performance Evaluation of a Multi-Radio Energy Conservation Scheme for Disruption Tolerant Networks.* In proceedings of the 8th ACM International Symposium on Mobility Management and Wireless Access, Bodrum, Turkey, October 2010.

5. I. Tumar, A. Sehgal, and J. Schönwälder: *Impact of Mobility Patterns on the Performance of a Disruption Tolerant Network with Multi-Radio Energy Conservation.* In proceedings of the 25th International Conference on Advanced Information Networking and Applications (AINA-2011), Biopolis, Singapore, March 2011.

A.2 Other Papers

1. A. Sehgal, I. Tumar, and J. Schönwälder. *Variability of Available Capacity due to the Effects of Depth and Temperature in the Underwater Acoustic Communication Channel.* In proceedings of IEEE OCEANS, Bremen, May, 2009.

2. K.D. Korte, I. Tumar, and J. Schönwälder. *Evaluation of 6lowpan Implementations.* In proceedings of the 4th IEEE International Workshop on Practical Issues in Building Sensor Network Applications (SenseApp 2009), IEEE, October 2009.

3. A. Sehgal, I. Tumar, and J. Schönwälder. *AquaTools: An Underwater Acoustic Networking Simulation Toolkit.* IEEE Oceans, Sydney, May 2010

4. A. Sehgal, I. Tumar, and J. Schönwälder. *Effects of Climate Change and Anthropogenic Ocean Acidification on Underwater Acoustic Communications.* In proceedings of IEEE Oceans, Sydney, May 2010

References

[1] P. Juang, H. Oki, W. Want, M. Maronosi, L. Peh, and D. Rubenstein. Energy-Efficient Computing for Wildlife Tracking: Design Tradeoffs and Early Experiences with ZebraNet. *ACM SIGPLAN Notices*, 37(10):96–107, October 2002.

[2] I. F. Akyildiz, D. Pompili, and T. Melodia. Underwater Acoustic Sensor Networks: Research Challenges. *Ad Hoc Networks (Elsevier)*, 3:257–279, 2005.

[3] I. F. Akylidiz, B. A. Ozgur, C. Chen, F.Fang, and W. Su. InterPlaNetary Internet: State-of-the-Art and Research Challenges. *Elsevier Computer Networks*, 43:75112, 2003.

[4] J. Ott and D. Kutscher. Drive-thru Internet: IEEE 802.11b for "Automobile" Users. In *Proceedings of the IEEE INFOCOM*, 2004.

[5] I. F. Akylidiz, X. Wang, and W. Wang. Wireless Mesh Networks: A Survey . *Elsevier Computer Networks*, 47:445487, 2005.

[6] I. F. Akylidiz, W. Su, and Y. Sankarasubramaniam E. Cayirci. Wireless Sensor Networks: A Survey . *Elsevier Computer Networks*, 38:393422, 2002.

[7] I. F. Akylidiz and I. H. Kasimoglu. Wireless Sensor and Actor Networks: Research Challenges. *Elsevier Ad Hoc Networks*, 2:351367, 2004.

[8] D. Culler, D. Estrin, and M. Srivastava. Overview of Sensor Networks. *IEEE Computer*, 2004.

[9] J. Partan, J. Kurose, and B. N. Levine. A Survey of Practical Issues in Underwater Networks. In *Proceedings of the 1st ACM international workshop on underwater networks, (WUWNet'06)*, pages 17–24, New York, NY, USA, 2006. ACM.

[10] J.A. Davis, A.H. Fagg, and B.N. Levine. Wearable Computers as Packet Transport Mechanisms in Highly-Partitioned Ad-Hoc Networks. In *Proceedings of the Fifth International Symposium on Wearable Computers*, pages 141–148, October 2001.

[11] S. Jain, K. Fall, and R. Patra. Routing in a Delay Tolerant Network. In *Proceedings of the 2004 Conference on Applications, Technologies, Architectures, and Protocols for Computer Communications, (SIGCOMM '04)*, pages 145–158, New York, NY, USA, August 30 - September 03 2004. ACM Press.

[12] J. Burgess, B. Gallagher, D. Jensen, and B. N. Levine. MaxProp: Routing for Vehicle-Based Disruption-Tolerant Networks. In *Proceedings of the 25th IEEE International Conference on Computer Communications, (INFOCOM'06)*, pages 1–11, April 2006.

[13] S. Farrell and V. Cahill. *Delay and Disruption Tolerant Networking*. Artech House, Inc., Norwood, MA, USA, 2006.

[14] H. Jun. *Power Management in Disruption Tolerant Networks*. PhD thesis, Georgia Institute of Technology, 2007.

[15] K. Fall. A Delay-Tolerant Network Architecture for Challenged Internets. In *Proceedings of the 2003 Conference on Applications, Technologies, Architectures, and Protocols for Computer Communications (SIGCOMM '03)*, pages 27–34, New York, NY, USA, August 2003. ACM Press.

[16] R.C. Shah, S. Roy, S. Jain, and W. Brunette. Data MULEs: Modeling a Three-Tier Architecture for Sparse Sensor Networks. In *Proceedings of the First IEEE International Workshop on Sensor Network Protocols and Applications*, pages 30–41, May 2003.

[17] W. Zhao, M. Ammar, and E. Zegura. A Message Ferrying Approach for Data Delivery in Sparse Mobile Ad Hoc Networks. In *Proceedings of the 5th ACM International Symposium on Mobile Ad Hoc Networking and Computing, (MobiHoc '04)*, pages 187–198, New York, NY, USA, May 2004. ACM Press.

[18] V. Cerf, S. Burleigh, A. Hooke, L. Torgerson, R. Durst, K. Scott, K. Fall, and H. Weiss. Delay-Tolerant Networking Architecture. RFC 4838, April 2007.

[19] R. H. Kravets. *Cooperative Solutions to The Dynamic Management of Communication Resources*. PhD thesis, Georgia Institute of Technology, 1998.

[20] G. Pottie and W. Kaiser. Wireless Integrated Network Sensors. *Communication of ACM*, 43(5):51–58, 2000.

[21] L.M. Feeney and M. Nilsson. Investigating The Energy Consumption of a Wireless Network Interface in an Ad Hoc Networking Environment. In *Proceedings of the Twentieth Annual Joint Conference of the IEEE Computer and Communications Societies, (INFOCOM'01)*, volume 3, pages 1548–1557, 22-26 April 2001.

[22] M. Stemm and R. H. Katz. Measuring and Reducing Energy Consumption of Network Interfaces in Hand-Held Device. *IEICE Transactions on Communication*, E80-B(8):1125–1131, August 1997.

[23] E. P. C. Jones and P. A. S. Ward. Routing Strategies for Delay-Tolerant Networks. *Computer Communication Review*, 2008.

[24] J. Shen, S. Moh, and I. Chung. Routing Protocols in Delay Tolerant Networks: A Comparative Survey. In *Proceedings of The 23rd International Technical Conference on Circuits/Systems, Computers and Communications (ITC-CSCC 2008)*, 2008.

[25] D.J. Goodman, J. Borras, N.B. Mandayam, and R.D. Yates. INFOSTATIONS: A New System Model for Data and Messaging Services. In *IEEE 47th Vehicular Technology Conference*, volume 2, pages 969–973, 4-7 May 1997.

[26] M. Ahmed, S. Krishnamurthy, R. Katz, and S. Dao. Trajectory Control of Mobile Gateways for Range Extension in Ad Hoc Networks. *Computer Networks*, 39(6):809–825, August 2002.

[27] H. Wu, R. Fujimoto, M. Hunter, and R. Guensler. An Architecture Study of Infrastructure-Based Vehicular Networks. In *Proceedings of the 8th ACM International Symposium on Modeling, Analysis and Simulation of Wireless and Mobile Systems, (MSWiM '05)*, pages 36–39, New York, NY, USA, October 2005. ACM Press.

[28] I. F. Akyildiz, D. Pompili, and T. Melodia. Challenges for Efficient Communication in Underwater Acoustic Sensor Networks. *SIGBED Rev.*, 1(2):3–8, 2004.

[29] Z. Peng, J. Cui, B. Wang, K. Ball, and L. Freitag. An Underwater Network Testbed: Design, Implementation and Measurement. In *Proceedings of the second workshop on underwater networks, (WuWNet'07)*, pages 65–72, New York, NY, USA, 2007. ACM.

[30] J.G. Proakis, E.M. Sozer, J.A. Rice, and M. Stojanovic. Shallow Water Acoustic Networks. *IEEE Communications Magazine*, 39(11):114–119, 2001.

[31] A. Vahdat and D. Becker. Epidemic Routing for Partially Connected Ad Hoc Networks. *Technical Report CS-2006, Duke University*, April 2000.

[32] A. Lindgren, A. Doria, and O. Schelén. Probabilistic Routing in Intermittently Connected Networks. *SIGMOBILE Mobile Computing and Communications Review*, 7(3):19–20, July 2003.

[33] D. B. Terry, M. M. Theimer, K. Petersen, A. J. Demers, M. J. Spreitzer, and C. H. Hauser. Managing Update Conflicts in Bayou, a Weakly Connected Replicated Storage System. In *Proceeding of The Fifteenth ACM Symposium on Operating Systems Principles*, December 1995.

[34] M. M. Bin Tariq, M. Ammar, and E. Zegura. Message Ferry Route Design for Sparse Ad Hoc Networks with Mobile Nodes. In *Proceedings of the 7th ACM international symposium on Mobile ad hoc networking and computing (MobiHoc'06)*, pages 37–48, 2006.

[35] Probabilistic Routing Protocol using History of Encounters and Transitivity (PRoPHET) Internet Draft. URL:http://tools.ietf.org/html/draft-irtf-dtnrg-prophet-05, Feb 2010.

[36] C. Bettstetter, G. Resta, and P. Santi. The Node Distribution of the Random Waypoint Mobility Model for Wireless Ad Hoc Networks. *IEEE Transactions on Mobile Computing*, 2(3):257–269, March 2003.

[37] C.E. Perkins and E.M Royer. Ad-Hoc On-Demand Distance Vector Routing. In *Proceedings in Second IEEE Workshop on Mobile Computing Systems and Applications, (WMCSA '99)*, pages 90–100, February 1999.

[38] E. Hyytiä and J. Virtamo. Random Waypoint Mobility Model in Cellular Networks. *Wireless Networks*, 13(2):177–188, April 2007.

[39] F. Bai, N. Sadagopan, and A. Helmy. Important: A Framework to Systematically Analyze the Impact of Mobility on Performance of Routing Protocols for Ad Hoc Networks. In *Proceedings of the Twenty-Second Annual Joint Conference of the IEEE Computer and Communications (INFOCOM'03)*, April 2003.

[40] I. Rhee, M. Shin, S. Hong, K. Lee, S. Kim, and S. Chong. CRAWDAD Data Set ncsu/mobilitymodels. http://crawdad.cs.dartmouth.edu/ncsu/mobilitymodels, July 2009.

[41] G. Anastasi, M. Conti, M. Francesco, and A. Passarella. *Ad Hoc Networks*, 7(3):537–568, May 2009.

[42] P. Santi. Topology Control in Wireless Ad Hoc and Sensor Networks. *ACM Computing Survey*, 37(2):164–194, June 2005.

[43] E. Fasolo, M. Rossi, J. Widmer, and M. Zorzi. In-network aggregation techniques for wireless sensor networks: a survey. *IEEE Wireless Communications*, 14(2):70–87, April 2007.

[44] I. Demirkol, C. Ersoy, and F. Alagoz. MAC Protocols for Wireless Sensor Networks: a Survey. *IEEE Communications Magazine*, 44(4):115–121, June 2006.

[45] S. Singh and C. S. Raghavendra. PAMAS: Power Aware Multi-Access Protocol with Signaling for Ad Hoc Networks. *ACM Computer Communication Review*, 28(3):5–26, July 1998.

[46] W. Ye, J. Heidemann, and D. Estrin. An Energy-Efficient MAC protocol for Wireless Sensor Networks. In *Proceedings of the IEEE INFOCOM*, pages 1567–1576, New York, NY, USA, June 2002.

[47] J. Polastre, J. Hill, and D. Culler. Versatile Low Power Media Access for Wireless Sensor Networks. In *Proceedings of the 2nd International Conference on Embedded Networked Sensor Systems, (SenSys'04)*, pages 95–107, New York, NY, USA, November 2004. ACM.

[48] W. S. Conner, J. Chhabra, M. Yarvis, and L. Krishnamurthy. Experimental Evaluation of Synchronization and Topology Control for In-Building Sensor Network Applications. In *Proceedings of the 2nd ACM International Conference on Wireless Sensor Networks and Applications, (WSNA'03)*, pages 38–49, New York, NY, USA, September 2003. ACM.

[49] T. V. Dam and K. Langendoen. An Adaptive Energy-Efficient MAC Protocol for Wireless Sensor Networks. In *Proceedings of the 1st international conference on Embedded Networked Sensor Systems (SenSys'03)*, pages 171–180, New York, NY, USA, 2003. ACM.

[50] W. Ye, J. Heidemann, and D. Estrin. Medium Access Control With Coordinated Adaptive Sleeping for Wireless Sensor Networks. *IEEE/ACM Transactions on Networking*, 12(3):493–506, June 2004.

[51] G. Lu, B. Krishnamachari, and C. S. Raghavendra. An Adaptive Energy-Efficient and Low-Latency MAC for Data Gathering in Sensor Networks. In *Proceeding of 18th International Parallel and Distributed Processing Symposium*, pages 224–231, April 2004.

[52] R. Zheng, J. C. Hou, and L. Sha. Asynchronous Wakeup for Ad Hoc Networks. In *Proceedings of the 4th ACM International Symposium on Mobile Ad Hoc Networking and Computing, (MobiHoc '03)*, pages 35–45, New York, NY, USA, June 2003. ACM Press.

[53] Y. Tseng, C. Hsu, and T. Hsieh. Power-Saving Protocols for IEEE 802.11-Based Multi-Hop Ad Hoc Networks. In *Proceedings of the Twenty-First Annual Joint Conference of the IEEE Computer and Communications Societies, (INFOCOM'02)*, volume 1, pages 200–209, 23-27 June 2002.

[54] Y. Tseng, C. Hsu, and T. Hsieh. Power-Saving Protocols for IEEE 802.11-Based Multi-Hop Ad Hoc Networks. *Computer Networks*, 43(3):317–337, 2003.

[55] Wireless LAN Medium Access Control (MAC) and Physical Layer (PHY) Specifications. IEEE Standard 802.11, June 1999.

[56] C. Schurgers, V. Tsiatsis, S. Ganeriwal, and M. B. Srivastava. Optimizing Sensor Networks in the Energy-Latency-Density Design Space. *IEEE Transactions on Mobile Computing*, 1(1):70–80, 2002.

[57] X. Yang and N. Vaidya. A Wakeup Scheme for Sensor Networks: Achieving Balance between Energy Saving and End-to-end Delay. In *Proceedings of the 10th IEEE Real-Time and Embedded Technology and Applications Symposium (RTAS'04)*, pages 19–26, Washington, DC, USA, 2004. IEEE Computer Society.

[58] H. Jun, M. H. Ammar, and E.W Zegura. Power Management in Delay Tolerant Networks: A Framework and Knowledge-Based Mechanisms. In *IEEE SECON 2005 Second Annual IEEE Communications Society Conference on Sensor and Ad Hoc Communications and Networks*, pages 418–429, 26-29 September 2005.

[59] H. Jun, M. H. Ammar, M. D. Corner, and E. W. Zegura. Hierarchical Power Management in Disruption Tolerant Networks with Traffic-Aware Optimization. In *Proceedings of the 2006 SIGCOMM Workshop on Challenged Networks, (CHANTS '06)*, pages 245–252, New York, NY, USA, September 2006. ACM Press.

[60] N. Banerjee, M.D. Corner, and B.N Levine. An Energy-Efficient Architecture for DTN Throwboxes. In *Proceeding of IEEE INFOCOM 2007*, Anchorage, Alaska, USA, May 6-12 2007.

[61] W. Zhao, Y. Chen, M. H. Ammar, M. Corner, B. N. Levine, and E. Zegura. Capacity Enhancement Using Throwboxes in DTNs. In *Proceedings of the IEEE Intl Conf on Mobile Ad hoc and Sensor Systems (MASS)*, Oct 2006.

[62] M. Anand, E.B. Nightingale, and J. Flinn. Self-Tuning Wireless Network Power Management. In *Proceeding of ACM Intl Conf on Mobile Computing and Networking(MobiCom'03)*, 2003.

[63] E. Shih, P. Bahl, and M. J. Sinclair. Wake on Wireless: An Event Driven Energy Saving Strategy for Battery Operated Devices. In *Proceedings of ACM Mobicom*, pages 160–171, September 2002.

[64] Y. Xi, M. Chuah, and K. Chang. Performance Evaluation of a Power Management Scheme for DTNs. *Mobile Networks and Applications*, 12(5):370–380, 2007.

[65] C. M. Sadler and M. Martonosi. Data Compression Algorithms for Energy-Constrained Devices in Delay Tolerant Networks. In *Proceedings of The 4th International Conference on Embedded Networked Sensor Systems (SenSys '06)*, pages 265–278, New York, NY, USA, September 2006. ACM.

[66] Z. M.Wang, S. Basagni, E. Melachrinoudis, and C. Petrioli. Exploiting Sink Mobility for Maximizing Sensor Networks Lifetime. In *Proceedings of the 38th Annual Hawaii International Conference on System Sciences(HICSS '05:)*, page 287.1, Washington, DC, USA, 2005. IEEE Computer Society.

[67] L. Berkhovskikh and Y. Lysanov. Fundamentals of Ocean Acoustics. *Springer*, 1982.

[68] A. Quazi and W. Konrad. Underwater acoustic communications. *IEEE Communication Magazine*, page 2429, March 1982.

[69] R. Coates. *Underwater Acoustic Systems*. Wiley, 1989.

[70] J. A. Catipovic. Performance Limitations in underwater acoustic telemetry. *IEEE Journal of Oceanic Engineering*, 15:205–216, July 1990.

[71] M. Stojanovic. Underwater Acoustic Communications. *Encyclopedia of Electrical and Electronics Engineering*, 22:688–698, July 1999.

[72] K. V. MacKenzie. Nine-Term Equation for Sound Speed in The Oceans. *Acoustical Society of America Journal*, 70:807–812, September 1981.

[73] K. V. MacKenzie. Discussion of Sea Water Sound-Speed Determinations. *Acoustical Society of America Journal*, 70:801–806, September 1981.

[74] Heinz G. Urban. *Handbook of Underwater Acoustic Engineering*. STN ATLAS Elektronik GmbH, November 2002.

[75] R. J. Urick. *Principles of Underwater Sound*. Peninsula Publishing, Los Altos, California, third edition, 1983.

[76] Albert F. Harris and Michele Zorzi. Modeling the Underwater Acoustic Channel in ns2. In *Proceedings of the 2nd international conference on Performance evaluation methodologies and tools (ValueTools '07)*, pages 1–8, 2007.

[77] A. Sehgal, I. Tumar, and J. Schönwälder. Variability of Available Capacity due to the Effects of Depth and Temperature in the Underwater Acoustic Communication Channel. In *Proceeding of IEEE Oceans*, May 2009.

[78] W. H. Thorp. Analytic Description of the Low-Frequency Attenuation Coefficient. *Acoustical Society of America Journal*, 42:270–+, 1967.

[79] W. H. Thorp. Deep-Ocean Sound Attenuation in the Sub- and Low-Kilocycle-per-Second Region. *Acoustical Society of America Journal*, 38:648–+, 1965.

[80] F. H. Fisher and V. P. Simmons. Sound Absorption in Sea Water. *The Journal of the Acoustical Society of America*, 62(3):558–564, 1977.

[81] M. A. Ainslie and J. G. McColm. A Simplified Formula for Viscous and Chemical Absorption in Sea Water. *Acoustical Society of America Journal*, 103:16711672, March 1998.

[82] M. Abolhasan, T. Wysocki, and E. Dutkiewicz. A Review of Routing Protocols for Mobile Ad hoc Networks. *Ad Hoc Networks*, 2(1):1 – 22, 2004.

[83] K. Akkaya and M. Younis. A Survey on Routing Protocols for Wireless Sensor Networks. *Ad Hoc Networks*, 3(3):325 – 349, 2005.

[84] C. Perkins and P. Bhagwat. Highly Dynamic Destination-Sequenced Distance-Vector Routing (DSDV) for Mobile Computers. In *Proceedings of the SIGCOMM '97*, pages 234–244, August 1994.

[85] V. D. Park and M. S. Corson. A Highly Adaptive Distributed Routing Algorithm for Mobile Wireless Networks. In *Proceedings of the INFOCOM '97*, page 1405. IEEE Computer Society, 1997.

[86] C. E. Perkins, E. M. Royer, and S. R. Das. Ad Hoc On-Demand Distance Vector (AODV) Routing. RFC 3561, July 2003.

[87] D. B. Johnson, D. A. Maltz, and J. Broch. DSR: The Dynamic Source Routing Protocol for Multi-Hop Wireless Ad Hoc Networks. In *In Ad Hoc Networking*, pages 139–172. Addison-Wesley, 2001.

[88] E. Cheng, Y. Qi, B. Sun, Z. Zhuang, and J. Deng. Research on Routing Protocol for Shallow Underwater Acoustic Ad Hoc Network. In *Proceedings of the 2008 ISECS International Colloquium on Computing, Communication, Control, and Management (CCCM '08)*, pages 533–537, 2008.

[89] P. Bose, P. Morin, I. Stojmenovic, and J. Urrutia. Routing with Guaranteed Delivery in Ad hoc Wireless Networks. *ACM Wireless Network*, 7(6):609–616, 2001.

[90] T. Melodia, D. Pompili, and I. F. Akyildiz. Optimal Local Topology Knowledge for Energy Efficient Geographical Routing in Sensor Networks. In *Proceeding of IEEE INFOCOM '04*, March 2004.

[91] E.S. Sozer, M. Stojanovic, and J. Proakis. Underwater acoustic networks. *IEEE Journal of Oceanic Engineering*, 25(1):72–83, January 2000.

[92] G. Xie and J.H. Gibson. A network Layer Protocol for UANs to Address Propagation Delay Induced Performance Limitations. In *Proceedings of IEEE OCEANS '01*, volume 4, page 20872094, November 2001.

[93] I. Vasilescu, K. Kotay, D. Rus, M. Dunbabin, and P. Corke. Data Collection, Storage, and Retrieval with an Underwater Sensor Network. In *Proceedings of the 3rd international conference on Embedded networked sensor systems (SenSys '05)*, pages 154–165, 2005.

[94] P. Xie, J.-H. Cui, and L. Lao. VBF: Vector-Based Forwarding Protocol for Underwater Sensor Networks. In *Proceedings of IFIP Networking*, pages 1216–1221, 2005.

[95] D. Pompili, T. Melodia, and I. F. Akyildiz. A Resilient Routing Algorithm for Long-term Applications in Underwater Sensor Networks. In *Proceedings of Mediterranean Ad Hoc Networking Workshop (Med-Hoc-Net)*, June 2006.

[96] D. Pompili, T. Melodia, and I. F. Akyildiz. Routing Algorithms for Delay-insensitive and Delay-sensitive Applications in Underwater Sensor Networks. In *Proceedings of ACM Conference on Mobile Computing and Networking (MobiCom)*, September 2006.

[97] J. M. Jornet, M. Stojanovic, and M. Zorzi. Focused Beam Routing Protocol for Underwater Acoustic Networks. In *Proceedings of the third ACM international workshop on Underwater Networks (WuWNeT '08)*, pages 75–82, 2008.

[98] B. Peleato and M. Stojanovic. Distance Aware Collision Avoidance Protocol for Ad-Hoc Underwater Acoustic Sensor Networks. *IEEE Communication Letters*, pages 1025–1027, December 2007.

[99] M. C. Domingo. A Distributed Energy-Aware Routing Protocol for Underwater Wireless Sensor Networks. *Wireless Personal Communications*, November 2009.

[100] Z. Guo, G. Colombi, B. Wang, J-H. Cui, D. Maggiorini, and G. P. Rossi. Adaptive Routing in Underwater Delay/Disruption Tolerant Sensor Networks. In *Proceeding of The Fifth Annual Conference on Wireless on Demand Network Systems and Services (WONS 2008)*, January 2008.

[101] M. C. Domingo and R. Prior. Energy Analysis of Routing Protocols for Underwater Wireless Sensor Networks. *Computer Communication*, 31(6):1227–1238, 2008.

[102] J. H. Cui, J. Kong, M. Gerla, and S. Zhou. Challenges: Building Scalable Mobile Underwater Wireless Sensor Networks for Aquatic Applications. *Special issue of IEEE Network on Wireless Sensor Networking*, May 2006.

[103] M. Dunbabin, P. Corke, I. Vasilescu, and D. Rus. Data Muling Over Underwater Wireless Sensor Networks Using an Autonomous Underwater Vehicle. In *Proc. IEEE International Conference on Robotics and Automation ICRA 2006*, pages 2091–2098, 15–19 May 2006.

[104] W. Zhao and M. H. Ammar. Message Ferrying: Proactive Routing in Highly-Partitioned Wireless Ad Hoc Networks. In *Proc. Ninth IEEE Workshop on Future Trends of Distributed Computing Systems FTDCS 2003*, pages 308–314, 28–30 May 2003.

[105] W. Zhao, M. Ammar, and E. Zegura. A Message Ferrying Approach for Data Delivery in Sparse Mobile Ad Hoc Networks. In *Proceedings of the 5th ACM international symposium on Mobile ad hoc networking and computing, (MobiHoc'04)*, pages 187–198, New York, NY, USA, 2004. ACM.

[106] B. Burns, O. Brock, and B. N. Levine. Autonomous Enhancement of Disruption Tolerant Networks. In *Proc. IEEE International Conference on Robotics and Automation ICRA 2006*, pages 2105–2110, 15–19 May 2006.

[107] B. Burns, O. Brock, and B. N. Levine. MORA Routing and Capacity Building in Disruption-Tolerant Networks. *Ad Hoc Netw.*, 6(4):600–620, 2008.

[108] Internet Engineering Task Force (2003) Power Saving in 802.11. URL:http://www1.ietf.org/mail-archive/web/manet/current/msg03227.html, Feb 2010.

[109] Chipcon. Smartrf cc1000: Single Chip Very Low Power rf Transceiver. http://www.chipcon.com.

[110] Basic form of Friis Transmission Equation. URL:http://en.wikipedia.org/wiki/Friis_transmission_equation, August 2010.

[111] III A. F. Harris, M. Stojanovic, and M. Zorzi. When Underwater Acoustic Nodes Should Sleep with One Eye Open: Idle-Time Power Management in Underwater Sensor Networks. In *Proceedings of the 1st ACM international workshop on Underwater Networks, (WUWNet'06)*, pages 105–108, Los Angeles, CA, USA, 2006.

[112] The network simulator ns-2.

[113] Y. Wang, P. Zhang, T. Liu, C. Sadler, and M. Martonosi. CRAWDAD Data Set Princeton/ZebraNet (v. 2007-02-14). http://crawdad.cs.dartmouth.edu/princeton/zebranet, February 2007.

[114] A. Porto and M. Stojanovic. Optimizing the Transmission Range in an Underwater Acoustic Network. In *Proc. of the MTS/ IEEE OCEANS Conference*. IEEE/MTS, September 2007.

[115] V. Rodoplu and M. K. Park. An Energy-Efficient MAC Protocol for Underwater Wireless Acoustic Networks. In *Proc. of the MTS/ IEEE OCEANS Conference*. IEEE/MTS, September 2005.

[116] W. Ye, J. Heidemann, and D. Estrin. An Energy-Efficient MAC protocol for Wireless Sensor Networks. In *Proceedings of the IEEE Infocom*, pages 1567–1576, New York, NY, USA, June 2002. IEEE.

[117] I. Vasilescu, C. Detweiler, and D. Rus. AquaNodes: An Underwater Sensor Network. In *Proceedings of the second workshop on Underwater networks (WuWNet '07)*, pages 85–88, New York, NY, USA, 2007. ACM.

[118] A.F. Harris, M. Stojanovic, and M. Zorzi. Idle-Time Energy Savings Through Wake-up Modes in Underwater Acoustic Networks. *Ad Hoc Networks In Press, Uncorrected Proof.*

[119] R. Jurdak, C. V. Lopes, and P. Baldi. Battery Lifetime Estimation and Optimization for Underwater Sensor Networks. *IEEE Sensor Network Operations*, Winter, 2004.

[120] Teledyne. Teledyne benthosmodem http://www.rdinstruments.com/nemo, May 2010.

[121] LinkQuest Modems http://www.link quest.com/html/intro1.htm, May 2010.

[122] EL. Freitag, M. Grund, S. Singh, J. Partan, P. Koski, and K. Ball. The WHOI Micro-Modem: An Acoustic Communications and Navigation System for Multiple Platforms. In *Proceedings of MTS/IEEE OCEANS*, 2005.

[123] A. Sehgal, I. Tumar, and J. Schönwälder. AquaTools: An Underwater Acoustic Networking Simulation Toolkit. In *Proceeding of IEEE Oceans*, May 2010.

[124] The National Center for Atmospheric Research. Temperature of Ocean Water. URL:http://www.windows2universe.org/earth/Water/temp.html.

[125] M. Ayaz and A. Abdullah. Underwater Wireless Sensor Networks: Routing Issues and Future Challenges. In *Proceedings of the 7th International Conference on Advances in Mobile Computing and Multimedia (MoMM '09)*, pages 370–375, New York, NY, USA, 2009. ACM.

Biography

Dr. Iyad Tumar is an Assistant Professor at Birzeit University. He received his Bachelor degree in electrical engineer (communications) in 2002, master degree in computational science in 2006 from Birzeit University in Palestine, and he received his doctoral (PhD) degree in smart systems in 2010 from Jacobs University Bremen. He was a member of Computer Networks and Distributed Systems group at Jacobs University Bremen. His research interests are resource management of disruption tolerant networks, wireless sensor networks, security in computer networks, underwater networks, and network management. He was a research associate and a member of EMANICS (European Network of Excellence for the Management of Internet Technologies and Complex Services) from 2007 - 2010, and he has been a member of the local organization of the 2nd International Conference on Autonomous Infrastructure, Management and Security AIMS2008.

SHAKER
VERLAG

ISBN 978-3-8322-9346-8